ABSTRACT

Title of Dissertation / Thesis: **The Influence of Landscape Position on Coastal Marsh Loss**

Andrew Stephen Rogers, Doctor of Philosophy, 2004

Dissertation / Thesis Directed By: Professor Michael Kearney, Department of Geography

Coastal marshes are considered as important features of the landscape that are at risk of loss. Accurately assessing their prospects for survival is difficult in view of the wide possible causes of loss, the large areas involved and that most research is done on relatively small parcels. This project examined the probability of conversion of marsh surface parcels to open water as a function of distance from roadways across marshes, tidal creeks, and upland areas, and the distance upstream, and the size of a

marsh parcel. These are understood to be stand-ins for hydrology, elevation and other factors that are more difficult to measure.

The study area was divided into a MidAtlantic coastal region and a large bays region comprising the Chesapeake and Delaware Bays. A semi-automated system was developed for measuring the extent and severity of coastal marsh loss using Thematic Mapper (TM) data. The data derived from the TM analysis were used to develop algorithms to examine the impacts of the five factors listed above. The factors were examined individually using ordinary least squares (OLS) regression, and collectively using logistic regression. The OLS regression revealed that distance from uplands and distance from the nearest tidal creek were highly correlated with marsh loss in both areas. For the Atlantic Coast, however, the loss was negatively related to distance from tidal creeks, the opposite of what was expected. Distance upstream was negatively correlated with marsh loss as predicted. The relationship between distance from roads and marsh loss indicated that marshes are healthier near roads than farther away. The relationship between parcel size and marsh loss was non-linear, with small and large marshes having a lower probability of degradation than mid-sized marshes. The logistic regression model is useful for identifying areas with higher probabilities of conversion to open water. Sea level rise (SLR), tidal range, easting and northing were examined for use with the logistic models. SLR and tidal range added no information to the bay areas, but sea level rise was weakly negatively correlated with marsh loss on the Atlantic Coast and tidal range was weakly positively related.

The Influence of Landscape Position on Coastal Marsh Loss

By

Andrew Stephen Rogers

Thesis submitted to the Faculty of the Graduate School of the
University of Maryland, College Park, in partial fulfillment
of the requirements for the degree of
Doctor of Philosophy
[2004]

Advisory Committee:
Professor Michael Kearney, Chair
Professor Court Stevenson
Professor Emeritus Ivar Strand
Professor John Townshend
Professor David Wright

Dedication

To my wife, Elizabeth Ann Rogers, and my three children, Suzanne Marie Mangeri, Michael James Rogers and Christopher William Geoffrey Rogers, without whose love and support this would not have been possible.

Acknowledgements

Coastal Marsh Project PIs

Michael Kearney, John Townshend, William Lawrence

Coastal Marsh Project Graduate Students

Jennifer Stevens, Janine Savage, David Stutzer, Kate Eldred, and Eric Rizzo

Committee Members

Michael Kearney, John Townshend, Ivar Strand, Court Stevenson, Dave Wright

Undergraduate Students

Deanna Guerieri and Nicole Hale

Proofreaders, boat carriers, critics and other assistants

Beth Rogers, Michael Rogers, Chris Rogers, Pam Heberer, Lisa Wainger, SeJong Ju, William Rogers, Anna Hight, and Rae Benedict

Funding and support

Chesapeake Biological Laboratory provided equipment and resources.

Applied Ordnance Technology, Inc., provided funding to the author.

NASA's Mission to Planet Earth funded the Coastal Marsh Project

Grant number: NAGW3758, Mr. Alex Tuyahov, Program Manager.

University of Maryland College Park sponsored the Coastal Marsh Project.

Table of Contents

List of Tables

List of Figures / Illustrations

List of Equations

Chapter 1: Introduction

Objective:

Research into coastal marsh loss has tended to focus on point or small plot measurements (e.g., Bricker-Urso et al., 1989; Cahoon and Reed, 1995; Craft and Broome, 1993; Bryant and Chabreck, 1998). These studies typically use a variety of techniques to estimate the ability of the marsh surface to keep up with changing sea levels, and involve historical analyses involving radioactive materials or stable isotopes (Chmura and Aharon, 1995; DeLaune et al., 1983a; Kearney, 1996), measurements of thickness of substrate, placing markers on the surface and measuring deposition at the point where the marker is placed over some period of time. These efforts have been critically important in developing an understanding of how marshes function. However, they cannot, by themselves, adequately address the underlying question of what is happening to coastal marshes and why. It is often difficult, or impossible, to relate findings at one location to other locations in the same marsh, much less locations in distant marshes. In addition, the methods tend to be very time and effort intensive.

Turner (1997) notes that the lack of clearly stated hypotheses for testing, quantification and prediction hinders good decision making for management. Further, due to not having carefully stated, testable hypotheses, researchers made diametrically opposed recommendations to the Louisiana government as to what actions would resolve the marsh loss in the Mississippi delta. This dissertation builds

on the knowledge gained from earlier studies, looks at factors that may lead to coastal marsh loss and that extend across all marshes, and the considers possibility of quantifying the influence of these factors. In doing so, it proposes five specific hypotheses to test.

The purpose of this research is to develop an understanding of the interaction between five factors, which can influence the conversion of coastal marshes to open water. The factors chosen to develop a multivariate spatial model are: 1) distance from the nearest road; 2) distance from the nearest tidal stream; 3) distance upstream from oceanic forcing such as the Atlantic Ocean or a major bay (such as the Chesapeake) where sea level rise could dominate the loss of marshes; 4) distance from the nearest upland; 5) total size of the parcel. These factors were chosen because they affect hydrology and sediment loading to the marsh surface and they, in turn, reflect subtle changes in elevation that are often on the order of a few centimeters. Their selection reflects the underlying assumption that hydrology, sediment supply, and elevation are key factors in marsh loss. These five factors will be discussed in more detail in the next section followed by a more general discussion of the interplay between marsh hydrology, sediment dynamics and marsh loss in Chapter 2. In addition, the factors chosen can all be derived from readily available information such as existing maps and remotely sensed data rather than requiring intensive and time-consuming field techniques that are often point-specific.

The specific factors examined in this dissertation reflect current thinking on tidal wetland loss and the value of coastal marshes (Cahoon and Reed, 1995; Kearney, 1996; Orson, 1996; Stevenson and Kearney, 1996; Van der Molen, 1997;

Bryant and Chabreck, 1998; Esselink et al., 1998; Evers et al., 1998; Boggs and Shepherd, 1999; Hazelden and Boorman, 1999;Kuhn et al., 1999; Roulet, 2000; Hartig et al., 2002; Kearney et al., 2002; Morris et al., 2002; Anastasiou and Brooks, 2003;Sun et al., 2003). The value of coastal marshes and factors affecting loss are discussed in Chapter 2.

The separate question of the rate of marsh vertical accretion versus sea level rise is not examined directly. However, if a marsh area is accreting at the appropriate rate, it will maintain itself as healthy marsh. If not, it will eventually drown. The expansion of marshes outside the study area is not examined, as areas outside the bounds of the study area are not examined.

Hypotheses:

The probability of a parcel of marsh being open water is directly related to specific landscape and related hydrological factors. This proposition can be rewritten as five specific hypotheses, as shown below. The null hypothesis for each of these specific hypotheses can be simply stated as follows: "The conversion of marsh surface to open water is a completely stochastic process, and it is not possible to infer that ponds are more or less likely to form in certain places based on this factor."

The hypotheses for testing the five factors are:

Hypothesis 1. The probability of a parcel being completely open water will be negatively related to the distance of the parcel from a road.

Hypothesis 2. The probability of a parcel being completely open water will be positively related to the distance the parcel is from the nearest tidal creek or man-

made ditch (e.g. mosquito ditches).

Hypothesis 3. The probability of a parcel being completely open water will be negatively related to the distance the marsh system containing the parcel is upstream.

Hypothesis 4. The probability of a parcel being completely open water will be positively related to the distance of the parcel from the upland.

Hypothesis 5: The probability of a parcel being completely open water will be negatively related to the size of the marsh parcel containing the grid cell.

These factors will be conditioned by the introduction of tidal range and local relative sea level rise to the model. The detailed rationales underlying the selection of these specific hypotheses are explained in subsequent sections.

Rationales for Selection of Hypotheses

Hypothesis 1:

Hypothesis 1 is that the installation of a paved road across a marsh encourages marsh loss in the vicinity of the road, but outside a buffer zone around the road where marsh stability may actually be enhanced. A road across a marsh may actually increase structural integrity in its immediate vicinity due to installation of materials suitable for road construction. The weight of a road constructed across a marsh may also push the immediately surrounding marsh up (Stevenson, pers. com, 1999). In addition, roads may be built on the most stable part of the marsh and often connect islands within the marsh.

There are two possible modes of response involved. Structures that prevent flow can limit the supply of inorganic material to the marsh surface. For example,

Allen and Rae (1988) found that marshes on opposite sides of a seawall along the Severn River in the U.K. had an average height difference of 1.2 meters, with the section of marsh that was still subjected to tidal flooding being higher. This may be due to drying of the peat on the non-tidal side (Bryant and Chabreck, 1998), resulting in compaction (Bricker-Urso et al., 1989) or lack of inorganic sediment input or both. Stevenson and Kearney (1996) note that building roads across marshes may limit their ability to trap sediment. In the absence of inorganic sediment input, the marsh surface can only accrete vertically via deposition of leaf and stem litter (above ground biomass) and development of rhizome systems (below ground biomass) (Boesch et al., 1994; Stevenson et al., 1988). The inorganic portion of the sediment may be more important as a nutrient than for its actual bulk volume (Bricker-Urso et al., 1989).

Bryant and Chabreck (1998) examined the impact of impoundments on marshes in Louisiana. They found that marshes impounded behind levees did not accrete as rapidly as areas of the same marsh outside the impoundments. They attribute this to several factors, principally a lack of inorganic sediment input, but also drying the marsh, which increases the oxidation rate of the organic fraction of the sediment. Where there is an impoundment, they further speculated that the only times the marsh surface would be nourished with mineral sediment was during storm events that overtopped the levees. Floods of this size, however, could easily remove the organic debris that forms much of the bulk of the marsh.

In other situations, roads may promote marsh loss through trapping water on one side of the road. If water becomes impounded behind a causeway, the soil will become anoxic and organisms may be subjected to longer periods of higher salinity.

Under extremely anoxic conditions sulfate is reduced to toxic sulfide (Kerner, 1993). Stevenson and Kearney (1996) suggest that the formation of oozes with "negligible structural integrity," such as underlie much of Blackwater National Wildlife refuge, may be a result of sulfate reduction and nitrate additions. These oozes contribute to the erodability of the marsh once the root mat is gone. Low plant productivity may be caused by the stress of anaerobic conditions (DeLaune et al., 1983b), which then causes reduced production of biomass. This can be especially problematic when low organic sediment input to the marsh is coupled with the low inorganic sediment input (due to the less effective trapping of mineral sediment from reduced aboveground biomass).

On the other hand, some flooding and the resulting anoxic soil conditions may actually improve the vertical accretion rate because organic debris in the oxic layer degrades rapidly and most of the bulk is lost. Degradation of peat under anoxic conditions is much slower than under oxic conditions (Halupa and Howes, 1995).

Hypothesis 2:

Hypothesis 2 is that formation of ponds will tend to take place away from tidal creeks, man-made ditches and similar sources of sediment-laden overwash. Several studies have plotted regressions of marsh vertical accretion rates vs. distance to nearest tidal creek (Esselink et al., 1998; French and Spencer, 1993; Hatton et al., 1983). All three showed vertical accretion rates are related to proximity to a stream, at least for short distances. This phenomenon reflects the rapid trapping of mineral sediment by the culms of the plants adjacent to tidal creeks, as marsh surfaces are

flooded during high tide (see Leonard and Reed, 2000).

However, this effect may be confounded by topography, as studies also find topography and vertical accretion rates to be correlated (Esselink et al., 1998; French and Spencer, 1993; Letzsch and Frey, 1980). In a study of a Louisiana salt marsh, Cahoon and Reed (1995) concluded that marsh topography exerted a strong influence on hydroperiod, with areas of lower topographic relief in some areas contributing to dramatic increases in hydroperiod, yielding greater accretion during extended flooding events. Nonetheless, despite the potential for increased flooding and deposition, the lowest areas of the marsh were found to be deteriorating rapidly, largely due to the fact that the lowest areas are interior marsh areas where limited influx of mineral sediments yields low rates of vertical accretion.

Similarly, the development of submerged upland marshes tends to result in marshes with poorly developed tidal creek systems. As the marshes spread inland, areas away from the tidal creeks can actually receive less inorganic sediment, relying solely on peat accumulation for vertical accretion (Stevenson and Kearney, 1996).

Hypothesis 3:

Hypothesis 3 is that coastal marsh loss is directly related to distance downstream. Coastal marsh loss, in the absence of anthropogenic factors, has been shown to be related to sea level rise (DeLaune et al., 1983, Downs et al., 1994). If this is true, then there should be a trend for downstream marshes (which are closer to both sea level and the sea) to disappear faster than upstream marshes. As sea level rises, the hydroperiod and salinity of lower marshes will change more than those

upstream. The plant communities in upstream marshes are more diverse and can still convert to salt-tolerant species. Downstream marshes are already likely to be maximally adapted to salinity and more regular hydroperiods with a few plant species that are already under stress. Therefore, when the salinity and hydroperiod increase, the marsh will be more likely to die (Nyman et al., 1995).

In the Great Lakes, where water levels can rise or fall over periods of decades, Keough et al. (1999) report in a review article that, in fact, this progression is what takes place. As the water rises, the more water-adapted species atthe water's edge are forced to shift back into the marsh, with subsequent displacement of less water tolerant species.

In one study, species distribution in terms of total numbers of species and in the species present changed abruptly going from fresh to oligohaline conditions. The numbers dropped dramatically from 18 species in the freshwater site, to three in oligohaline conditions and five in mesohaline areas (Latham et al., 1991).

A preliminary study of four sites along the Patuxent River, MD, (Rogers, unpublished data) found that species richness was weakly correlated (0.38) with distance upstream from the river mouth. However, the marsh farthest upstream had twice the species richness as the most downstream marsh.

Hypothesis 4:

Hypothesis four is that the probability of a parcel being completely open water will be positively related to the distance of the parcel away from the nearest upland area. Upland should provide several benefits to the marsh immediately adjacent to it.

One, of course, is simply elevation: the marsh adjacent to the upland is generally higher than the rest of the marsh farther away since the marsh surface rises in elevation inland. Secondly, if the marsh was formed by deposition onto a substrate as sea level rose over the last few millennia, then the depth of peat will be less near the upland and this may provide more stability to the marsh. In addition, there will be fresh water runoff, which will both provide sediment and reduce the salinity of the adjacent marsh. The logic behind this hypothesis is that near the upland, there will be both a slight elevation change and that the marsh substrate may be shallower with firmer soil underneath near the upland.

The distance to the nearest upland was added as a parameter after a brief preliminary study (Rogers unpublished data) looked at 24 plots spread along four transects along the Patuxent River. In this study, four parameters - salinity, soil redox[1] potential, amount of bare soil and the plant species richness - were measured and related to distance upstream and distance from the shore. Six 1-meter-square plots were sampled in pairs along each transect line at 0, 15 and 30 meters from the shore. The plots in each pair were five meters from either side of the transect. The expectation in collecting these was that redox potential would decrease moving from the shore (where there is often a levee) into the interior, which often retains water between tidal cycles. Also, the salinity and percent bare soil were expected to increase along each transect. These expectations were not met, however. Salinity did

[1] "Redox potential: The tendency of oxidation – reduction reactions to occur. An oxidation – reduction reaction occurs when an oxidizing agent, often oxygen, acquires electrons from a reducing agent such as carbon or hydrogen."

increase in some cases, but it was not consistent. This may reflect the difference in the sizes of the marsh areas sampled, with some being narrower strips between the adjacent upland and the river.

This study also found that redox potential was weakly correlated with distance from the Patuxent River. However, the redox potential was highest near the river shore (perhaps a levee effect due to greater sediment influx), lower 15 meters inland and higher again at 30 meters for the marsh where the distance from shore to upland was shortest. This may indicate that the proximity of the upland helped reduce the soil anoxia by greater aeration due to flushing from the upland gradient of soil/substrate pore water by throughflow. Due to the above observations, distance from the nearest upland was added as a factor to be tested.

Hypothesis 5:

Hypothesis 5 is that marsh loss rates are negatively related to total parcel area. As parcels of a marsh become smaller and smaller, the edge exposed to erosion becomes much greater compared to the amount of marsh that is left to erode. Based on this reasoning, small parcels should disappear faster than large parcels. Conversely, small parcels of marsh may be resistant to loss, because no part of the marsh is far from the sediment input sources. Also, small marshes are likely to be the least erodible areas of a larger marsh that have been left behind and may tend to represent areas that are linked closely to uplands. Only large parcels have enough interior area to develop ponds with sufficient surface area for waves to develop. Similarly, newly-formed channels can help remove sediment more expeditiously from

the marsh (DeLaune et al., 1983a), as well as serving as loci for interior pond formation (see Kearney et al., 1988).

This hypothesis is distinctly different from the others in several ways. Effects related to size of the parcel are liable (as noted above) to be related to a variety of other effects. This hypothesis was introduced to determine how selection of the size of a marsh parcel in a study affects conclusions about its vulnerability. If there is no size dependency, then studies of small marshes can be applied to large marshes and vice versa. If there is a size dependency, then this has to be considered in making comparisons across marsh size ranges.

Effects of Scale:

Measurements of the same property at different scales may yield different causal relationships. For example, local biological dynamics can dominate at small scales, but physical processes tend to dominate at larger scales (Wiens, 1989). Furthermore, quite different effects can explain the same phenomena at different scales. For example, leaf litter decomposition at the local level is explained by the properties of the litter and the decomposers. However, at regional scales, climatic variation accounts for most of the difference (Meentemeyer, 1984). In terrestrial ecosystems, physical factors tend to operate at regional or continental scales, whereas these physical effects are overcome by biological drivers at local scales. However, plant communities can influence climate at regional scales and plant growth can be affected by microtopography and edaphic factors (Wiens, 1989). These effects will be discussed in separate sections below.

This principle can be seen to operate in coastal marshes. Plant canopies in experimental flumes affect water velocity and, therefore, deposition and erosion of sediment (Shi et al., 1995). Moreover, they are largely responsible for the organic fraction of the vertical accretionary budget (Kearney et al., 1988). However, ultimately both factors are modulated by sea level rise. On the other hand, two identical inputs can have completely different relationships at different scales (Wiens, 1989). Wiens notes, for example, that Least Flycatcher and American Redstart populations are negatively correlated on local scales, but positively correlated on regional scales. This is presumably because of interspecific competition at small scales, but usage of identical habitats that dominates at regional scales.

In addition, Wiens identifies "grain" and "extent" as limits on scale. The grain is the smallest parcel size that is measured; the extent is the total study area. In this study, the grain size is 28.5 meters and the largest extent is approximately 1000 kilometers. This means that any variation smaller than 28.5 meters is invisible to this project. No tidal creeks smaller than 28.5 meters were used as inputs and small bodies of water were not recorded as such. The formation of small ponds, as long as they do not occupy over 50% of a pixel, is not observed. The trends measured by Rogers (unpublished) in chemistry, species richness, salinity, and bare soil across the marshes would not be visible in this study, although the trends going upstream are visible. In addition, while the impact of large populations of herbivores would be visible, small eat-outs might not be. The overall result of this is that the biotic, inorganic and microtopographic drivers of the beginnings of pond formation cannot be observed at the scale of this study.

The five factors proposed for examination as part of the hypothesis would be expected, like the weak, strong, electromagnetic and gravitational forces, to act over different ranges with different strengths. If there is a correlation of loss with size, that would be strictly related to the immediate parcel of marsh. The impact of roads, causeways, levees and similar structures that block water and sediment movement would be expected to be greatest over distances of tens to hundreds of meters. Distance from the nearest tidal creek would be a factor that would operate at most at the scale of a single marsh. The distance of the marsh upstream, on the other hand, would certainly influence the sedimentary dynamics of individual marshes, but as a phenomenon probably is best observed over the length of an entire river system.

Chapter 2: Coastal Marshes

The Value of Coastal Salt Marshes

Coastal marshes are important for a number of reasons. In brief, marshes are viewed as traps for various pollutants and CO2 (Craft and Broome, 1993, Roulet, 2000) as well as sediment (Hutchinson et al., 1995). Under some circumstances, they can also be sources of sediment (Stevenson et al., 1988; Wang et al., 1993) and nutrients (Childers et al., 1993). The current focus on global carbon cycles makes carbon sequestration an especially important value. As long as coastal marshes maintain themselves with regard to rising sea level, they will continue to sequester carbon, because they have to build substrate.

It has been widely believed that detritus from marshes contributes to the estuarine/marine food webs (Odum et al., 1995; Peterson and Howarth, 1987). Wetlands provide habitat for a variety of resident species, both plant and animal, including nursery areas for young fish and shellfish (Browder, 1985; Minello et al., 1994; Rozas, 1995; Schenker and Dean, 1979). Marshes are also critical habitat for many migratory bird species (Daborn et al., 1993; Erwin, 1996, Gabrey et al., 1999).

Coastal Salt Marsh Loss Factors

Coastal salt marshes are often considered to be geologically transient systems (Dame and Childers, 1992) that are sensitive to any changes in hydrology, hydroperiod or salinity (Kuhn et al., 1999; Morris et al., 2002) and are currently being lost (Figure 1). Some of the factors contributing to this loss are the position of a marsh in the landscape,

chemistry, sediment supply, marsh structure, sea level rise, anthropological impacts, fauna, flora, and history.

Each of these factors will be discussed below, however, not all of these factors are examined as part this dissertation.

Landscape Position

The position of a marsh in the landscape will determine much about the hydrology, hydroperiod and salinity (Morris et al., 2002). For example, in any one marsh, the high marsh will, by virtue of its slightly higher elevation and distance from the stream channels, have a lower hydroperiod than the areas of the marsh at lower elevation and closer to sea level. The high marsh, however,

may have areas subject to very high salinity stresses if tidal water is trapped and evaporates, especially above the MHW mark, because it may be several weeks before another tide comes in and dilutes it back to normal seawater salinity (Frey and Basan, 1985). Deposition rates and tidal range are positively correlated (Letzsch and Frey, 1980; Stevenson et al., 1986) with tidal range affected by several factors, including coastal setting, and local topography.

Chemistry

The chemistry of estuarine intertidal marsh soils has some common characteristics, which distinguish it from other soils. The salinities tend to be high, as do concentrations of sulfide ion, and reducing conditions tend to prevail over oxidizing conditions below the soil surface (Anastasiou and Brooks, 2003). On a local scale, marsh

chemistry is strongly influenced by hydroperiod and salinity. Although tidal water can sometimes be trapped in the upper marsh and become highly saline as the water evaporates, the overall incoming tidal water will be lower in salinity farther upstream.

Increasing salinity tends to make particulates flocculate and precipitate. This occurs at relatively low salinities, however, so that fresh water coming downstream will have its sediment load stripped relatively far upstream. This causes marshes upstream to have relatively more sediment input than marshes downstream (see Kearney and Ward, 1986), but more at the margins than the interiors. For example, Jug Bay in Maryland has been filling in for over a century (Heinle and Flemer, 1976) as marshes grow from the edges of the bay. Thus, one effect of being at the freshwater-saltwater interface is that marshes will tend to be expanding.

Sediment Supply

Stevenson and Kearney (1996)) suggest that regional variations in sediment supply may be a major factor in marsh loss and survival in the Chesapeake Bay. Marshes of the western shore of the Chesapeake, where sediment influx is undoubtedly higher due to physiography (the Fall Line) and extensive land clearance, tend to be stable or growing while the relatively sediment-starved marshes of the Eastern Shore are being lost. In the Baie du Mont Saint Michel, France, there is a positive sediment budget. The salt marshes are growing at a current estimated rate of 90,000 meters2 per year (Haslett et al., 2003), so even in the face of rising sea level, with enough sediment supply marshes can still grow.

Marsh Structure

Tidal marshes have a characteristic structure dominated by the interaction between tidal range and marsh topography (Stevenson et al., 1986). In tidal marshes, , the incoming tide flows over the creek banks, and because the sediment carrying capacity is directly related to velocity, the bulk of the sediment is deposited on the creek banks, building stable levees with a large percentage of inorganic material (Esselink et al., 1998; French and Spencer, 1993; Hatton et al., 1983; (Kearney et al., 1988)). However, if insufficient sediment is available for transport, or for other reasons, levee building may not always occur, as has been reported for marshes along the lower Nanticoke River in Maryland (Kearney et al., 1988).

The interior of the marsh typically receives little inorganic input (Kearney et al., 1988, 1994; French and Spencer, 1993), and the sediment there frequently consists of organic material derived from local plant production, although some organic material may be imported by flooding (Cahoon and Reed, 1995).

These landscape features are important in the face of sea level rise. If the low marsh areas fail to keep up with sea level rise, they will likely drown first. However, rising sea level may eventually convert the high marsh to low marsh.

Kearney et al. (1988) discuss three geomorphic types of land loss.

> "(1) shoreline retreat (Figure 2)
>
> (2) widening of tidal creeks (Figure 3)
>
> (3) interior ponding" (Figure 4 and Figure 5)

Shoreline retreat is a result of wave erosion and is thought to account for only 1% of coastal marsh loss in the U.S. (Gosselink and Baumann, 1980). Widening of tidal

creeks (Figure 3) is caused by erosion along tidal creek banks, which is most prevalent in estuarine meander marshes where growth of tidal networks can be promoted (Kearney, et al., 1988; Gammill and Hosier, 1992). It is similar to creek bank erosion just before bankfull stage in rivers, but in this case probably reflects rising tidal prisms due to sea level rise. Burrowing animals, such as crabs and bivalves, may play a role by weakening the marsh sediments (the root mat) and facilitating erosion (Frey and Basan, 1985). In some coastal marshes of the Chesapeake Bay, creek bank erosion has accounted for as much as 20 - 30 percent of total marsh loss since 1938 (Kearney et al., 1988).

Interior ponding (Figure 4 and Figure 5) begins with the formation of small pannes which can form from eat-outs by ducks, geese, and muskrats, but are likely a response to slow rates of vertical accretion begins with the formation of small pannes (Stevenson et al., 1985). When water stays on the surface in these pannes too long, plant roots are subjected to stress due to the long periods of anoxic soil conditions. The prolonged exposure to higher salinity and anoxia may kill the plants whose roots hold the substrate together. Once the plants die, the sediment can become resuspended due to tidal or storm action and removed with the ebb tide. Bryant and Chabreck (1998) discuss this removal of plant detritus from impounded areas. The mobility of sediments in and out can make a large difference in this process. If sediments are readily available for import, the panne may be refilled (Mitsch and Gosselink, 2000), especially when sediment is remobilized after hurricanes.

Eventually, the panne may become a permanently filled pond. At this point, the pond can begin to grow as more plants at the periphery die, and more sediment is resuspended and removed during storm events. Eventually, neighboring ponds will begin

to coalesce and become large enough that storm-driven waves can begin to actively erode the edges (Kearney et al., 1988, Stevenson et al., 1985).

Sea level rise

Rates of sea-level rise for much of the Eastern Seaboard and Gulf Coast are generally held to be the underlying cause (Dame and Childers, 1992; Kearney et al., 1988; Kearney et al., 2002; Stevenson and Kearney, 1996) for the dramatic decline (approximately 50%) in marsh acreage since 1900 (Gosselink and Baumann, 1980). Marshes in some places cannot migrate inland due to land form constraints such as the Pleistocene Talbot terrace landward of some Nanticoke River marshes (Kearney et al., 1988) or due to human intervention, such as bulkheads (Titus, 1998), or by being completely surrounded by the sea, such as Bloodsworth Island (Downs et al., 1994). The studies of the relationship of marsh development to sea level rise raise concerns about marsh survival in the 21st century, when the global sea level trend may accelerate due to greenhouse warming (Nyman et al., 1995). Reflecting this uncertainty, Bricker-Urso et al. (1989) concluded that the New England marshes might be characterized by a maximum vertical accretion rate that, if exceeded by local relative sea level rise, will cause these marshes to disappear.

The impact from sea level rise is not distributed evenly over the course of a tidal river. Figure 6 shows that maximum sediment input will occur where the tidal range is highest (Morris et al., 2002), which is not necessarily at one end of the river system. As relative sea level rises, water that is more saline will move into the system, hydroperiods will increase, resulting in increased duration of hypoxic soil conditions. Plants at the

lower end of the river are already the most salt-tolerant species. Therefore, as the hypoxia kills the existing plant community, there are no other plants capable of replacing it. At the fresh water end, however, plant community shifts can allow the marsh system to continue. Even *S. alterniflora*, among the most adapted of coastal marsh plants to rising salinity, will eventually succumb to drowning (Mendelssohn et al., 1982).

Anthropological Impacts

However, coastal marshes are also being threatened by a variety of human activities including oil and gas extraction (Dijkema, 1997; White and Morton, 1997; White and Tremblay, 1995), urban development, sediment diversion, and possibly other factors, such as road construction (Stevenson and Kearney, 1996). Marsh management techniques may also promote loss (Gabrey et al., 1999). Such techniques include marsh burning in fall or winter, or structural marsh management (SMM), which uses levees and water control systems to regulate the hydroperiod of enclosed areas (Gabrey et al., 1999; Kuhn et al., 1999). Both approaches can limit the vertical accretion by reducing detrital inputs (in the case of marsh burning) or mineral sediment inputs (in the case of levees and other hydroperiod controls). In a study of four hypotheses explaining loss of marshes in Louisiana, the losses correlated with canals and accompanying dredge spoil levees lining the canals (Turner, 1997). The combination of canals, which drain water, and levees, which prevent overwash, has the double impact of lowering the water table in the wetlands while simultaneously preventing tidal overwash from reaching the marsh surface with nutrients and sediment.

Fauna

In addition to these factors, animal populations may influence the health of marshes in various ways. Snow geese (Gabrey et al, 1999) and *Nutria* (Carter et al., 1999) both eat the plant roots. At Jug Bay Wetlands Sanctuary in Maryland, carp are implicated in consuming young wild rice plants (Baldwin, pers. com.), and year-round resident Canada geese eat the seedpods as they are growing in the spring. Oyster reefs may, in some cases, significantly change water – flow and sediment dynamics. This may help nutrient retention, aiding the development of bar-built estuarine marshes (Dame and Childers, 1992).

Nutria, an invasive species, may cause destruction of the marsh substrate by grubbing for roots. Evers et al. (1998) found that, although *Nutria* could not be shown to be more destructive than waterfowl, they can cause reductions in plant biomass and productivity. They also found that areas grazed by both waterfowl and *Nutria* tend to be more affected than areas grazed by only one. Grace and Ford (1996) discussed the impact of *Nutria* on Louisiana marshes from the findings of numerous other scientists and their own work. Their finding, using simulated herbivory, was that some marsh plants (*Sagittaria lancifolia* in particular) can recover quickly even after suffering stress from storm-induced salt water intrusion.

Flora

The interaction between plants and marsh degradation can be quite complex. Plant communities can help to stabilize the marsh by trapping sediment and providing litter (Morris et al., 2002). For *Spartina alterniflora,* the maximum growth occurs when

the plants are below the mean high tide (MHT). In North Inlet, South Carolina, much of the *S. alterniflora* is above its optimal position and is stunted. However, as sea level rises, plants respond with more growth, which traps more sediment, which maintains the elevation (Morris et al., 2002).

The high marsh is only slightly higher than the low marsh, but the elevation difference is just sufficient to decrease the hydroperiod so that different plant species grow there. For example, *Phragmites australis* tends to grow in the high marsh and invade low marsh areas (if salinities are very low). Even in the low marsh areas *P. australis* produces more biomass than *Spartina patens* in the same environment, and the material is more resistant to microbial degradation (Windham, 2001). It follows from this that *P. australis* can contribute more inorganic material to the marsh surface than *S. patens,* at least under some conditions.

Stribling and Cornwell (2001) note that upper marsh areas - where salinity stresses are lower - are often subjected to high fluctuations in nutrients, especially from farm run off. While the fluctuations present an additional stress, the additional nutrients support increased plant growth. Increased plant production would cause an increase in sediment trapping.

This dissertation will not look at the impacts of different plant communities or different biomass production rates specifically because plant communities cannot be differentiated by the remote sensing techniques used. However, plant community interactions to marsh topography are part of what drives the effects being studied. In examining the proposed five factors, both the influence of plant communities and the drivers of plant community development in the salt marsh are being reviewed indirectly.

Histories

The marsh areas under study have different histories. The salt marshes of the Delaware Bay were dissected by mosquito control ditches dug in the 1930's by the Civilian Conservation Corp. Areas were impounded in the 1950's and 1960's to provide habitat for waterfowl and some areas were historically used for salt hay farming. About 4% of the tidal wetlands along the Delaware Bay have been filled for residential, commercial or industrial uses since 1950. This low rate (about 0.1% per year) of loss is associated with limited human population below the Delaware Memorial Bridge and large amounts of wetlands held in public and private preserves (Sullivan et al., 1991).

The Delaware Inland Bays have in excess of 6,573 acres of tidal wetlands (Weston, Inc., 1992). Over 2,000 acres were lost from 1938 – 1973 (Weston, Inc., 1992). Natural losses are attributed to sea level rise, natural succession, the hydrologic cycle, erosion, sedimentation and fire. Human induced losses are attributed to drainage and channelization, filling for development, dredging, pond construction, timber harvesting, and water pollution and waste disposal (Tiner, 1985).

The Albemarle-Pamlico Sound is the largest sound formed behind barrier beaches on the East Coast (Stanley, 1993). Although the region is relatively undeveloped, human activities such as draining, dredging and filling in connection with agriculture, housing development and forestry still change the marshes (Stanley, 1993). In 1962, there were an estimated 4,897 hectares of salt marsh in Pamlico Sound and none in Albemarle Sound (Wilson, 1962). There are eight times as many acres of nontidal and brackish marshes as salt marshes in Pamlico Sound. Large areas of marsh were previously altered by mosquito ditches and creating impoundments for waterfowl. A moratorium on

ditching has been in place and future losses from direct human impacts should be minimal (Kuenzler and Marshall, 1973; Steel, 1991).

The different histories for each of these areas will cause differences in outcomes as to rates and locality of marsh loss. However, by averaging data from the entire East Coast, the general trends will be isolated and impact of the individual histories will be lessened in the aggregation.

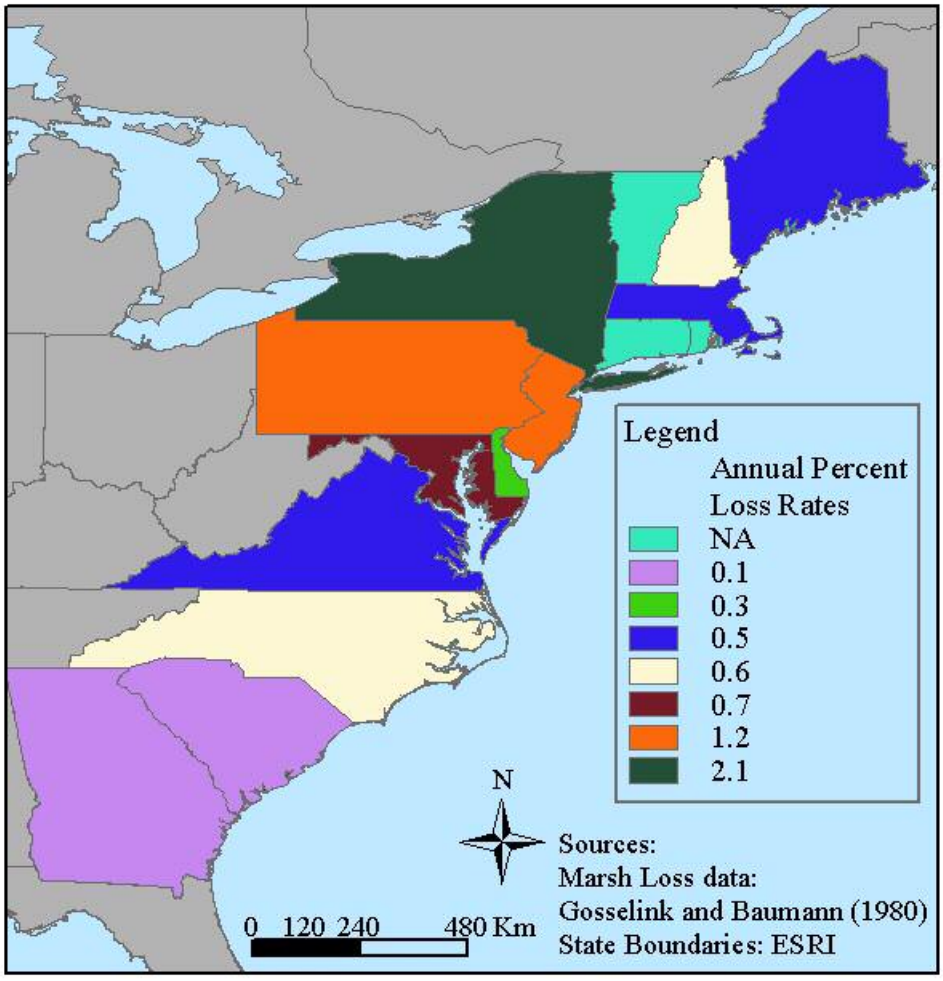

Figure 1. Variations in Annual Marsh Loss Rates along the East Coast.

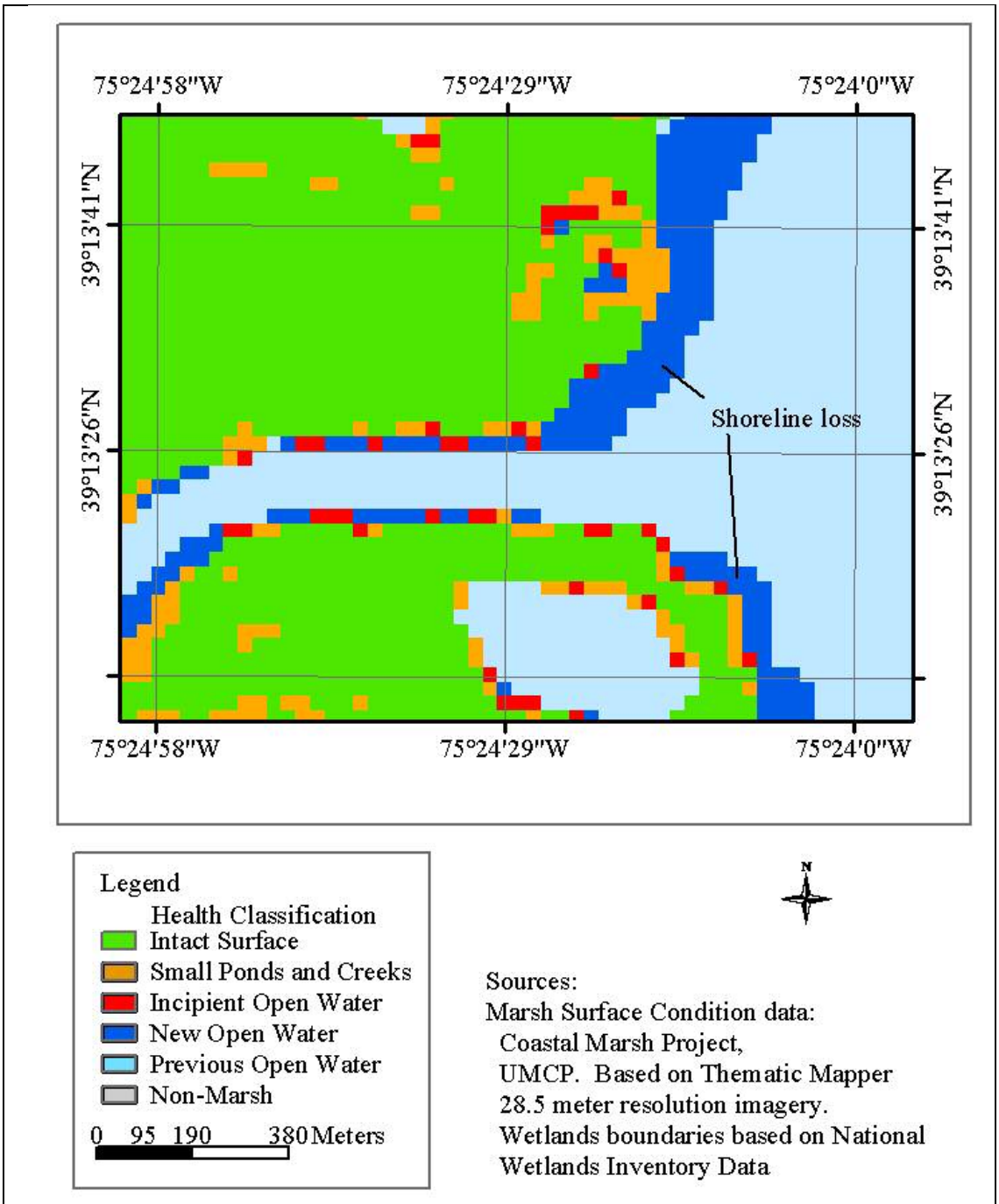

Figure 2. Shoreline Erosion

This figure shows erosion along the western shore of the Delaware Bay.

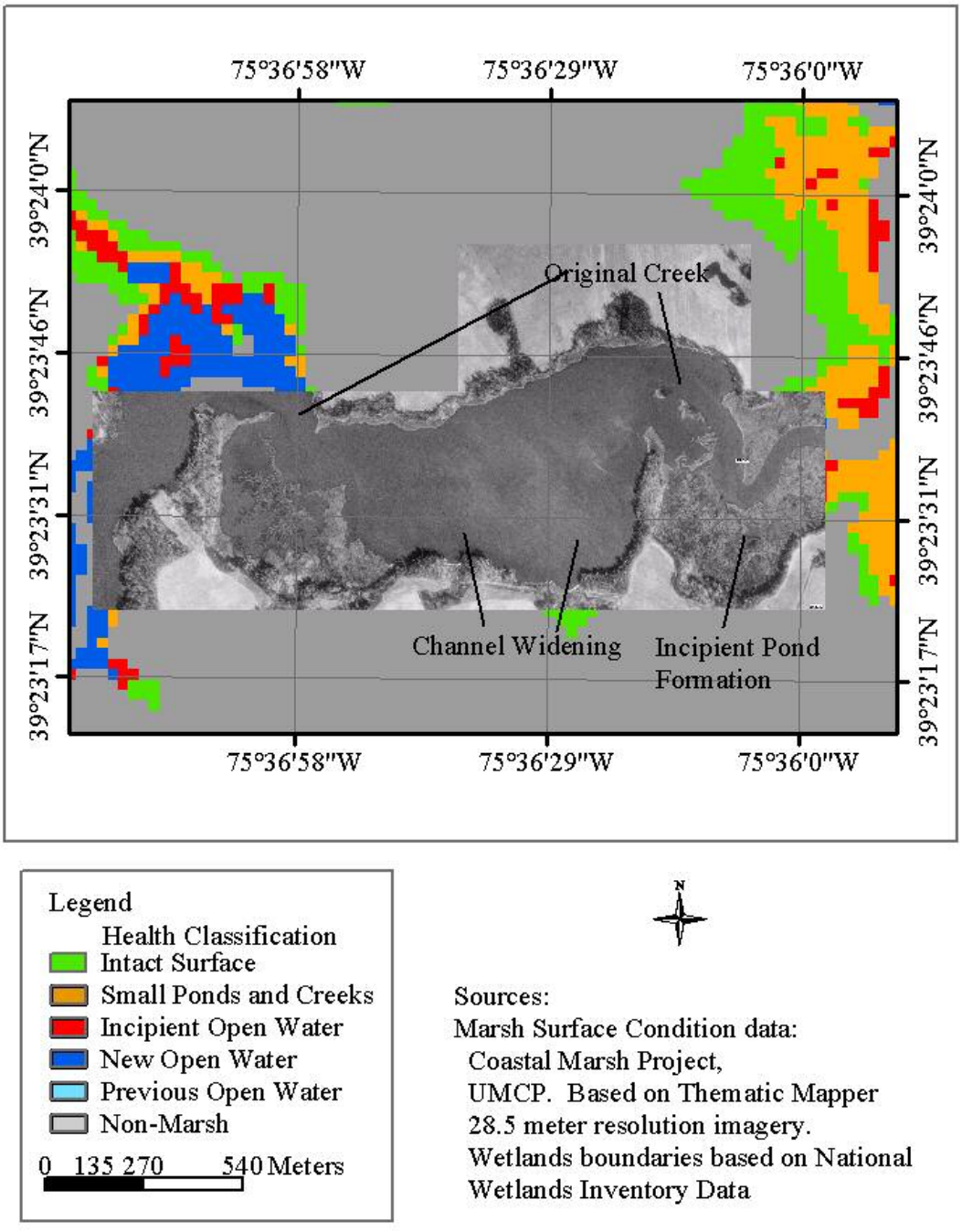

Figure 3. Tidal Creek Widening

The gray-scale is a March, 1992, aerial photograph of the area. The picture shows how the CMP data relates to areas of change in the photograph.

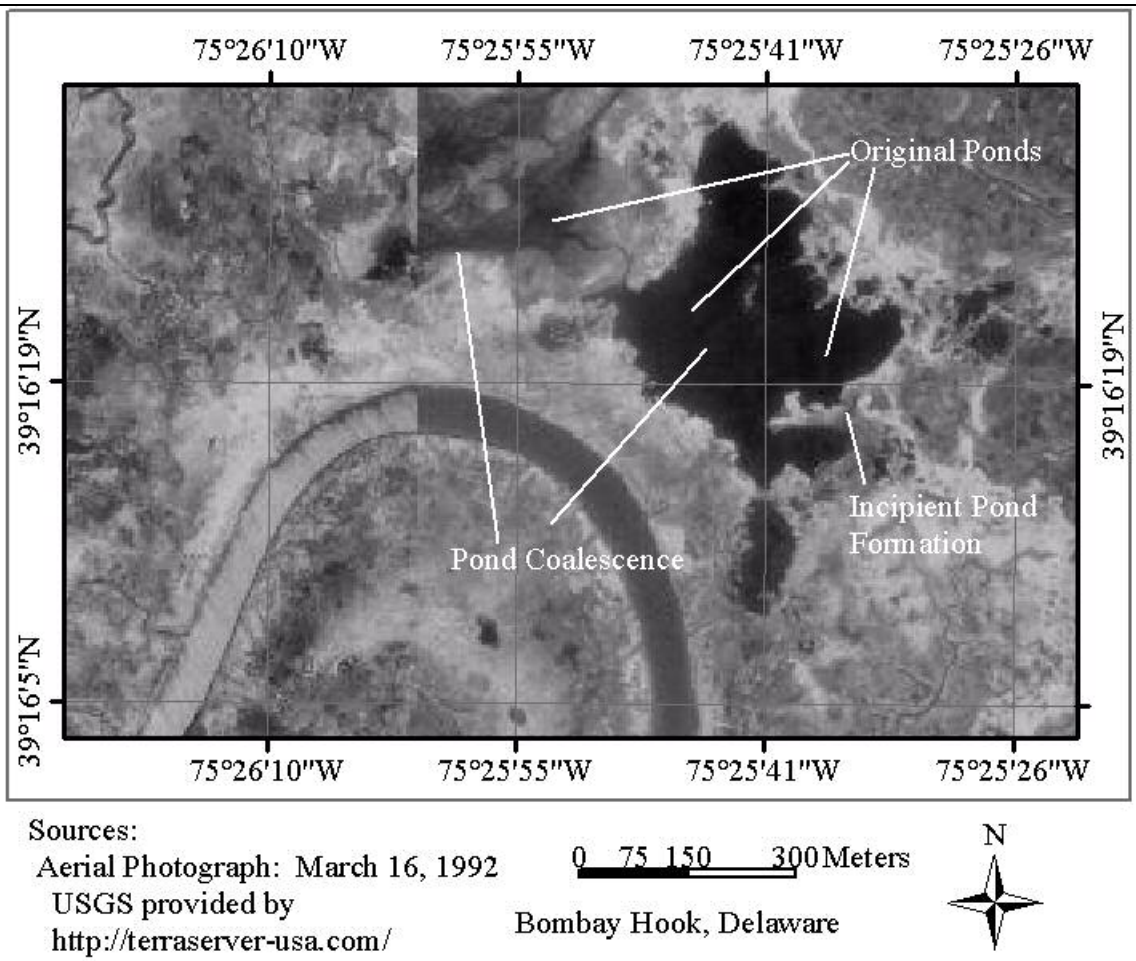

Figure 4. Pond Expansion.

This figure shows the current area of some ponds in Bombay Hook, Delaware. The Coastal Marsh Project analysis of the same area is shown in Figure 5. The light blue areas in Figure 5 show the area of the ponds at the time of the NWI.

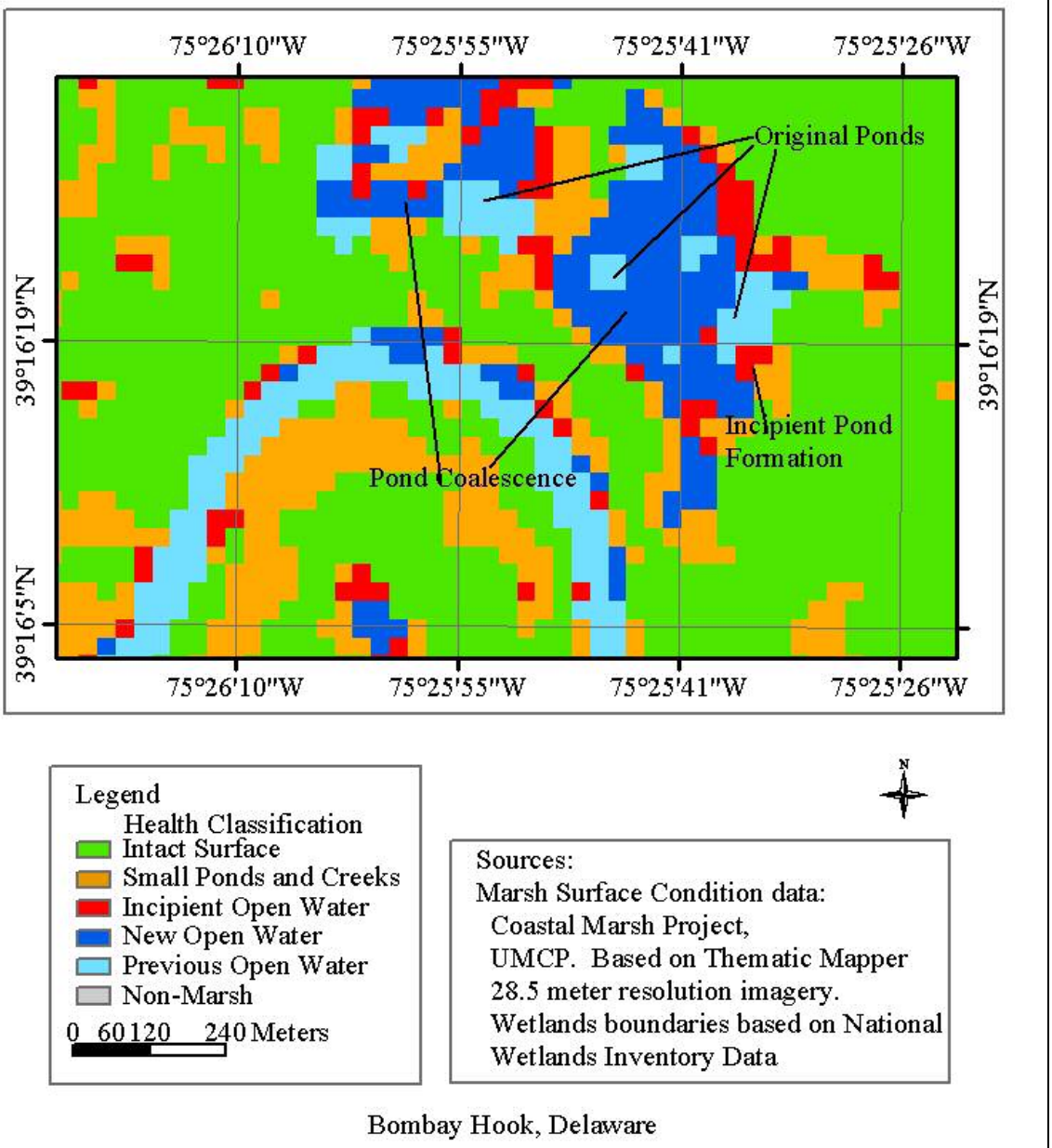

Figure 5. Pond Growth Seen in Coastal Marsh Project Data.

This is the same area shown in Figure 4. The growth of ponds and appearance of new ponds can be identified as shown by the arrows in Figure 5.

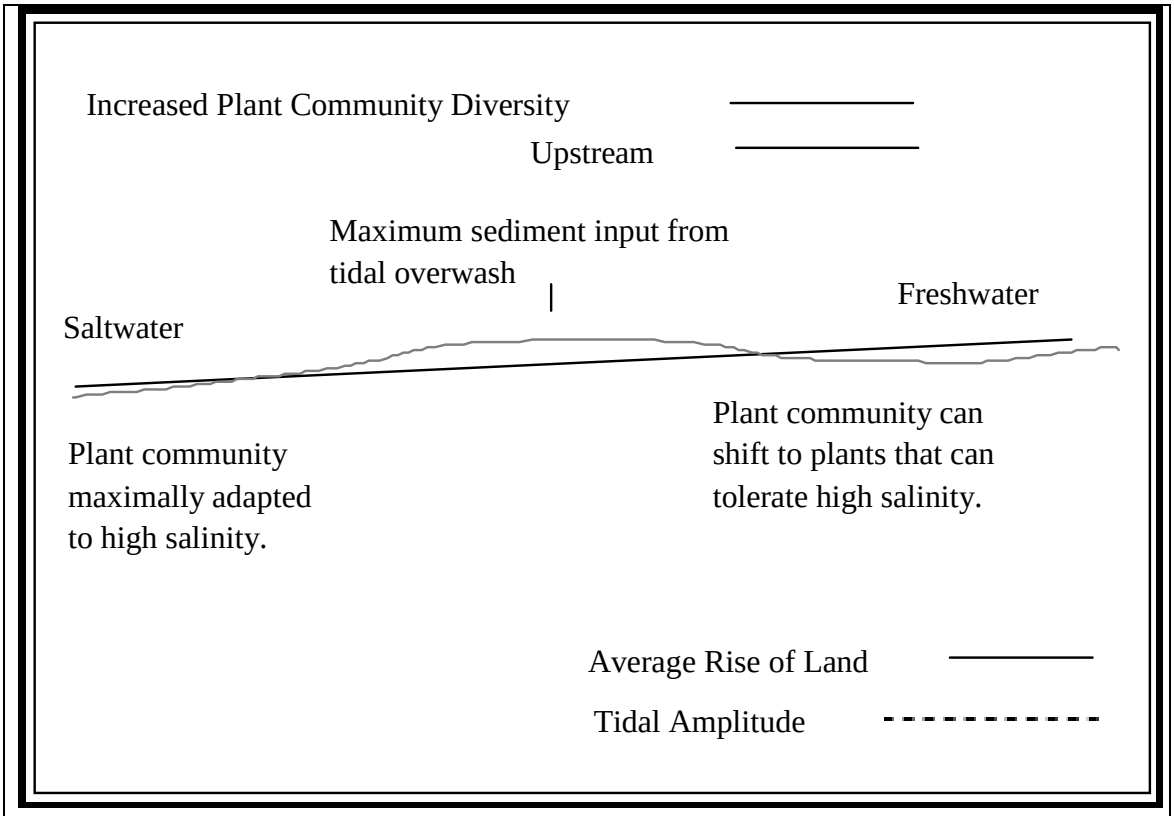

Figure 6. Changing Impact of Sea Level Rise along a River.

This picture is only an example. The maximum tide could be in other places along the system, including the freshwater portion.

Chapter 3 Remote Sensing:

Problems in Assessing the Risk of Loss

The Need for a Remote Sensing Method

Marsh loss has been shown to occur through the processes of pond formation and growth, tidal creek expansion and shoreline erosion discussed above. These processes produce distinctive large and small-scale physical changes in the marsh surface (Kearney and Stevenson, 1989). Based on the different stages of marsh loss, Kearney et al. (1988) developed a marsh surface condition index (MSCI) to classify marshes in the Nanticoke River estuary according to their degree of degradation. This classification recognized five categories of marsh surface condition ranging from intact "healthy" marsh to completely degraded marshes (essentially open water). Assessing whether a marsh belongs in one category or another is based on the presence, relative location, and number of key attributes that are generally identifiable on high quality aerial photographs (preferably large-scale color photography). Although several of the intermediate categories employ tonal or textural characteristics, this method relies on gross pattern recognition and, thus, determining the absolute size or position of the individual features is neither fundamental nor critical. It avoids one of the major pitfalls of conventional change detection approaches that inherently rely on a high degree of planimetric precision: inaccurate registration of base points between different generations of images. However, aerial photography is very expensive to update despite its advantages in terms of accuracy and ability to record species differences (Rice et al., 2000).

Satellite data are available on a regular schedule at a comparatively moderate price. This MSCI does not work well with Thematic Mapper (TM) satellite imagery, however. The visual analysis is time-consuming and susceptible to interpreter bias. More importantly, from the perspective of marsh conservation, purely visual inspection of TM imagery, which lacks the detail of large-scale aerial photography, generally cannot detect reliably the very earliest stages of marsh loss when remediation efforts may be most successful.

Spatial limitations of field-work based studies

Most studies of marsh loss and related topics such as vertical accretion rates, examine only small areas, even if the individual plots are spread over a wide area. Gross et al. (1993), for example, studied above-ground and below-ground *Spartina alterniflora* biomass production at five sites scattered from Nova Scotia to Georgia. For many other studies, sample sizes ranged from 2 to 27 sites with study areas ranging from 20 meters to 100 km. (Bricker-Urso et al., 1989; Craft and Broome, 1993; Dame and Childers, 1992; Esselink et al., 1998; French and Spencer, 1993; Hatton et al., 1983; Halupa and Howes, 1995; Hutchinson et al., 1995; Kaye and Barghoorn, 1964; Ke et al., 1994; Kearney et al., 1988; Kearney et al., 1994; Kelley et al., 1995; Kokot, 1997; Leonard et al., 1995; Morrison et al., 1990, 1990; Murray and Spencer, 1997; Netto and Lana, 1997; Nyman et al., 1995; Orson et al., 1990; Orson and Howes, 1992; Osgood and Santos, 1995; Pethick, 1981; Ramsey et al., 1997a; Van der Molen, 1997; Wang at al., 1993; Wray et al., 1995). The small size of these studies is appropriate because it is a scale on which humans can make detailed measurements of chemistry, current velocities, sedimentation rates and

other parameters. However, it is difficult to integrate the data across larger areas, in part because the parameters measured can fluctuate widely over small distances (Rogers, unpublished data). Using such data, and the numerous data points collected by other researchers, does not lend itself to aggregation of losses and reliable estimation of losses in areas not sampled. Moreover, the rapidity of marsh loss processes in its later stages (cf. Kearney et al., 1988), even for those areas for which relatively recent information is available, can quickly make site investigations and aerial photography data outdated.

Updating the status of marsh condition involves organizing and conducting new and often time-consuming field or aerial surveys. Moreover, because the data derived in this manner is generally not immediately amenable to digital analysis, incorporation in broader synoptic assessments of coastal marsh change can involve further lengthy processing. For many areas, such as the Atlantic coastline where there are hundreds of thousands of hectares of marsh, the scale of such a task is clearly daunting.

Only two studies, the CoastWatch Change Analysis Program (C-CAP) program (NOAA) and the National Wetlands Inventory done by the U.S. Fish and Wildlife Service, are comparable in size to the output of this project – they are both, in fact, much larger, and are the subject of debate. Both of these are extremely labor intensive requiring 1000's of person-hours to accomplish. As late as 1994, it was stated, "The CoastWatch program will be national in scope and require ... many agencies and investigators ..." (Civco et al., 1994). Therefore, a study comprising the area used here has never been undertaken with the ease and repeatability of this study.

Image Analysis

Remotely sensed data are difficult to interpret, especially in areas where the pixels are likely to be highly mixed composites of surface types (Mathieu et al., 1994; Foody and Cox, 1994; Huete, 1986). In most marshes, there is vegetation of various types, bare soil and open water in various size patches mixed heterogeneously. At any site, for example, surface water may be visible between the shoots of emergent, erectophile vegetation, or may occur in large open ponds or creeks. At larger scales, patches of vegetation may vary in size from a few meters to several hectares.

Mixture modeling has the potential to recover actual percent coverages despite this complexity (Mathieu et al. 1994; Foody and Cox, 1994). Nevertheless, mixture modeling has certain inherent limitations. Traditionally, a linear model is assumed, but a linear combination of spectra does not necessarily reproduce measured composite scene spectra (Borel and Gerstl, 1994).

Linear mixture modeling is based on certain assumptions. The most important assumption is that the signal received at the satellite from any ground parcel is simply the additive sum of the reflectances of all the surface covers in the parcel, weighted by the fraction of the parcel occupied by each surface cover. The standard linear mixture model for three endmembers and three spectral bands may be represented as:

Equation 1.

$R_i = \sum \rho_{ij} f_j + e_i$, summed from j = 1 to n.

where n is the number of bands, ρ_{ij} represents the reflectance of surface cover type j in band i, f represents the fraction of the pixel covered by cover type j and e

represents random error in band i. The following restrictions are assumed in linear mixture modeling:

1) Any pixel on the ground is made up of a composite of spectrally pure cover types - the spectra of these cover types are used as endmembers in the analysis.

2) The signal received at the satellite is the linear, weighted sum of the radiances from each cover type in the pixel.

3) The percent of the pixel that each cover type occupies can be recovered by inverting Equation 1 and solving for each f_j.

4) The number of endmembers cannot exceed the number of spectral bands used.

5) All the f_j's must sum to one.

6) $0 < f_j < 1$ for all f_j's.

To make sense, the endmembers must be selected from the boundary of the data space (Mathieu-Marni et al. 1996) and must be consistently in the same place.

Analysis of remotely sensed images is often done by a classification scheme that assigns a single cover type to each pixel or polygon in an output map. In a supervised classification, spectral signatures are developed by having an analyst choose pixels in the satellite image that contain the feature of interest. The computer then generates a signature for that cover type. In unsupervised classification, the computer analyzes the image and breaks it into spectral classes. In either supervised or unsupervised classification, once the spectral signatures are calculated, every pixel in the scene is tested to determine which spectra it matches most closely.

Mixture analysis techniques, in contrast to traditional classification systems, can assign more than one value to a pixel. Most pixels are mixtures of various surface covers

(Huete, 1986) and mixture modeling attempts to calculate the fractional covers. Donoghue et al. (1994) compared linear unmixing and maximum likelihood classification (MLC) and found that both were 90% accurate in delimiting the intertidal vegetation. While both produced poorer results in the intertidal zone, linear unmixing proved better able to map pioneer vegetation such as *Spartina anglica* and *Salicornia fragilis* than the MLC.

Mixture models and classification procedures often have serious inherent flaws. They are not reproducible across scenes, and they cannot properly interpret the sometimes excessive number of soil and vegetation endmembers present in a scene (Smith et al., 1994; Williamson et al., 1994) nor do they include non-linear scattering (Borel and Gerstl, 1994). To overcome the high variability inherent in scenes, the tendency in many efforts is toward more complexity in the models (e.g., Roberts et al., 1993). This approach can only work to the extent that the inputs are linear and there are no more actual endmembers than input independent data channels.

Typical mixture modeling is based on the assumptions of linearity outlined above (Fung and LeDrew, 1987; Bierwirth et al., 1990a,b; Gong et al., 1991; Mackin et al., 1990; Holben and Shimabukuro, 1993; Roberts et al., 1993; Settle and Drake, 1993; Cherchali and Flouzat, 1994; Foody and Cox, 1994; Puyou-Lacassies et al., 1994; Smith et al., 1994; Williamson, 1994; Mathieu-Marni et al.,1996a,b). Most of these authors and others (Harsanyi and Chein, 1994) rely on rotating the data matrices and scene-by scene ground referencing to improve reliability. Obviously, scene-by scene collection of ground reference data reduces the utility of remote sensing to some degree.

Selection of endmembers

Endmembers are the required spectral endpoints for unmixing multispectral data. There are four general methods for obtaining them. Spectra can be : 1) collected in a laboratory setting (Bierwirth, 1990a,b); 2) collected in the field; 3) extracted from the image to be unmixed (Cherchali and Flouzat, 1994; Gong et al., 1991; Mackin et al (1990); Puyou-Lacassies et al., 1994); 4) derived, for example, by Varimax rotation of the principal components (Mathieu-Marni et al., 1996 a, b). These can also be combined. Williamson (1994) used PCA, the spectral distribution of the data and ground reference data to select endmembers.

Novo and Shimabukuro (1994) derived spectra in the field for their three endmembers (using a Spectron SE590); however, the endmembers chosen are spectrally similar being chlorophyll a, DOM (Dissolved organic material) and TSS (total suspended solids). They state that, although there were confounding factors at each station used for a pure endmember, they did not use laboratory spectra because such spectra for phytoplankton suspensions typically do not match field spectra. Spectra were analyzed over the range from 400 - 800 nm, and then by analyzing the fractions and residuals from unmixing their data, they refined the spectral regions needed to produce the best results. Then they developed a regression equation between the model data and measured concentrations of their three endmembers. This method is essentially the same as using image-derived data since the SE590 data was what they analyzed.

Although endmembers gathered in a laboratory offer assurance of consistency and accuracy, there is no assurance that they represent endmembers as defined in the spectral space of the image (Gong et al., 1991; Smith et al., 1990a, b). Moreover, there is also no

assurance that they match the spectra of real objects in the environment despite the fact that those object may be made of the same material (Bierwirth, 1990a). However, for distinguishing between spectrally similar targets, such as various soil types, it has the advantage over image-derived spectra of providing the ability to resolve closely related spectra. Image or laboratory derived spectra, to be reliable across scenes, require standardization of the scenes with radiometric and atmospheric correction. Laboratory-derived spectra have the additional limitation of narrowing the variance associated with the cover type sought, perhaps eliminating marginal areas inappropriately. Endmembers selected from the image itself are more likely to represent true endmembers, take into account the natural variability of the endmembers and the conditions under which they are found, but may not actually represent any given physical material such as could be identified in the laboratory. Nonetheless, regardless of the method by which the spectra are derived, ultimately ground referencing is required.

For the purposes of the research only interested in three surface covers – soil, water and vegetation – are of interest. These spectra are quite diverse and well known (Richards, 1986). The water and vegetation endmembers are readily distinguishable by a variety of methods including finding relatively pure training sites in the image and locating them at predictable places in plots of various spectral bands.

Pixels representing bare soil are also easily identified in the image, although identifying them in a spectral plot is not simple. There are several reasons for this. The spectra of soils, although consistent in shape, can vary considerably in brightness. For instance, the organic soils of the Delmarva Peninsula and sand in South Carolina both

exhibit a monotonic increase from Band 1 through Band 5 although the sand is extremely bright and the organic soils are not.

Another complication is that senesced vegetation can look a lot like soil. Gausman et al. (1975) plot the spectra of crop residues and soils. The soils and residues have very similar spectra, and the crop residue is very dissimilar to live plant. In another study, crop residues and soils were found to be spectrally similar, only differing in their amplitude at given wavelengths. In fact, wavelengths around 2100 nm were required to distinguish crop residue from soil reliably, due to a cellulose/lignin absorption feature at that wavelength. This is much farther into the IR than the NDX bands (Daughtry, 2001). If separating senesced vegetation from soil were necessary for this project, this would be a good wavelength to use. However, that separation is unnecessary here.

This could cause confusion, except that for this project there is little consequential difference between dead plants and soil. The main point of interest being that neither is water. In both PCA space and raw spectral space, there is no single endmember that captures soil effectively. When spectral endmembers from one scene were applied to different scenes of the same area (Wingate, MD) the results were at least reasonable, even though somewhat noisy. The same endmembers applied to South Carolina, however, made the entire North Inlet marsh system appear to be open water. With ground reference data in hand and considerable effort, a soil endmember was finally located in the South Carolina image that produced correct results. Nonetheless, this hardly describes a method that can be used by others. In fact, when several different people attempted to select a soil endmember from diverse scenes using PCA, the results were extremely disappointing. One would expect a good correlation between the spectra

derived from PCA in different scenes; however, in some cases they were negatively correlated with each other. In addition, the PCA plots featured other pixels as the endmembers, not soil.

Laboratory spectra can be ruled out due to the lack of a reliable water spectrum (Kirk, 1994), and because an inordinate number of soil spectra would be required to cover all the soil types encountered in this research work. PCA-derived endmembers are not of much use due to the low likelihood of selecting an actual soil endmember – and, again, the large number of soil spectra that would be required. Vegetation ratio indices such as the normalized difference vegetation index (NDVI) rely on the soil line in plots of red vs. infrared reflectance. Because most soil spectra fall on or near this line and the intercept of the line is close to zero, a wide range of soils will have nearly identical NDVI values (Huete, 1989).

The New Technique

The technique used here is a hybrid of traditional classification and mixture model analysis. Although the resulting classification is a single value for each pixel, the classification is based on using mixture modeling to calculate the percentage water in the pixel rather than statistical or quasi-statistical manipulations of the spectral data – for example, maximum likelihood classification or clustering techniques.

The power of the technique is based, not on complex mathematical or image assessment techniques, but on simplifying the task of the remote sensing to the extent possible. The current work focuses on a single parameter - the percentage of water in a pixel rather than a variety of issues such as plant health or community structure. Because

there is no intention to differentiate plant species or soil types, the remote sensing model can be greatly simplified. It is similar to some of the mixture modeling techniques, shown above, which are reasonably accurate. However, the current technique is less affected by the variability of soil, water and vegetation spectral responses than a simple linear model.

The analysis is further simplified by conversion of the data space so that there are mathematically only three endmembers. Automation is possible because it is not necessary to extract endmembers from each image, nor are large banks of spectral endmembers that might be present in the image necessary. One set of three endmembers can be used with all images to unmix coastal marshes (Rogers and Kearney, 2004). .

The technique relies on high-quality atmospheric correction (Fallah-Adl et al., 1996; Liang et al., 1997; Donoghue et al., 1994) and the use of spectral indices similar to the Normalized Difference Vegetation Index (NDVI). Although normalized differences are used for vegetation mapping (e.g. Baret and Guyot, 1991) and have been used for water mapping (McFeeters, 1996), spectral indices have not been used in a mixture model analysis previously.

The transformed indices (Kearney et al., 2002; Rogers and Kearney, 2004) are calculated as follows for the Normalized Difference Water Index (NDWI), Normalized Difference Vegetation Index (NDVI) and the Normalized Difference Soil Index (NDSI):

Equation 2. NDWI

NDWI = (Band3 - Band5) / (Band3 + Band5)

Equation 3. NDVI

NDVI = (Band4 - Band3) / (Band4 + Band3)

Equation 4. NDSI

NDSI = (Band5 - Band4) / (Band5 + Band4).

All bands refer to Thematic Mapper band numbers. These bands represent reflectance ranges of 630 - 690 nm (Band 3), 760 - 900 nm (Band 4) and 1,550 – 1,750 nm (Band 5). Because the technique relies on several normalized difference indices, it is referred to hereafter as the NDXI technique.

This transformation redistributes the data points so that NDWI places surface covers that are brighter in Band 3 than Band 5 at the top of the scale. The NDSI and NDVI behave similarly for band pairs 5 and 4, and 4 and 3, respectively. Because of the characteristics of surface reflectance, this will normally result in soil-dominated pixels having the highest values on the NDSI, green vegetation-dominated pixels having the highest values on the NDVI, and water-dominated pixels having the highest values on the NDWI. Non-photosynthetic or senesced vegetation may be confused with soil and a few soils maybe confused with vegetation. However, as the purpose of this process is to separate water from everything else, potential confusion of the vegetation and soil endmembers is expected to have limited impact on the overall model. The resulting indices are then unmixed using the principles of linear unmixing already described.

The output of this remote sensing technique is the input for the risk model.

Various Issues with the NDXI Technique

Normalized Difference Indexes

Quarmby et al. (1992) state that the NDVI cannot be used in a mixture model because, being a ratio, it violates the assumptions of mixture modeling. Principally, it is

not expected to scale with changing area. However, tests with real data have shown that it does scale with changes in area (see Rogers and Kearney, 2004). On the other hand, randomly assigned pixel values do not produce normalized difference indices that scale when averaged over different areas. This would indicate that the NDXI technique measures real properties of the surface, and that the real properties are fractional coverages of the various scene components. The NDVI has been shown to be functionally related to absorbed photosynthetically active radiation (Asrar, 1984; Sellers 1985, 1987), which is of interest in global vegetation studies. The NDVI is used for global vegetation monitoring because it helps compensate for changing illumination, surface slope and other extraneous factors (Lillesand and Kiefer, 1994).

Consider the case for water:

In a pool of infinitely deep, uniform water, the illumination at any depth would be given by

Equation 5.

$I_z = I_0 * e^{-kz}$, where z = depth and k is the extinction coefficient

The backscattered irradiance from a layer at any depth would be

ρI_z

where ρ is the reflectance of a thin layer.

The upwelling light just below surface from a layer at depth z would be:

Equation 6.

$I_s = \rho I_z * e^{-kz}$

and the total upwelling light just below the surface from the entire water column for a particular wavelength is then

Equation 7.

$$R = \int_0^z \rho I_0 e^{-2kz} dz$$

or

Equation 8.

$$R = \rho I_0 (e^{-2kz} - e^0) / (-2k)$$

or

Equation 9.

$$R = \rho I_0 (1 - e^{-2kz}) / 2k .$$

For an infinitely deep pool, e-2kz -> 0.

Therefore,

Equation 10.

$$R = \rho I_0 / 2k .$$

Putting this into the normalized difference form,

Equation 11.

$$NDXI = (R_1 - R_2) / (R_1 + R_2)$$

and assuming that the incident radiation has been corrected for atmospheric haze and illumination angle, gives:

Equation 12.

$$NDXI = (\rho_1 I_1 - \rho_2 I_2) / (\rho_1 I_1 + \rho_2 I_2)$$

which, for pure water, is a constant. This research, of course, deals with estuarine water, which is more variable.

The above calculations ignore the effects of the light entering the water and leaving the water. For the moment, we will assume that on average this is constant as well. In Equation 12, the below surface upwards radiance is for a point. If each of the radiances were integrated over an area, the area would simply cancel. The same basic logic would also apply to pixels of pure, homogeneous vegetation or pure, homogeneous soil. Further, for mixtures of soil, vegetation and water the radiance in each pixel for one band would be

Equation 13.

$$TotalArea * R = TotalArea * \sum_0^n f_i \rho_i$$

where n is the number of surface cover types. In the normalized difference, the TotalArea would again divide out.

Several factors may affect the reflectance. Among these are the non-Lambertian properties of leaves, soil and water. The resulting anisotropic reflectance function is called the bidirectional reflectance distribution function (BRDF). For TM data, the change in view angle on each sensor sweep is about 7.5 degrees off nadir. According to Myneni and Asrar (1994), the change in top of the atmosphere NDVI over this range of view angles is negligible.

Secondly, the solar zenith angle will affect both the irradiance and the refraction/reflectance of light at the surface. The atmospheric correction algorithm compensates for the changes in irradiance on a seasonal and latitudinal basis. The

Fresnell equation and Snell's law predict how much light will be reflected and how strongly the light that does penetrate the surface will be refracted (Ingle and Crouch, 1988). The solar angle for latitudes of interest in this work will vary between 30 and 48 degrees during the late spring to early autumn time frame of the images used. This will cause a change of approximately 30% in surface reflection and approximately 1% decrease in transmission into the body of water. Because most of the reflection will be specular[2], it will not enter into the satellite sensor's field of view. The 1% change in transmission into the water will not cause a significant change in upwelling light.

The depth of the water and bottom reflectance will also affect the results. The above calculations hold for infinitely deep water, so the question arises: How deep does the water have to be before it can be considered to be of infinite optical depth? Given that the TM data are quantized as eight bits, the smallest change detectable would be 1/256 of the reflected radiation. Any change in reflectance smaller than that amount will not be recordable. For the three TM bands used in the NDXI technique, the "infinite" depths are calculated based on where the e^{-2kz} term falls below 1/256 of the reflected radiation using the data in Table 1. Using values of 10%, 50% and 30% (estimated from Townshend et al., 1988) as the reflectance values for Bands 3, 4 and 5 respectively, gives the values in the "Infinite depth" column of Table 1.

Pure water was used for Bands 4 and 5 because measurements of absorption in estuarine waters at those wavelengths are unavailable, for the obvious reason that not

---

[2] Specular reflection occurs when the angle of reflectance of a ray of light from a surface equals its angle of incidence. A mirror is a specular reflector.

much light is returned. For these bands, bottom reflectance will only be a factor in Band 3 and of some consequence in Band 4. For Band 5, however, by the time a body of water gets as shallow as 3 μ it is, arguably, not a body of water any more. What this means is that for shallow, clear water, there will be a bottom reflectance component in Band 3. For the three indices chosen, Band 3 – Band 5, Band 4 – Band 5 and Band 3- Band 4, this will only affect the NDWI signal. The key to the NDWI signal is that it interprets surface covers that are brighter in Band 3 than Band 5 as being water. If the water were more algae or sediment laden, Band 3 would be brighter than Band 5. If the water is perfectly clear in a pixel, Band 3 will be brighter than Band 5. The calibration will be different for these two cases, but the overall effect should be that water will look like water.

Table 1. Absorption Properties of Water at Various Wavelengths

Lambda (nm)	absorption	Infinite depth (meters)	Thematic Mapper Band	λ(nm)	Water Type	Source
650	0.5 / m 3	8	Band 3	630 - 690	Estuarine water	Prieur and Sathyendranath, 1981
760	0.0256 / cm	0.9	Band 4	760 - 900	Pure water	Shifrin, 1988
1500	10000 / cm	2 E-07	Band 5	1,550 – 1,750	Pure water	Shifrin, 1988

3 This extinction coefficient is for 1 gram chlorophyll a per cubic meter which is low for the Chesapeake Bay. (Rogers, 1994)

NDVI

The normalized difference vegetation index (NDVI) was developed based on the spectral response of vegetation in the red and NIR, specifically Bands 1 (0.58 - 0.68µ) and 2 (0.725 - 1.1 µ) of NOAA's Advanced Very High Resolution Radiometer (AVHRR). The index is defined as (NIR - Red) / (NIR + Red), where NIR equals the reflectance of the surface being measured in the near infrared and Red is the reflectance in the red region of the spectrum. The reflectance of vegetation in these spectral regions is dominated by two factors. The reflectance is very low in the red region due to absorption by chlorophyll (Gates et al., 1965). Reflectance in the NIR is dominated by scattering from the interfaces between cell walls and air spaces in the leaf (Peterson and Running, 1989; Gausman et al., 1969). Leaf reflectance spectra are also affected by water absorption bands and other properties, but these are either not within the spectral range of interest here or are of less significance than the chlorophyll absorption and mesophyll (Walter-Shea et al., 1992) scattering. For instance, leaf NIR optical properties are little affected by pigments (Maas and Dunlap, 1989). However, leaf water content may directly affect NIR scattering. As leaves lose water, this reduces cell turgor, which can affect the relative cell surface, intracellular air spaces, and consequently reduce NIR reflectance (Levitt and Ben Zaken, 1975).

Separating Plant and Algae-Laden Water Signals

Because green plant reflectance in the IR is dominated by structure of the plant, there is no corresponding increase in water reflectance even at high algal concentrations. The reflectance of water in the IR is dominated by the absorption of water and the particulate load (Tyler and Stumpf, 1989) and although there is an increase in reflectance associated with increased particulate counts in the water, it is unlikely ever to exceed the reflectance of the same water body in the red region.

Figure 7 shows calibrated radiances for nine locations in the Patuxent River collected in June 1992, by the author. It is not possible to calculate exact TM-comparable NDVI's for these without applying a spectral response function for the TM's sensors. However, an approximation can be obtained by summing across the spectral bands and ratioing the results. It can be seen (Table 2) that there is some variation in the NDVI based on the changes in the water column. If NDVI exclusively were used to extract results, this would pose a more serious problem. However, with three endmembers the water with higher sediment and/or algae concentrations will be shown not to be pure water when it is unmixed. It is obvious, however, that no matter how much algae is added to the water, it will not look like a mixture of vegetation and water. For NDXI, measurements are all made with Bands 3, 4 and 5. Bands 4 and 5 are well beyond the reflectance maximum of water containing chlorophyll a and its various derivatives and gelbstoffe (the combination of long-chain fulvic and humic acids that give natural water its yellow - brown color). The region between the absorption maxima of various photopigments is where the highest variability in water reflectance typically occurs (

Figure 7).

Effects of Tides and Rain

Field spectra are of great value in understanding the likely impact of various changes on the received spectrum. For example, Stutzer (1997) measured the changes in reflectance of wetland plants as water depth changed over the expected microtidal range in Blackwater National Wildlife Refuge and surrounding marshes as part of his work for the Coastal Marsh Project. The result showed that the 0 -10 % range of water in a vegetated area could not be differentiated from the 10 - 20% range, due to tidal fluctuations. However, tides in the microtidal range could not raise water levels high enough to make healthy vegetated areas look like they were moderately deteriorated (20 - 30% water),.

Endmembers

How accurate are the endmember spectra? Table 3 lists NDVI values for open water calculated from the two images. The mean values are at the low end of the range in Table 2, which are calculated from the spectra in

Figure 7. This means that the spectra represented in Table 2 with higher chlorophyll concentrations would be correctly unmixed as having other properties. These numbers are scaled 0 - 255, so the difference in means represented in Table 3 is about

2%. The number of replicate pixels makes it clear that we have captured the signature of water very reliably.

Table 4 shows the spectra for all three endmembers in both TM bands and normalized difference bands. The normalized difference transformation reduces the standard deviations in most cases. Spectra extracted from various scenes match well with published spectra (e.g., Richards, 1986).

General Improvement Over Standard Linear Unmixing:

The four panels of Figure 8 show spectral data from a computer-generated set of pixel values. The data actually comprises 7 spectrally distinct endmembers, three soils (red), two waters (blue) and two vegetations (green). The data was generated from three spectral bands representing the Thematic Mapper Bands 3, 4 and 5. A problem arises immediately in trying to interpret the data because there are only three bands of input data but seven spectral endmembers. One might think of adding extra TM bands to the data input, but this has severe limitations. There are only 7 bands in TM data, and there is information overlap between them (Townshend et al., 1988). Due to the variability of reflectances of different materials, this situation of having more spectral endmembers than input channels is liable to persist even with larger numbers of bands. Because there are only three spectral channels available, only three spectral endmembers can be assessed at one time.

In this case, two of the soil endmembers closely resemble each other, as do the pairs of vegetation and water endmember spectra. The problem can then be reduced to four endmembers. Standard linear mixture modeling still cannot cope with the number of

endmembers present in a typical scene. In fact, every endmember selection will be wrong (Figure 8).

If you select the actual endmembers on the graph, you will always get a wrong answer. For example, if the soil endmember on the upper right in the PCA plot were chosen, the soil endmember on the lower left would be unmixed as though it were some proportion of the upper right soil endmember. Similarly, the soil endmember in the middle of the Band 3, 4, 5 plot would show unmix as 50 percent soil using standard techniques.

The NDXI transformed data, however, are much better behaved. The water and vegetation endmembers do not get closer to each other, but the soil endmembers are now almost identical (Figure 8).

Table 2. Pseudo NDVIs Calculated for Spectra in

Figure 7.

Spectrum	Pseudo-NDVI
1	90.01136
2	82.9563
3	94.03216
4	93.00153
5	90.94593
6	96.68848
7	90.25289
8	76.38511
9	69.02303
	Mean 87.03
	Std. Dev. 9.129

Figure 8 Panels b, c and d compare the results of unmixing synthetic data with both a linear model and the NDX transformation. Based on this one might argue for the linear model. However, the strength of the NDX model is in its consistency. Table 5 shows this. The table shows the results of applying the same mixing algorithm to several 1000 pixels with randomly assigned fractional cover values. Although each unmixed dataset gives a strong linear relationship with the input fractional covers, for the linear

method the regression coefficients change significantly every time. The NDX coefficients remain relatively consistent. The pixels were mixed using a non-linear model with variation built-in.

Table 3. NDVI'S for Open Water From Images			
	Mean NDVI	Std. Dev.	n (samples)
Scene 1	75.1	1.48	376
Scene 2	70	2.1	2520

Table 4. NDXI values calculated from TM data.			
Cover Type	Channel	Mean	Standard Deviation
Water	3	43.08	3.04
	4	44.33	3.41
	5	21.27	1.62
	NDWI	167.35	2.08
	NDVI	126.71	2.48
	NDSI	81.07	1.72
Vegetation			
	3	39.6	0.89
	4	194.26	3.09
	5	92.29	2.64
	NDWI	75.12	1.48
	NDVI	207.76	1.00
	NDSI	80.49	1.62
Soil			
	3	67.33	13.74
	4	108.94	21.11
	5	163.39	31.21
	NDWI	72.94	1.13
	NDVI	154.72	1.24
	NDSI	150.11	0.46

Potential Problems with the Method

There are several potential problems with the technique used. Because the scene is converted so that there are only three endmembers, substances such as clouds, cloud-shadows, roads, and, in fact, everything will be placed somewhere in this spectral space. Because we operate on the assumption that the three endmembers represent soil, water and vegetation, other surface covers must be removed by other means. The National Wetlands Inventory (NWI) classified data are used to remove the non-marsh areas. Clouds and cloud-shadows are removed largely by hand. In areas for which there are multiple images, clouds and cloud shadows can also be removed by image overlays, replacing the bad pixels in one scene with clear pixels from another.

Table 5. Variations in output using computer-generated in input for PCA and normalized difference (NDX) transformations.

Method	Intercept	Slope	R-square
PCA	-18.047	1.13486	0.80
PCA	-64.417	1.385	0.89
PCA	-28.26	1.20489	0.83
NDX	20.499	0.7589	0.91
NDX	16.248	0.77568	0.90
NDX	16.0323	0.78364	0.90

This represents three scenes created randomly from standard inputs. Each scene was unmixed by the two different techniques and the results are shown here. The input data for all scenes were created using the same endmember spectra and randomization techniques for generating pixel values. The PCA output is quite different between scenes, whereas the NDXI values remain constant. All are scaled 0 - 255.

Secondly, although there should be no problem differentiating water from the other two endmembers in general, at the margins there are problems in assigning meaning to the interpretation. Particularly the cases of very shallow water vs. very wet mud, or

very sediment-laden water vs. very wet mud are problematic. IR radiation is highly absorbed by water, which is why the IR bands were chosen for the much of the work. This means that even in relatively shallow water bottom reflectance will not have much effect (because Band 3 will still be brighter than Band 5). However, as the water depth approaches zero, there will be a depth at which the underlying soil becomes very apparent, even in the IR. It is not yet clear how to separate this from the case of very wet mud.

Essentially, these two questions transcend the scope of image analysis, because neither is entirely clear from ground observations. One is, at what water depth should the surface classification change from wet mud to water over sediment? The second is, what is the proportion of water: sediment at which the change from mud to sediment-laden water occurs? Because of this, an arbitrary cutoff was used that excluded areas featuring less than 10% vegetation and more soil than water.

Remote Sensing Validation:

Several of the authors combined data sources in a GIS (Donoghue et al., 1994; Hinson et al., 1994; Ramsey and Laine, 1997). Ramsey and Laine (1997) combined aerial photography with TM data as a means of validating the TM. They found that the TM classifications were 77 - 81 % accurate, but performed poorly in change analysis of a complex marsh system. Hinson et al. (1994) compared the use of ground reference data with NWI data as a means of assessing the accuracy of remotely sensed image classification. They found that ground reference data always gave a higher accuracy for

the image analysis than was found from comparing the imagery directly to the NWI. NWI data are used in the current study to classify the marsh, not assess the results.

Legend for Figure 7	
Color	Line
	1
	2
	3
	4
	5
	6
	7
	8
	9

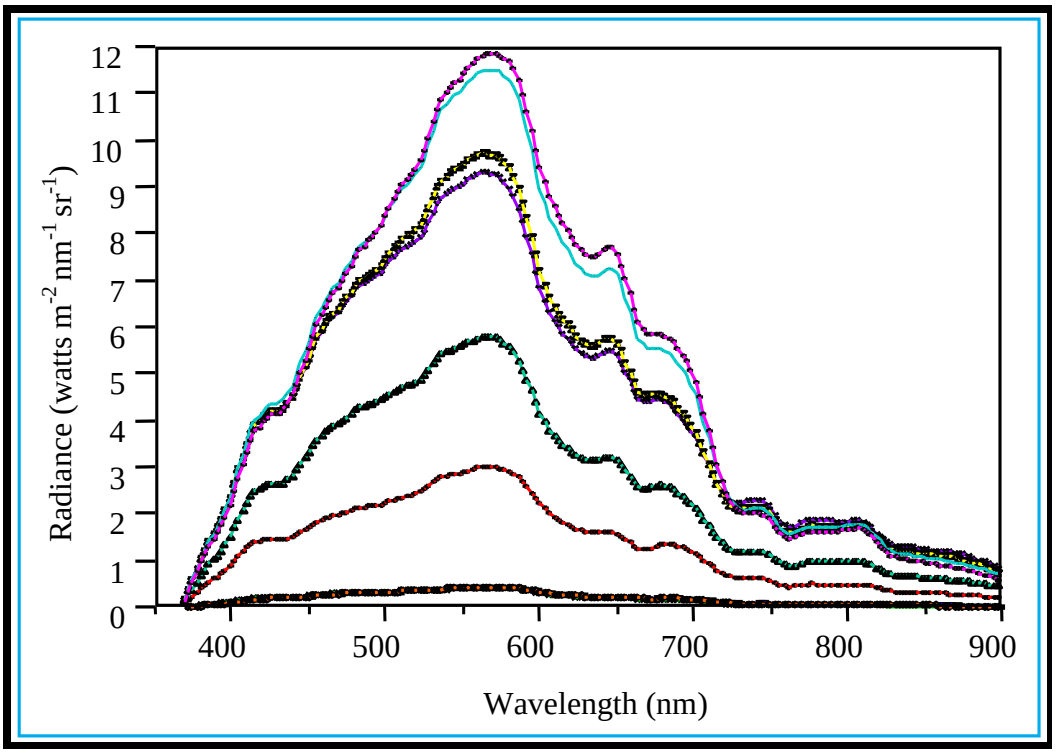
Radiance (watts m-2 nm-1 sr-1)
0
1
2
3
4
5
6
7
8
9
10
11
12
400
500
600
700
800
900
Wavelength (nm)

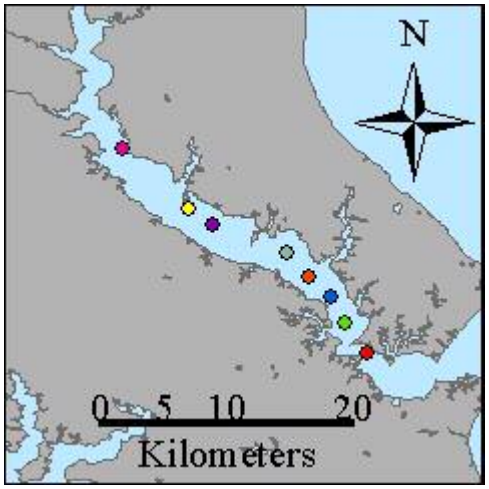
N
0 5 10 20
Kilometers

Figure 7. Patuxent River Spectra (June 2, 1992)

The curves represent different hyperspectral scans of the Patuxent River collected with an SE590 scanning spectrometer mounted on a boom on a boat, approximately 1 meter above the water. Point 8 is missing from the map.

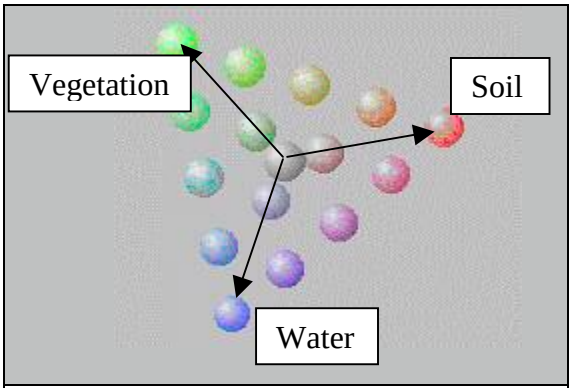

Panel a. The actual fractions of soil, water and vegetation in each pixel. A perfect unmixing of the data would look exactly like this, and, in fact, this diagram is what all unmixing algorithms are based on for three endmembers. Each point in this graphic represents two or three different combinations of the spectral endmembers, but constant proportions of soil, water and vegetation.

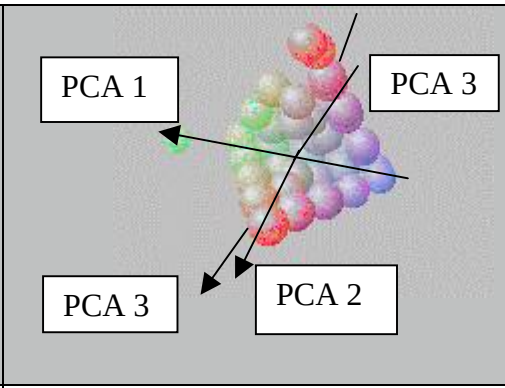

Panel b. Principal Component Analysis (PCA) transformation of the data. The data is split into two planes. No matter which endmembers are selected, many of the pixels will be misinterpreted. PCA numbers are arbitrary.

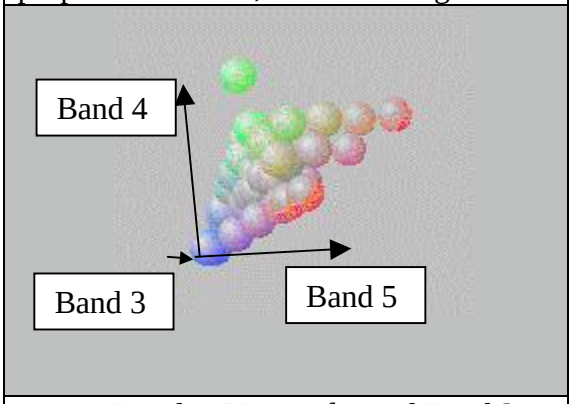

Panel c. Untransformed Band 3, 4 and 5 data. Note the separation between the soil endmembers. One soil endmember is at the extreme right; the other two appear in the middle. Whichever soil endmember is picked will give incorrect results for the other types of soil. Band 3 is perpendicular to the panel surface.

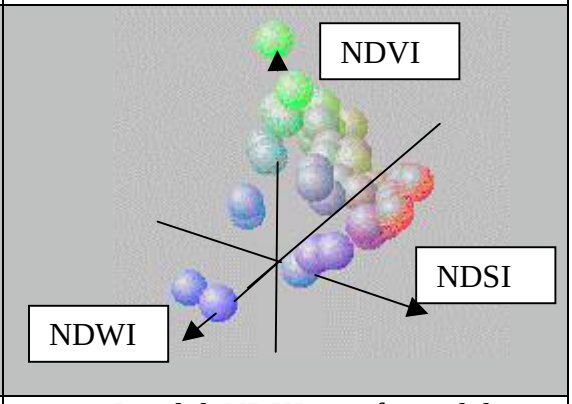

Panel d. NDXI transformed data. The endmembers of each type lie relatively close to each other and all the data lies within one slightly curved plane. There is, however, some distortion. The lumpiness is caused by the pixels of identical fractions but with different endmembers only slightly separating from each other.

Figure 8. Four different views of the dataspace.

Explanations accompany each panel. The axes in each panel meet at the origin. The arrows point in the positive direction.

Chapter 4: Methods

Definition of Study Area

The study area is the MidAtlantic Region of the U.S. (Figure 9), defined here as the East Coast between approximately 34 ° to 40 ° North latitude where Coastal Marsh Project data exists. Legislation defining the MidAtlantic Region for the purposes of the MidAtlantic Regional Marine Research Program defined the area as the coastal area from Cape May, New Jersey, to Cape Fear, North Carolina. The area in this study matches that definition very closely, extending slightly farther both North and South. The study area is split into two zones. The Chesapeake and Delaware Bays comprise one zone. The other zone contains the Atlantic Coast barrier island marsh, the mainland marshes along Pamlico and Currituck Sounds and Great Egg Harbor. The mainland marshes could have been put in the inland marsh group with the large bays, but due to their narrowness and proximity to the coast were left in the coastal group.

This study area was chosen to minimize variation related to climate and other variables while defining an area containing a large amount of data. In particular, the MidAtlantic marshes lie on the coastal plain, differentiating them from the geomorphology of New England marshes to the north (Mitsch and Gosselink, 2000). South of the MidAtlantic region, there are changes in productivity, tidal regimes, and climate. Furthermore, marsh loss rates decline precipitously below North Carolina (Gosselink and Baumann, 1980).

Coastal marshes under consideration are those classified as “estuarine intertidal” and subclassified as either emergent or scrub-shrub (Cowardin et al., 1979) by the U.S. Fish and Wildlife Service in the National Wetlands Inventory (NWI).

The Chesapeake and Delaware estuaries are defined as drowned river valleys (Pritchard, 1967). The marshes along the Atlantic Coast, however, have different origins. The Albemarle and Pamlico Sounds are “bar-built” estuaries, either former shallow marine areas or flooded coastal plains (Pritchard, 1967). On this basis, the study area was divided into two large subsets – the bay area, comprising the Chesapeake and Delaware Bays, and the Atlantic Coast – comprising everything else.

A test area, comprising the Blackwater, Transquaking, Nanticoke and Wicomico rivers and the surrounding area, was selected for development of algorithms. It was chosen as a test area because the area enclosed has a very high fraction of marshes, the area has been well studied and is known to the author.

Effects Investigated in the Study

Five hypothesized effects are studied in this dissertation, along with other effects included for completeness of the model in Chapter 6. The effects hypothesized to impact marsh health are distance from land, distance from roads, distance from tidal creeks, distance upstream from the nearest major bay or ocean, and marsh parcel size. The additional effects are sea level rise, mean tide, northing and easting. The term “effect” in this chapter refers to one of these 9 items unless otherwise specified or made obvious by the context. These are fully detailed in Chapter 1.

Factors Not Investigated in the Study

Some factors that were included in the proposal were not included in the final study.

Nutria

Nutria are thought to have an impact on the survival of wetlands (Carter et al., 1999). However, no numerical data on *Nutria* densities were found that could be used in a model such as was developed for this research. Moreover, it is not known how pervasive *Nutria* impacts are on other marshes in the middle Atlantic Region, or even what population numbers are involved.

Management regime

Informal conversations with staff at BNWR led to the conclusion that accurate management data reflecting any significant length of time would be difficult to locate. Additionally, this is not amenable to numeric interpretation. For example, if a parcel of marsh was not burned for three years and then not burned for five years, how would this scenario compare to a marsh that had been flooded to create ponds and then drained? Each management regime would have to be treated as a separate binary input, most of which would be ones for only small areas. Utilizing binary input codes on management regimes would not reflect differences due to the scale of this project.

Age of roads

It was proposed that older roads would have more time to impact to marsh health then newly constructed ones and that, therefore, the age of roads should be

included as a parameter. However, two things led to dropping this as a parameter. First, it was discovered that thousands of road segments were involved, making collection of accurate data difficult. Furthermore, should the road be dated from when it was an unpaved shell road or when it was paved?

Secondly, using the date of the roads implies somehow retrogressing the marshes to their state when the roads were built. USGS maps of Blackwater show that there were ponds present at the time the Shorter's Wharf Road was paved. Did the paving cause the ponding or had these ponds formed previously? It was not feasible to ascertain the marsh condition prior to road building; therefore, an alternative approach was utilized. The National Wetlands Inventory (NWI) coverage was delineated as time zero for the studied marshes. Using the NWI provided a concrete temporal base line against which to make measurements.

Ditches

A search of the on-line databases found only one article on ditches. Therefore, this was dropped as a topic.

Software:

The work was undertaken using Environmental Systems Research Institute's ArcView, ArcInfo 7.x and ArcGIS 8.2 products, and PCI Inc.'s image analysis software. The statistics in Chapter 5 were calculated with SAS JMP statistical software. The statistics in Chapter 6 were calculated using ArcGIS.

Data Sources and Preparation

The raw inputs to the data model are National Wetlands Inventory (NWI) data, U.S. Census Bureau TIGER files for road data, Thematic Mapper (TM) satellite imagery and ground observations. The TM and NWI data were combined to create the Coastal Marsh Project (CMP) data. The National Atmospheric and Oceanic Administration (NOAA) provided Tidal and sea level rise (SLR) data (www.noaa.gov). These datasets, combined with some ground reference data and aerial photography, comprise the inputs to this research. CMP or NWI data are used interchangeably for areas outside the marsh (open water or upland).

The CMP data were created with a semi-automated image processing and interpretation technique to classify TM pixels representing coastal marshes in the test area with respect to their degree of deterioration (Kearney et al, 2002; Rogers and Kearney, 2004). The pixels represent 28.5-meter square parcels on the ground.

Data sources

Landsat Thematic Mapper (TM) satellite imagery (specify path and row, and dates)

Any TM images that were acquired without georeferencing were georeferenced using the USGS quad maps. Registration was done to less than 1 TM pixel (28.5 meters) accuracy in both the horizontal and vertical axes. A second-order polynomial fit was used with approximately 40 ground control points for each image to project the unmixed data applying the values of the nearest neighbor in the input to the output pixels.

Prior to rectification, Thematic Mapper images were atmospherically corrected using the method of Fallah-Adl et al., (1996). The resulting data are in reflectance units after correcting for haze, solar zenith angle, and solar distance from the earth. This allows the remaining steps to be standardized for all scenes. Image data were put into a PCI database and transformed into three normalized difference indices the Normalized Difference Water Index (NDWI, Equation 2), Normalized Difference Vegetation Index (NDVI, Equation 3) and Normalized Difference Soil Index (NDSI, Equation 4) (Rogers and Kearney, 2004) as described in Chapter 2.

Several diverse TM images were transformed and endmembers selected using PCI's scatterplot (SPL) and visual outlier removal (VOR) subroutines. Pixels representing each of the three endmembers selected were located in the image and, by examining their spectra and using positional data from the scene were determined, in fact, to represent water, soil, or vegetation. From these image-derived spectra, one set of endmembers was chosen to represent the most extreme endmembers and these were applied to all images.

The three normalized difference indices were unmixed using PCI's unmix subroutine to create three percent cover channels - one each for soil, vegetation and water. Pixel values that would have fallen below 0 were reset to 0. Pixels where the vegetation is less than 10% and there is more soil than water were flagged as outside the scope of the wetlands model (Rogers and Kearney, 2004).

Clouds were masked by selecting any pixel with a DN greater than 80 in TM band 1. The value of 80 was based on preliminary analysis of the images. Remaining clouds and cloud shadows were masked by hand. Ground reference data from

fieldwork and aerial photography were used to create a calibration curve to convert the mixture model results into actual percentages. The images used were late spring to early fall, so there was no snow cover; and buildings, roads and other non-marsh surface covers were all removed by applying a mask based on the NWI polygons. Ramsey et al. (2001) made a similar use of NWI masks to perform analysis of coastal marshes for the Coastal Change Analysis Program (C-CAP). They used NWI masks to separate classes that could not be separated spectrally in TM images such as estuarine and palustrine marshes.

After processing, the individual images were combined into larger coverages. To do this, it is assumed that all interferences with the recorded signal (atmospheric haze, high tide, recent rainfall) make the marsh in the pixel look more degraded than it is. Therefore, to assign a value where images overlap, the lowest percentage water value from the input pixels was assigned to the output pixel. In this way, incorrectly classified pixels can be corrected, and pixels that were covered by clouds or shadows in one image may be replaced by clearly viewed pixels from another to produce a final product.

Where bodies of water meet the land surface of the marsh, pixels will tend to be mixed. This is unavoidable and will cause an overestimation of marsh loss along shorelines and creek banks. Because there is no way to know if this is really happening, or if the pixels aligned correctly with stream banks, such points cannot be rejected outright, but cannot be taken too seriously, either.

National Wetlands Inventory Data

NWI digital wetlands data were available as 7.5-minute orthophotoquads, stored in Digital Line Graph Level 3 Optional (DLG-3 Optional) format. Many are now available as Arc/Info exchange files. The coverages were digitized using Arc/Info software with the NWI classification codes assigned as attributes. These maps were produced by the U.S. Fish and Wildlife Service and delineate most of the wetlands in the U.S.

A mask was made of the NWI data. It separates the estuarine intertidal marshes of scrub shrub or emergent plants from uplands, open water and other wetlands. This NWI mask was converted to a grid and combined with the TM data so that all non-marsh, open water or unusable pixels were flagged in the final output and the remaining marsh pixels were categorized by the fraction of the pixel that is open water as calculated from the scene. The mask was used for the calculations of distance from uplands.

Updated coverages were downloaded from the NWI website in December, 2002 and inserted into the NWI coverages that had been compiled by the Coastal Marsh Project. However, in most cases the NWI data was not used directly, but the finished Coastal Marsh Project data, which already incorporated the NWI data, was used instead.

The USGS provides general metadata for the NWI maps. The metadata states, among other things, that reference files from 1902 to 1995 were used. However, the aerial photography on which it is based ranges in date from Feb. 1971 to Nov. 1997. Further, they state that the NWI system does not correspond with other jurisdictional

wetlands maps, it does not include wetlands that were not readily visible in the aerial photography and there is a size limit based on the scale of the input maps, which was variable.

U.S. Geological Survey (USGS) orthophoto quad maps

USGS Orthophotoquad paper maps were used to georeference images and provide detailed information on various areas when on-line sources were not available.

U.S. Census Bureau TIGER Files

U.S. Census Bureau TIGER Files were downloaded from the ESRI website in 1999. These files were used to provide locations of streets and roads throughout the study area. An attempt was made to use TIGER water boundaries to supplement the NWI water boundaries, however there were conflicts between the datasets so TIGER files were dropped from the water boundary processing.

Field sites

During the course of the marsh project several field sites were investigated (Figure 10). The techniques ranged from simply looking at the site and estimating the percentage water to going over the site with a line marked at one-meter intervals and noting whether the marsh under the rope was water, land or vegetation at each point. The transects were chosen randomly. Field sites were located predominantly in the test area defined above, North Inlet, South Carolina, and the Delaware Bay marshes on the western side of the bay. None of these sites, including the North Inlet site, is good representatives of the marshes in North Carolina.

Aerial photography.

USGS aerial photographs were obtained from http://terraserver-usa.com/ and used in mapping and verification of some data as shown in some figures.

Tide Gauge Data

Mean tide and sea level rise data (Figure 11) were obtained from the National Oceanic and Atmospheric Administration (NOAA) and used in the marsh loss model (Appendix B).

Creating the distance data:

All the distances were calculated using ESRI's costdistance function. This function takes two inputs: a mask and a cost grid. The cost grid assigns a resistance value or cost for traversing each unit of surface area. In this study, the units are meters. The mask contains a set of discrete source points in a grid. The non-source points in the grid must be NULL values. The costdistance function calculates the least cost path from each gridcell in the output grid to each source in the input grid using the costs assigned in the cost grid. If the entire costgrid were set to 1, then the distance calculated will be the actual physical distance. For example, using the marsh data and a resistance of 1, the cost of traversing one grid cell from side to side would be 28.5, the width of a cell in meters multiplied by the cost per meter. If the same cell were traversed on the diagonal, the cost would be 28.5 * 21/2. Any NULL values in the cost grid are treated as impenetrable cells, and the least cost path must go around them.

Although the costdistance function requires the non-source points in the mask to be NULL values, many ESRI functions, which use the same information, require the masks to use 0 instead of NULL values. In the amls listed in Appendix C, the masks are often converted from the null to the zero form for this reason.

A separate mask had to be generated for distance from each effect type (land, tidal creek, downstream limit and roads). In the stream mask, all water bodies that had no discernible connection to tidal streams were removed because they would not be suppliers of sediment or oxygenated, estuarine-salinity water to the surrounding marsh surface. The tidal creek hypothesis is based on the view that creeks supply nutrients, sediment and flushing to the marsh. Bodies of water that are not connected to the tidal creek network (or that are only marginally connected) would not be expected to supply incoming tidal water at sufficient velocity to carry sediments to the surrounding marsh surface, if, indeed, they flush the marsh surface at all. However, they were left in the road and upland mask files, because they would still act as barriers to hydrological impacts. Each effect type, due to the grid cell size, has a minimum thickness of 28.5 meters.

Distance upstream:

Distance upstream was calculated in three steps, excluding the creation of various masks. The first step was to determine the furthest point downstream. This was determined in a somewhat subjective manner by drawing a line that roughly paralleled the shoreline, with the exception of river mouths were it was drawn as a straight line (Figure 12). On areas such as the Outer Banks, the line went almost completely around the barrier islands. The purpose of this line was to establish a

reference that represented a hydrostatic minimum for the adjacent land and waterways. Once the baseline downstream position was determined, it was converted to a grid, along with a mask of the shoreline including a cost grid. The ESRI function costdistance was then used to calculate the distance to every grid cell upstream within the river and creek boundaries from the nearest point on the downstream line for a line following the tidal creeks.

To assign a value to pixels in the marsh a similar mask was applied and the eucdistance function was applied. This function applies the nearest value from a mask (the river and stream edges, in this case) to each cell in the output grid. The results of this are shown in Figure 12.

Before running the costdistance function, the streams were clipped wherever they became only 1 pixel wide. This served to eliminate ponds that were attached to the main channel by a narrow creek, as well as narrow meandering creeks.

Distance from nearest tidal creek:

The NWI data were used to define all tidal creeks. First, a mask was created showing areas on the marsh surface that were water, road or upland (streammask2.aml). Then the water_process.aml was run. The upstream distance calculation was used as the beginning of this operation. The clipping of small channels and calculation of upstream distances allowed easy removal of many interior ponds. Those not visibly connected with a channel or that were clipped off, simply had no distance upstream calculated and could be removed. The algorithm after that is much more convoluted and is included in whole in Appendix C. Once tidal creeks were defined, the distance from each point in the marsh to the nearest creek had to be

calculated. The output of water_process.aml is a file called allcreeks, which is an attempt to remove ponds while leaving as much of the creek system as possible. The possibility of doing this by hand was examined, but discarded because of the hugely subjective interpretation it creates.

Allcreeks was used with a cost grid to create the distance grid. For creeks it was determined that their influence would end at other water bodies, roads or uplands.

None of the amls turned out to be complete, so some manipulation by hand was undertaken at the completion of some of the amls. These steps were kept the same and are outlined in the "Processing Steps for All Input Grids" section of Appendix C.

Distance from nearest road:

The road distance calculation also started with the creation of a mask. This mask process was designed to differentiate between roads that crossed marshes and those that merely touched them. The first step was to identify all road segments that touched a marsh. The second step was to eliminate those that coincided with upland or that merely came to the marsh edge and ended there. This mask was then used as input to a number of functions. For the road distance calculation, the next step is "road_process.aml". This aml further processes the mask and attempts to differentiate between roads that impede water flow and those that do not. This step was necessary as the hypothesis was based on the assumption that roads affect hydrology. Those that do not affect hydrology are of no interest in this analysis. In brief, a costgrid is created in which each water pixel has a resistance value of 1 and

each marsh pixel was assigned a resistance of 100. The value of 100 was chosen after trying several different values for resistance to flow across the marsh. This value caused the model water flow to stay within the creek banks more rather than flowing long distances over the marsh to reach a pixel. This allowed an approximation of a flow distance to be calculated. The costdistance function always calculates the least cost path. In this case, there will be a trade off between coming farther upstream versus calculating across diagonals of the marsh pixels. The costdistance will be minimized somewhere between

Distance = Nwater + Nmarsh * 100

And

Distance = (N – Y)water + (Y2 + Nmarsh2)1/2 * 100

Where Nwater refers to the distance upstream to the stream point nearest the marsh pixel in units of pixels. The Nmarsh is the number of pixels in the shortest distance from the marsh pixel to the water and N – Y is the distance along a stream that would give the shortest costdistance to the marsh pixel in question if traversing marsh and traversing water had the same cost. This also assumes, for simplicity, a relatively straight stream, which is not likely in a marsh. This formulation simulates the flow of tidal water in and out of the marsh, by assuming that flood tide water reaching a point in the marsh will get there by the least cost path.

Use of this function allows the algorithm to determine which roads impede the flow of water by comparing the costdistance to pixels on either side of the road. After some examination of the data in the test zone, a difference of 13,000 was found to be effective in separating the roads into two categories. This value implies an

actual difference of 4.5 pixels traversed. The actual calculation was accomplished by placing a 5x5 window over each grid cell that contains road surface, and then comparing the minimum and maximum values. The expected maximum difference (maximum – minimum), if the water is flowing parallel to the road on both sides, would be 28.5 * 4 * 100 (width of a pixel, times 4 pixels, times the resistance due to traveling over ground). If the road runs diagonal to all the pixels, it may get included as having an effect because the diagonal maximum difference expected would be 16,207, or slightly larger than the cutoff value in some cases. However, making the cutoff larger would also exclude road segments that should be included.

The road cost grid was defined by assuming that the influence of a road, being primarily hydrological in nature, would end at another road, stream or upland area. These areas were set to NULL, which terminates the cost function calculation in that direction.

Distance from nearest upland

The landmask was created by reassigning the CMP marsh upland category a value of 1 and all other categories a value of NULL. The impact of uplands being modeled includes both runoff and structure. In Blackwater National Wildlife Refuge, for example, the marsh substrate clearly thins as you approach the various islands, much as the water around an island gets shallower closer to shore. Because it is not possible to know how far this effect stretches, the effect of uplands was determined not to be influenced by surface features such as streams or roads. Therefore, the cost function was set to 1 for all pixels.

Distance from Random Points

To test if randomly spaced sources would produce a regression with probability of marsh loss, approximately 5% of the marsh surface cells were randomly assigned to be sources and distances were measured from these points just as for the other effects, such as roads or land boundaries. This was done to test whether or not the processing itself or other unknown processes were affecting the outcome of the regressions of probability of loss on distance from some effect. It was done after the other regressions were performed, and many produced very high R^2 values.

Size of Marsh Parcel

To calculate the size of a parcel of marsh, the CMP data were converted from a grid to a polygon coverage, the four marsh health categories were set to 1, and everything else was set to zero. Polygons of like value were then merged using the merge function. Each polygon in a coverage has an attribute containing the area of the polygon. The polygons were converted back to grids using the area attribute as the value assigned to each cell.

Sea Level Rise

Sea level rise data were acquired from NOAA for points (Appendix B) along the coast. These data were interpolated using inverse distance weighting to give a value to every marsh pixel based on the two nearest actual measurements. Along

parts of the North Carolina coast, this meant some points were calculated from points as much as 200 km distant.

Tidal Range

Tidal range data were acquired from NOAA for the East Coast (www.noaa.gov). These data were also interpolated using inverse distance weighting to assign a value to each marsh pixel based on the two nearest actual measurements.

Dependent variable

To perform the analysis it was necessary to compute the probability of marsh loss. One way to do this was simply to use the percent water in each pixel as the dependent variable. However, according to the original formulation of the MSCI, a certain amount of open water is good in a healthy marsh. There will be small ponds creeks. Furthermore, small amounts of water on the marsh may be a result of recent rain events or simply the tide being high at the time of the data collection. Therefore, the numbers at the low end of the scale were not meaningful. Only about 2 – 5% of the marsh exceeded 50% water in any given pixel, so at the high end of the scale, data were virtually non-existent. To be consistent with the Coastal Marsh Project analysis, any parcel estimated to be 50% or more open water was considered "totally degraded" or "open water" for the purposes of this research. All other pixels were considered to be “not totally degraded”.

Testing the Individual Effects (Chapter 5)

The response variable being examined here is the probability of becoming open water, and was calculated as follows. For each effect type, (distance from a

road, distance from upland, parcel size, etc.) the distances (or size of parcel) were normalized to a scale of 1 – 100, and converted to integers to yield 100 categories (this was represented by an integer grid containing the values 1 – 100). In ArcInfo terminology, a zone is defined as a set of grid cells all having the same value, whether or not they are contiguous, therefore each integer value defines a zone. For each zone, the number of cells in category 4 (totally degraded) was calculated as well as the zonal area. From this the probability of a point in the marsh becoming open water could be calculated from:

P = area degraded / total area in zone.

The normalized distances and the probabilities were then converted to natural logarithms and plots were made of the regression of the probabilities on the distances. This explains why the distances were scaled from 1 – 100, instead of 0 – 100, as zero has no natural log. The distance from land zones are shown in Figure 13.

The conversion to natural logarithms is necessary to give the data a Gaussian distribution. The data are almost all based on distances from some feature, so the input data can be thought of as source cells and target cells. The number of target cells per source cell diminishes with distance from the source cells, hence, each zone, defined as all the cells at some distance plus Δx from a source cell will have a number of cells defined by

Equation 14. Distribution of target cells

$$y = g(\int dx / x)$$

where g() accounts for other factors in the number of cells, y is the total number of cells in a zone, x is distance, and the definite integral over dx is implied. Therefore, y

= g(ln(x)). Defining the zones on equal widths of ln(distance) tends to redistribute the number of cells per zone more normally. Because total degradation is a rare condition, based on the total marsh surface area, the distribution of probability values will tend to follow a non-Gaussian distribution, also. In particular, they will tend to follow an e-x distribution, which can also be corrected to a Gaussian distribution by the natural logarithm function.

Statistics: Chapter 5

Autocorrelation

When dealing with spatial data, the question of autocorrelation becomes important. Cliff and Ord (1973) define spatial autocorrelation as "If the presence of some quantity in a county (sampling unit) makes its presence in neighboring counties (sampling units) more or less likely, we say that the phenomenon exhibits spatial autocorrelation". Anselin (1988) and Davis (2003) stress that this is a functional relationship.

Equation 15. Autocorrelation

$$y = \rho Wy + X\beta + \varepsilon.$$

β is a vector of parameters for the exogenous variable matrix, X, ρ is the coefficient of the spatially lagged dependent variable, y, and ε is a, possibly autocorrelated, disturbance term. W is the weight matrix (Anselin, 1988).

For this analysis, the W matrix may be thought to contain several interpretable influences (the subjects of the hypotheses) plus others that are not known. Particularly, in the presence of a road, where y = p(deterioration), the weight matrix values would be

hypothesized to increase as the distance from the road increased, if that were the only influence. Several factors may be in operation in a given area. To extract the one of interest, the data are organized by the effect being studied. This essentially becomes an exercise in signal extraction. By summing the data in a way to emphasize the signal of interest and to average the rest, the signal of interest will be amplified and non-correlated inputs (noise) will be reduced by the averaging. This applies both to the other influences in the W_1 matrix, as well as the exogenous inputs included in $X\beta$. Any autocorrelation due to measurement error has been reduced through resampling of the original data, atmospheric and solar angle correction, and the NDXI technique, which tends to reduce between-band autocorrelation.

The possibility of endogeniety arises with the regression of distance from roads on marsh health. Roads are likely to be built where the surface or subsurface is solid. For a regression of marsh health on distance from roads, the health of the marsh may have been an important factor in the location of the road.

Modeling Landscape Effects in Coastal Marsh Loss (Chapter 6)

To develop a model using the topography-related effects examined in Chapter 5, the data were examined to find the most relevant inputs. These were assembled into stacks in ESRI's Grid program. Each stack was then converted to a set of principal components using the princomp function. The CMP marsh data was converted to a grid that had the value of 1 wherever the marsh was totally degraded, 0 everywhere else there was marsh and "no value" past the edges of the marsh. This marsh grid and the principal components were written to a sample file by the grid

program Sample, where the all the values in each grid are aligned geographically. This sample file then was used as the input for Grid's regression command, which was run using the "logistic" and "brief" options. This procedure produces the coefficients for a logistic regression (discussed in detail in Chapter 6) and the rms and chi-square values.

Model grids were then calculated and compared to the original data to check for goodness-of-fit. A standard G-adjusted value was calculated for each result and compared to the chi-square values. The sample for the Bay areas model was a subset of approximately 1000th of the entire data set, randomly chosen but weighted to increase the number of totally degraded pixels. The sample for the Atlantic Coast was the entire dataset. These choices were based on which method produced the best results.

Statistics: Chapter 6

Principal Components

To ensure that the independent variables used in the regression model are independent, principal components of a matrix of the measured variables were calculated (Hosmer and Lemeshow, 2000). These are guaranteed to be orthogonal. Because principal components analysis (PCA) was not used to reduce the number of variables by compressing the bulk of the variability into a few variables, all the PCA variables were used in the final analysis (Davis, 2003).

Autocorrelation

Autocorrelation is not specifically addressed in Chapter 6 and will have some impact on these results.

Regression

The data used for this research has several characteristics that make ordinary least squares (OLS) regression of the raw variables inappropriate. The dependent variable being investigated is best expressed as a simple binary choice - the marsh is either totally degraded or it is not. Logistic regression calculates the probability of an event occurring or not occurring. A linear model is not appropriate for this type of response variable for several reasons. The error terms are heteroskedastic. The variance of e = p (1-p), where p is the probability that degradation = TRUE. P is dependent on X, so the assumption that the error term does not depend on the Xs is violated. As P can have only two values, the error terms are not normally distributed. Linear regression, of course, uses a range of y that is not bounded by one and zero. Hence, if used for probability calculations it can return probabilities greater than 1

Logistic Model

The logistic model is:

$$\ln[p/(1-p)] = \boldsymbol{a} + \boldsymbol{B}X + e$$

where:

a is the constant term coefficient,

B is a vector of coefficients on the independent variables,

X represents the vector of independent variables

e is the error term

p = probability(Y=1)

The probability, p, is calculated by:

$$p = [e(a + BX)]/[1 + e(a + BX)]$$

or

$$p = 1/[1 + e(-a - BX)]$$

If $a + \boldsymbol{B}X$ equals 0, then p = 0.5; as $a + \boldsymbol{B}X$ gets larger, p asymptotically approaches 1, and as $a + \boldsymbol{B}X$ gets smaller, p asymptotically approaches 0.

Model Fitting

Estimation by maximum likelihood

The goal of maximum likelihood estimation (MLE) is to find the parameter values that make the observed data most likely. If P(X|p) represents the probability of an event X given the model parameters p, then L(p|X) represents the likelihood of the parameters given the data. Logistic regression finds a best fitting equation by using a maximum likelihood method. This maximizes the probability of getting the observed results given the fitted regression coefficients. As a result, different tests of statistical significance are required for logistic regression than are used in OLS regression.

The likelihood function (L)

$$L = \Pi(X = xj)$$

calculates the likelihood of predicting the dependent variable values observed given a set of parameters for the model (Upton and Cook, 2002). As the function increases, the probability of observing the Xs in the sample increases. MLE is used to find the coefficients (a, B) that maximizes the log of the likelihood function (LL < 0).

Overall model performance

Several statistics can be used for comparing alternative models or evaluating the performance of a single model. One of these, the model likelihood ratio (LR), or chi-square, statistic is

$$LR[i] = -2[LL(a) - LL(a,B)]$$

where the model LR statistic is distributed chi-square with i degrees of freedom, and where i is the number of independent variables. The "unconstrained model", LL(a, Bi), is the log-likelihood function evaluated with all independent variables included and the "constrained model" is the log-likelihood function evaluated with only the constant included, LL(a). The Model Chi-Square statistic is used to determine if the overall model is statistically significant.

Another evaluation of the model is to use a contingency table to determine the accuracy of the predictions. The percent correct statistic is calculated on the assumption that if $p > 0.5$, then the pixel is degraded. Otherwise, the pixel is assumed not totally degraded. There is no equivalent to the OLS regression R^2 statistic in logistic regression (Hosmer and Lemeshow, 2000).

Remote Sensing

Synthetic Data

Several sets of synthetic data were created for this modeling effort using SAS-JMP® on a Macintosh® computer. Three cover fractions were created (f1, f2, f3). To insure a high probability of a pure pixel for any of the three surface cover types, and evenly distribute the potential for any one cover type to be either high or low in any given pixel, they were calculated by first generating a random variable, x1, that was between 0 and 1. This random variable was skewed toward 1, with a mean value of 0.6. A second random variable, x2, was calculated between 0 and 1 - x1. A third number, x3 = 1 - x1 - x2, was calculated for each pixel. One third of the values of each variable were then assigned to the water, vegetation and soil fractions. Once the surface cover fractions were determined, synthetic reflectance data had to be calculated. Two methods were used: simple linear mixing and non-linear mixing with noise added to both.

Noise was added to the reflectance spectra to test whether it could be successfully removed by the NDXI procedure. Noise in the reflectance spectra was added to the linear mixture model above by:

Equation 16. Multiple Scattering.

$$R_i = (\rho_{wi} + S_{wi} e_{wi}) f_w + (\rho_{vi} + S_{vi} e_{vi}) f_v + ((\rho'_{si} - \rho_{si}) e_s + \rho_{si}) f_s$$

where the e's represent random variation in the endmembers and $\rho'_{si} - \rho_{si}$ represent the bright and dark soil spectra, s_{wi} , and s_{vi} represent standard deviations of

water and vegetation, and ρ_{wi} and ρ_{vi} represent the reflectances of water and vegetation.

The non-linear model used is a modification of one of the models of Borel and Gerstl (1994). Borel and Gerstl's model incorporated one cover type (soil) beneath the vegetation. This model allows the substrate to vary between 100% soil and 100% water in each pixel. As a first-order approximation, each pixel in this model is treated as though the mixture of soil and water is completely homogeneous and constant across the pixel. The reflectance immediately above the leaf layer is given by:

Equation 17.

$$R_f = R_v + R_g .$$

The individual components R_v and R_g are given by:

Equation 18. Scattering from Vegetation.

$$R_v = \rho_v * f_v + \tau f_v \rho_{ws} (1 + f_v(\tau - 1)) / (1 - \rho_v \rho_{ws}))$$

Equation 19. Scattering from Soil/Water.

$$R_g = \rho_{ws} (1 + f_v * (\tau - 1)) / (1 + f_v \rho_v \rho_{ws})) .$$

where

$\rho_{ws} = \rho_w f_w/(f_w+f_s) + \rho_s f_s/(f_w+f_s)$.

R_v and R_g represent the reflectances of the leaf layer and the substrate, τ is the transmissivity of the leaf layer, f_v is equal to LAI (Leaf Area Index) for LAI less than 1, ρ_{ws} is the average reflectance of water and soil in any pixel. Borel and Gerstl (1994) also modeled reflectance for LAI $\geq$ 1, but that model was not applied here.

Datasets of ten thousand points were created using the non-linear model and unmixed using PCI's unmix algorithm with two different procedures. In one procedure, the principal components were calculated, endmembers selected in PCA space, and then the endmembers were used in TM space to unmix the pixels using bands 3, 4, and 5. This is referred to as the "PCA" procedure. The second procedure was to run the NDX transformation on TM bands 3, 4 and 5, use the NDWI and the NDSI to select endmembers and then unmix the data in the NDX data space (referred to as the NDX procedure).

Identification of endmembers from real images was undertaken using PCI's Imageworks® and EASI/PACE® programs. When using principal components, the first two principal components of the dataset were calculated and a scatterplot made of them. The points in the two-dimensional scatterplots representing water, soil and vegetation were identified at the extrema of the data, flagged, and the actual pixel locations identified. These pixels were used as training sites to create spectra for the three endmembers. The reflectance data were then unmixed using PCI's unmix algorithm (Gong et al. 1991) and subsequent analysis performed with SAS-JMP®. The unmix program uses singular value decomposition to solve for the unknown percentage cover fractions. For the NDX operation, a set of standard endmembers were extracted from actual scenes and applied across all synthetic datasets.

To examine the effects of non-linear mixing directly on the data, one set of 498 points was generated with reflectances calculated both with and without non-linear mixing. No random variations were permitted in this dataset, so that only the difference between linear and non-linear mixing could be examined.

Non-linear reflectance in water or soils was not modeled because the spectral bands chosen have very little reflectance from water, except Band 3. The latter band may penetrate sufficiently into water to produce significant backscatter from bottom sediments. However, detection of water depends on Band 3 being brighter than Bands 4 and 5, which should make the water look more like water in the NDXI transformation. This is important because if the reflectance is sufficiently bright in Band 3, it may cause a pixel to appear like more than 100% water.

Real Data

The method of defining endmembers used here is similar to that of Williamson (1994), who used PCA, the spectral distribution of the reflectance data and ground reference data to select endmembers. The points representing endmembers were carefully screened after being selected in two-dimensional scatterplots. They were all examined spectrally to determine the degree to which they fit expectations for the various spectra, and they were also examined geographically within the context of the image. Water and vegetation pixels were relatively easy to find, as large expanses of open water and forests characterized most of the images. By comparison, soil spectra were a little more difficult to obtain. Sandy beaches provided the one ready source; the rest had to be carefully examined. Knowledge of the area being examined was used to support choices of individual pixels. It was found that even for the PCA method, the quickest way to identify potential endmembers accurately was to use plots of NDWI versus NDSI. Pixels flagged by this method could be used to find and identify the training pixels in the PCA space.

A subset of 67,600 points was extracted from an atmospherically corrected Thematic Mapper Scene, 16/37 1992, and used either as TM image data or transformed according to the NDX algorithms above. Two sets of one thousand random points were selected from this subscene. The first set was truly random, but did not have many soil-dominated pixels. The second set was weighted, based on their spectra, to contain more soil-dominated pixels.

The preliminary field validation and image processing used to provide the data here are discussed in Kearney et al. (1995). Ground reference data were collected in Blackwater NWR, Maryland, and Winyah Bay, South Carolina, by visually assessing areas on the ground and estimating the percentage water. The assessed locations were geographically located with GPS and then referenced back to the analyzed images.

To determine whether the transformed TM data would scale spatially or not several TM scenes were tested. For the first half of the test, each NDX value was calculated and then the pixel values averaged together in 10 by 10 squares to get the following equation:

Equation 20. NDX Average

$$NDXave = \left(\sum_{i=1}^{100} [(BandA - BandB)/(BandA+BandB)]_i\right)/100 \quad .$$

Alternatively, the TM pixel values were averaged in 10 by 10 squares and subsequently transformed into NDX axes for the following equation:

Equation 21. TM Average

$$TMave = (\sum_{i=1}^{100} BandA_i - \sum_{i=1}^{100} BandB_i) / (\sum_{i=1}^{100} BandA_i + \sum_{i=1}^{100} BandB_i)$$.

The results of these two transformations were then regressed against each other to show that the NDX results scale with changes in geographic extent (Rogers and Kearney, 2004).

The preceding discussion covers work that was done for the Coastal Marsh Project from 1992 – 1996 as well as work that was done strictly by the author in the period 1996 to the present.

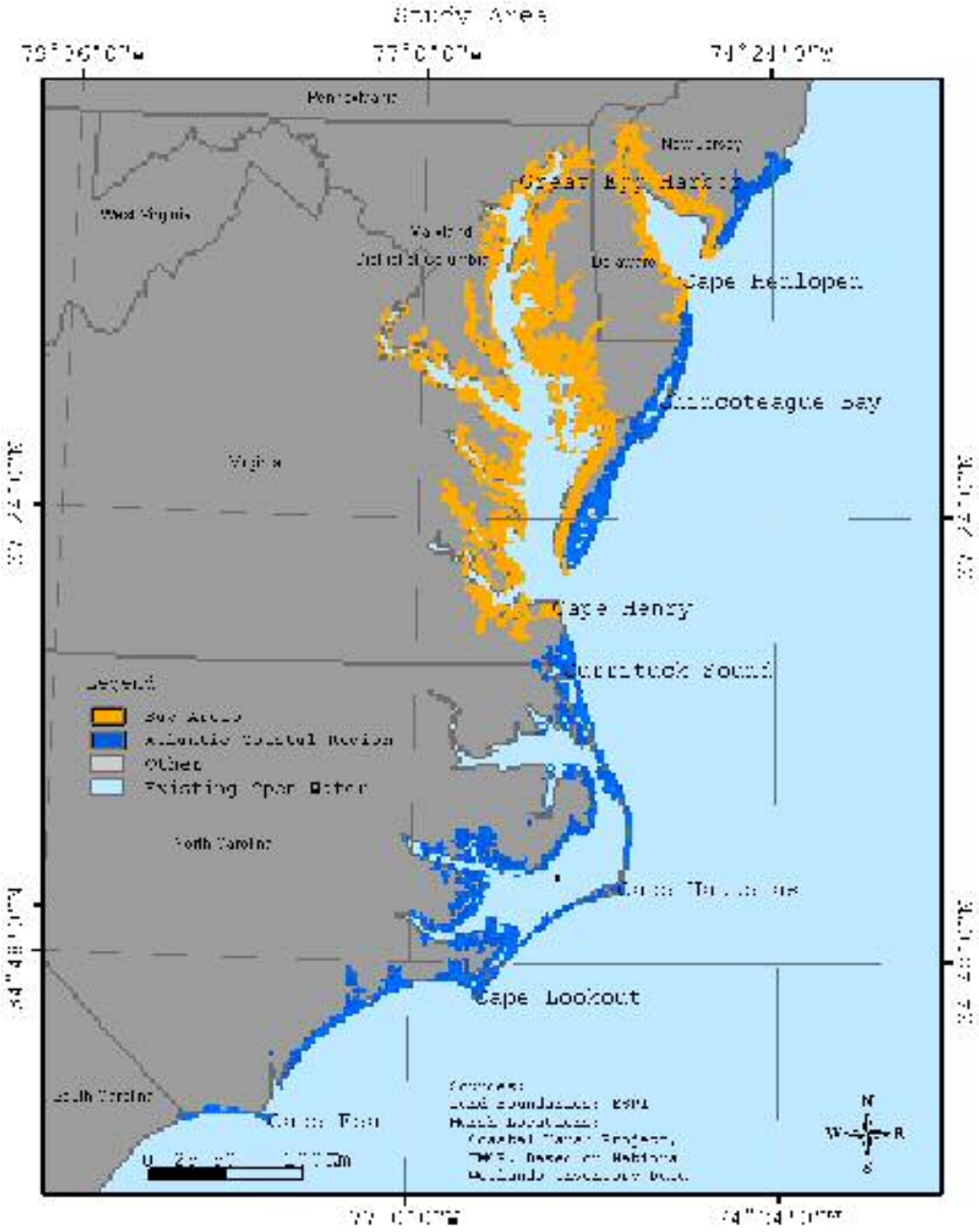

Figure 9. The two zones of the study area

The Chesapeake and Delaware bays, where the marshes are larger and more insolated from the ocean, were put in one zone. The barrier island marshes and the mainland marshes behind Cape Hatteras were put in the second zone.

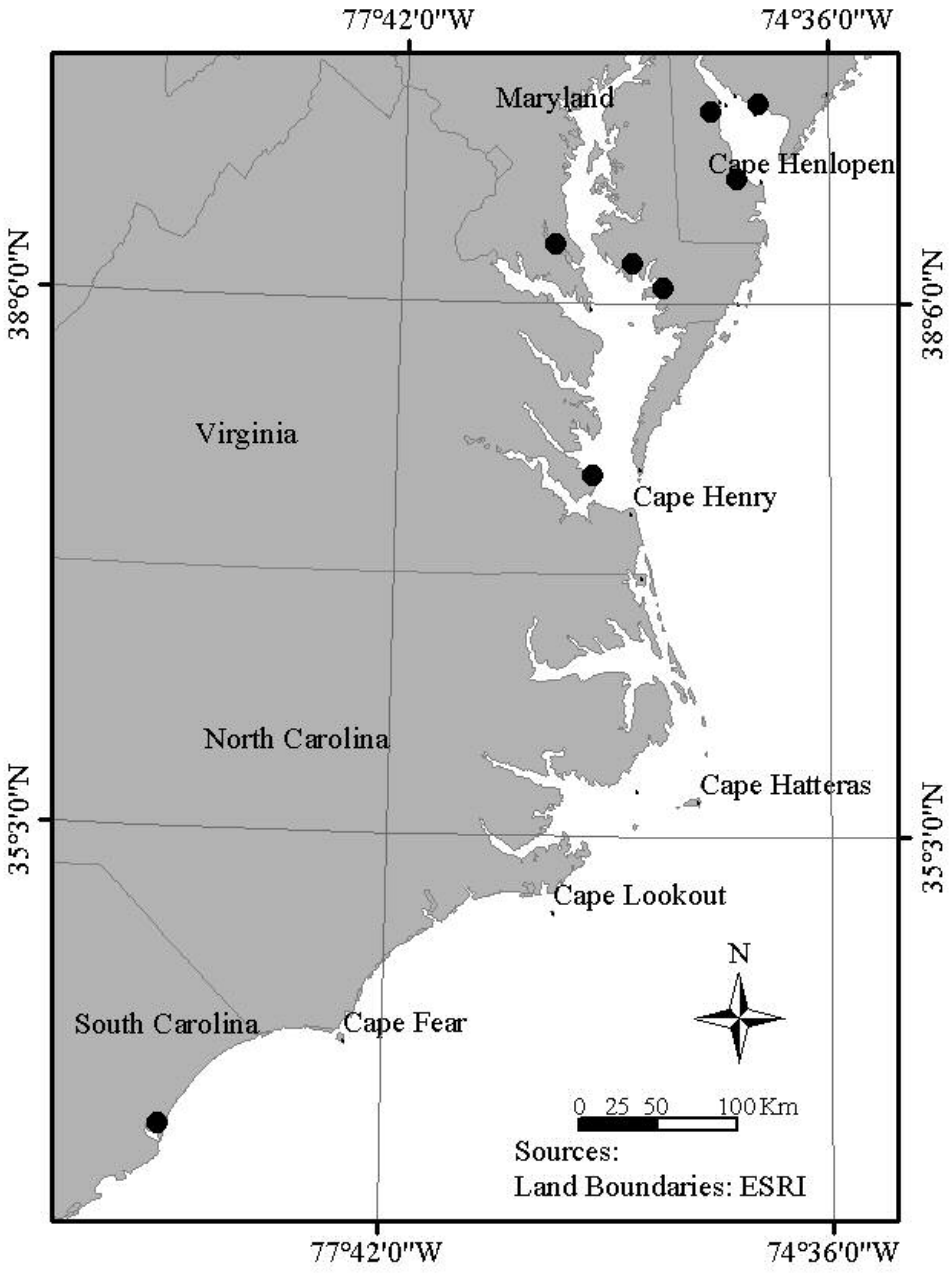

Figure 10. Validation Sites

The dots shown represent general sites where the remote sensing technique was calibrated or validated.

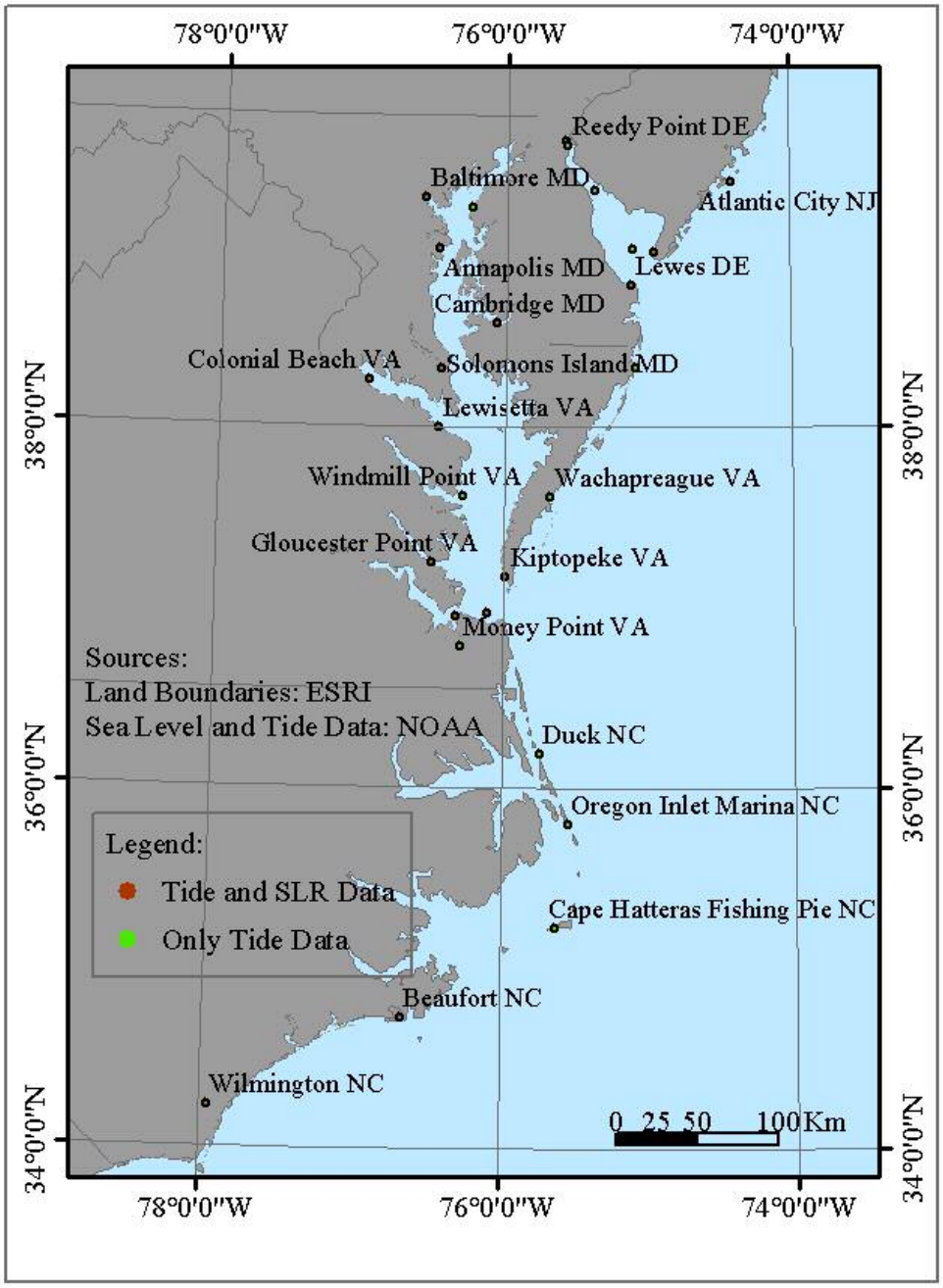

Figure 11. Tide Gauges and Sea Level Rise Data Points.

This shows the location of NOAA's tide gauges, which are the source of the sea level rise, and tidal range data used in this dissertation.

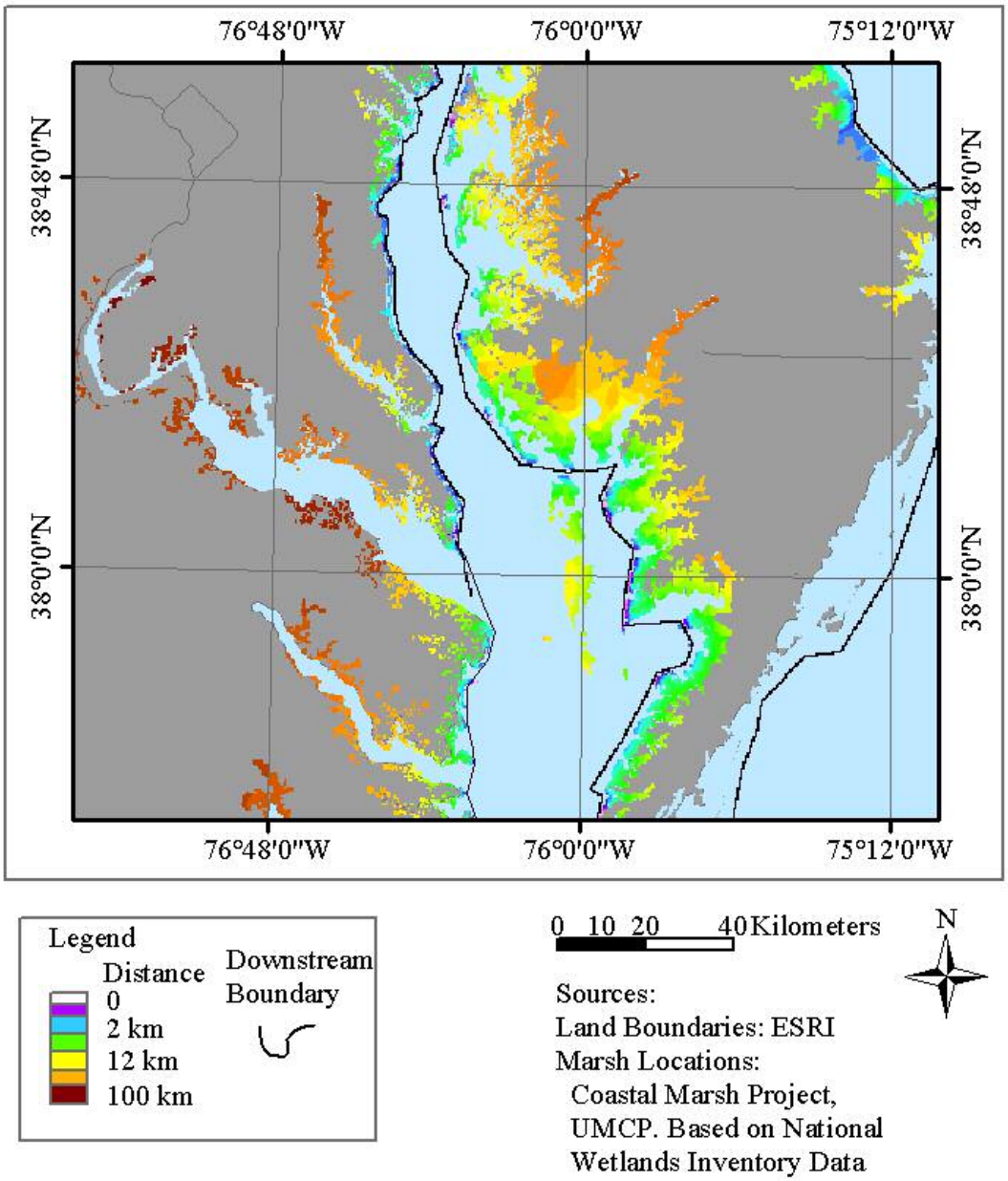

Figure 12. Upstream Distance in the Chesapeake Bay

The dark line along the coast in this figure is the line defined to be the downstream limit from which distances were measured. The colored zones represent bands of marsh at different distances upstream from the nearest point on this line.

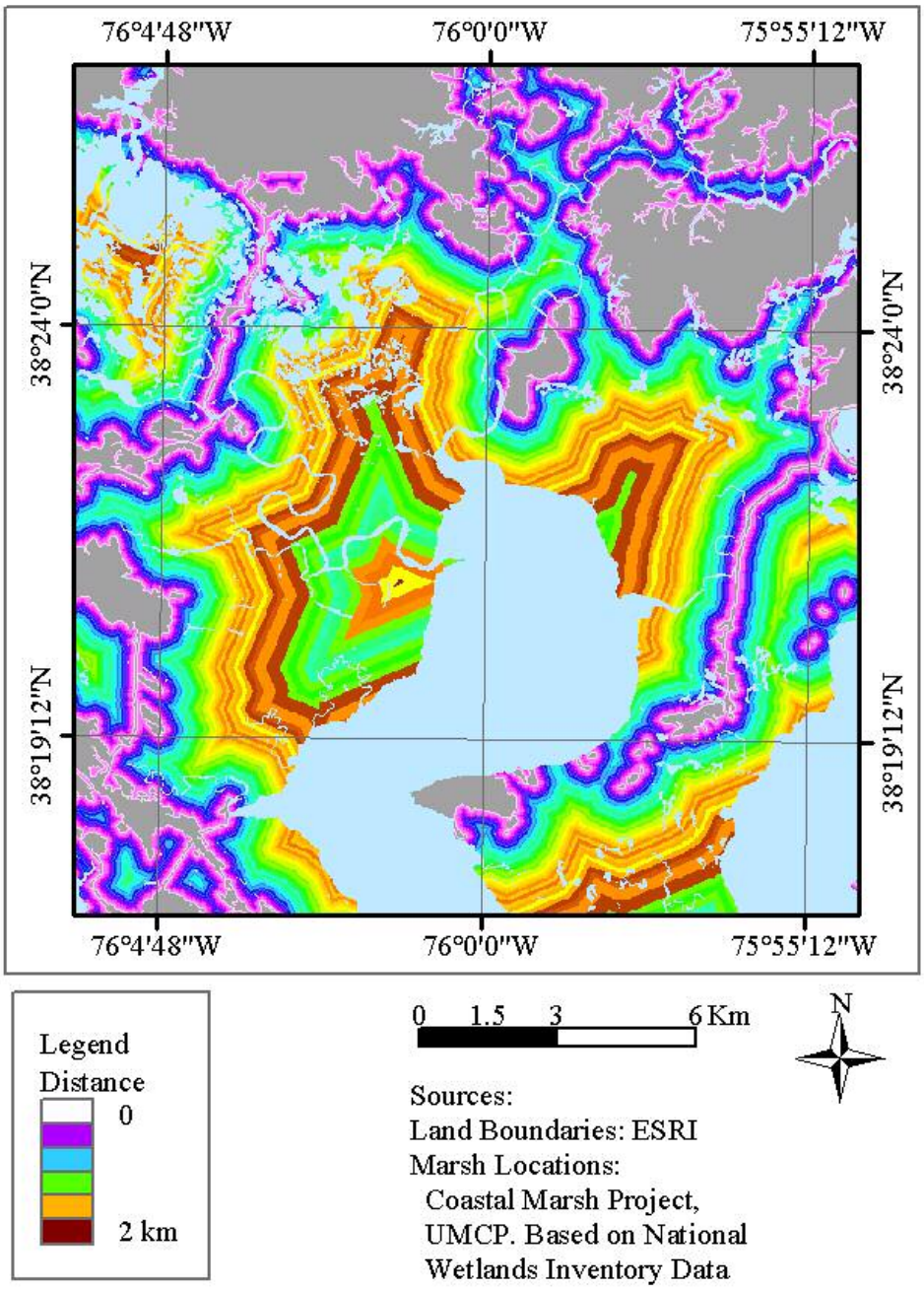

Figure 13. Distance from land represented as zones.

The colored bands represent the zones of marsh that are all a constant distance from the nearest upland.

Chapter 5: Testing the Hypotheses

One goal in this study is to test several hypotheses regarding factors that might be correlated with marsh loss. The other is to develop a multiple regression model of marsh loss using those same factors. The results of the multiple regression model will be presented and discussed in Chapter 6. This chapter focuses solely on the testing of the four hypotheses presented in the proposal, plus an additional one added later. The hypotheses are discussed fully in Chapter 2, but are restated below for convenience. Each section in this chapter consists of the hypothesis, the Bay Area (Chesapeake and Delaware Bays) results, the Atlantic Coast results and a conclusion.

The Coastal Marsh Project assessed the condition of coastal marshes from New England to northern Florida. This study uses the results from the middle of New Jersey to southern North Carolina as shown in Figure 14. The study area covers both Atlantic Ocean coastal areas and estuarine marshes, principally on the Chesapeake and Delaware Bays, but some smaller ones are scattered along the coast. The coloration of Figure 14 is based on the Coastal Marsh Project output but has been reduced to show two categories of pixels – those below 50% open water and those 50% and above open water. The two-class system shown in Figure 14 shows the data actually used to calculate the probabilities of total deterioration.

The descriptive text associated with Figure 14 is based on the Marsh Surface Condition Index, which in turn is based on how estuarine marshes are thought to

deteriorate (Kearney et al., 1988). This may have nothing to do with backbarrier island marshes or those on the far side of Currituck Sound, which are barely separated from the open ocean by a thin chain of islands. The back barrier marshes may also be stable with much higher amounts of open water in ponds and streams than the estuarine marsh systems. In addition, marshes that are developing may look exactly like marshes that are disappearing in remotely sensed data. However, for purposes of this discussion, the terms deteriorated and degraded will be applied to both marsh systems to denote marshes that have become 50% open water after the delineation of the NWI data.

Coastal marshes under consideration are those classified as "estuarine intertidal" and subclassified as either emergent or scrub-shrub (Cowardin et al., 1979) by the U.S. Fish and Wildlife Service in the National Wetlands Inventory (NWI).

Validation

Limited new validation of the Coastal Marsh Project dataset was done. However, the original validation is very encouraging as to the accuracy of this analysis. In one study on the Delaware Bay, it was found that the CMP classification was 83% accurate for classification into four classes (Stevens, 1997). This analysis compares the percent water calculated by the remote sensing model with percent water observed by analysis of aerial photographs, which was backed up with visits to ground sites. For a two-level classification (Table 6) the accuracy is nearly 100%. Other efforts have further validated the work (Kearney et al., 2002).

Table 6. Validation of Coastal Marsh Loss Project Data on the Delaware Bay

		Actual		Row Totals
		Healthy	Degraded	
Assessed	Healthy	178	1	179
	Degraded	0	6	6
	Column Totals	178	7	185
	Percent assessed correctly			
	Healthy	99	G-Adjusted	47.2051
	Degraded	100	Chi-square value	10.828
	Total	99	Level of Significance	0.001

1 A value of 10-15 was added to the zero-valued cell in the contingency table to calculate the G value because the calculation involves a logarithm. The 100% correct for assessed degraded reflects the fact that all six pixels assessed as degraded were, in fact, degraded.

Hypothesis 0. (Random points as causes of marsh loss)

Before examining the stated hypotheses, the results of using randomly assigned pixels as an effect needs to be addressed. Figure 15 shows a clear relationship between probability of marsh loss and distance from randomly chosen points. What Figure 15 demonstrates is that the distribution of degraded pixels is

clumpy and that they are rare. Because total degradation is a rare event, (approximately 5% of the pixels are degraded) any randomly chosen location is likely to be far away from a degraded pixel. This graph has three notable sections. From 0 to about 100 meters there is no strong trend. From about 100 meters to 300 meters, there is a strong increase in probability of degradation (p(degradation)). After that point, there is very little continuing relationship. Three kilometers is the maximum distance possible from one of these random points in the marsh. This was tested on the Atlantic Coast marshes.

Hypothesis 1. (Roads as causes of marsh loss)

The probability of a parcel being completely open water will be negatively related to the distance of the parcel from a road, with the caveat that close to the road the marsh may be healthy for the reasons stated in Chapter 1. Therefore, the deleterious impact may be expected to start some distance from the road. This was tested on both the Atlantic Coastal region and the Bay Area. Regressions of the data for this hypothesis are shown in Figure 16 and Figure 17.

In both Figure 16 and Figure 17, the marsh nearest the road is the least likely to have degraded in the recent past. Contrasting Figure 16 and Figure 17 with Figure 15, p(degradation) increases immediately adjacent to the road but not next to the random pixels. The pattern remains coherent to a distance of 3 km in both Figure 16 and Figure 17, but this probably is because it is possible to be farther from a road in the marsh, then it is to be from one of the randomly chosen pixels. Overall, the regression of probability of marsh loss on distance from roads in the bay area does

not look significantly different from the random effects in Figure 15, except that the R^2 is lower. It also directly refutes the hypothesis.

One complication of the method used is that degradation that occurred prior to the NWI analysis must be included as existing open water. It is beyond the scope of this study to attempt to regress the landscape to what it was in some pristine state. Therefore, areas like Blackwater National Wildlife Refuge (BNWR), which show serious degradation close to the road, relative to 1938, will not show up as degraded areas in this study.

Bay Area

For the bays, the distance to maximum degradation is about 400 meters. Figure 18, Figure 19 and Figure 20 show close ups of two areas. In Figure 18 and Figure 20 p(degradation) data are mapped. Each figure has a hypothetical transect, marked with various distances. In Figure 18, the two lines mark the beginning and the end of the plateau in Figure 16. There seems to be some impact up to about three kilometers. After that, the graph (Figure 16) no longer forms a coherent line, although there is still a strong increase in marsh degradation with distance. Figure 18 and Figure 20 map the wide swings in probability of loss after that distance.

Figure 19 is the same area as Figure 18, but in this figure the marsh health index is shown. The two-hatched boxes represent the approximate bounds of the data "plateau". The box to the east of Shorter's Wharf Road clearly captures the bulk of the recent marsh loss in that direction. There is less loss to the west of the road, but much of it is captured by the box on that side. Just to the west of this map, however,

is a large area of marsh loss in the midst of the lake in BNWR. This probably accounts in part for the scatter towards the right side of the graph in Figure 16.

Atlantic Coast

Figure 17 shows a similar result with marsh health decreasing with distance from the road until a dramatic shift in probability of loss at about 3 km. It is quite tempting to attribute this result to the same factors as in the bays. However, an examination of the available data leads to the conclusion that this is a result of other correlates discussed below.

Figure 21 shows a typical coastal marsh. Many of them form narrow strips along the shoreward side of barrier islands, or strips along the coast of the mainland. Typically, they have much more of their total edge open to a large body of water than the estuarine marshes of the bays. This means that is unlikely for hydrological impacts from a road to spread very far. The transect along the small island in Figure 21 makes this point.

The roads in the Atlantic Coast area themselves are different in that they are usually closely associated with upland areas so it is quite natural that the marsh will be healthy near the road. Presumably, the road was built there because the marsh was stable. In Figure 22, there are numerous roads with marsh on both sides connecting the mainland and the barrier islands between Cape May and Great Egg Harbor. Examination of aerial photos and USGS orthophotoquads indicates that there may be more marsh present than is seen in the Coastal Marsh Project/NWI dataset. However, the roads do form points of stability in the marsh so the marsh immediately adjacent

to them is healthy. This is an area heavily managed by humans, so the result may not be incidental. Because the marshes are healthy near the roads, it then must follow that degraded areas are going to be further away and this will produce the trend seen in Figure 17.

Figure 22 also shows the mainland marshes south of Great Egg Harbor. These marshes exhibit some of the longest distances from a road to the end of the marsh in this dataset. However, the roads are far up in the marsh. Note the position of Route 585 where it crosses the marsh. It may have some influence in limiting freshwater input into the lower marsh, but it stretches credulity to imagine that it could have an impact on areas bordering the major river 8 kilometers away. It may well be a factor in the degradation upstream, however, if it prevents drainage from the upper marsh areas.

Figure 22 also illustrates another interesting feature of this analysis. There are roads crossing the marsh farther upstream than Route 585 but they do not show up in this analysis. That is because Route 585 would have been considered a solid barrier to water movement and therefore, even though the roads cross the marsh upstream, they would not be shown to impact the ebb and flow of tidal waters.

An additional complication of the method is that there is an inherent decrease in the amount of data available at longer distances. Every grid cell on a road has at least one and possibly two grid cells in the surrounding marsh that are closer to it than to any other grid cell on the road. This means that for extreme distances only a few marshes, or perhaps one, will dominate the characterization of the marsh. In this

case, the marsh on Great Egg Harbor and two in North Carolina seem to dominate this measurement.

Conclusion to Hypothesis 1

The evidence for the estuarine marshes of the Delaware and Chesapeake Bays does not support the hypothesis and are indistinguishable from random inputs. For the Atlantic coast marshes, the evidence would suggest that roads do not have any demonstrable negative impact on the surrounding marshes and may serve to stabilize them.

Hypothesis 2. (Distance from large tidal streams)

The probability of a parcel being completely open water will be positively related to the distance of the parcel from the nearest tidal creek. Tidal creeks were defined as those that occupied in excess of one pixel width for their entire length and were present in the NWI data.

Bay Area

Figure 23 shows two strong trends. At the immediate creek edge, the marsh is more degraded and p(degradation) drops quickly for about 150 meters. Immediately next to the water body, this is probably an artifact of misregistration and the impossibility of spectrally distinguishing the water in the river from ponds on the marsh. Often there are degraded areas immediately behind the levee of a river, and these may be responsible for the higher level of degradation at 50 – 100 meters from the creek edge. From 250 meters to 3 km the anticipated increase in p(degradation) toward the interior of the marsh occurs. The two regression lines drawn represent the

two independent processes operating on marsh degradation with respect to sources of water. After 3 km, there is no longer a discernible pattern. Figure 24 shows the pattern of calculated degradation for the entire two bay area. Predictably, BNWR appears as a very degraded area. In Figure 25 and Figure 26, the tidal stream effects-related loss can be compared directly to the Coastal Marsh Project output. There is a good deal of correspondence, particularly in the upper reaches of the streams. It is not expected that there would be a perfect match.

Atlantic Coast

Figure 27 shows the result of regressing the ln(probability of being open water) on the ln(distance from the nearest tidal creek or water source). This is a very strong regression, showing continual declines in p(degradation) over the entire breadth of the marsh. This graph shows quite powerfully that Figure 15 is not the only possible outcome and that real effects are being detected. The Atlantic Coast marshes appear very wet at the edges and get healthier going inland for about 800 meters, on average. This does not agree with the hypothesis. The bulk of the marshes in this category have their edges almost entirely exposed to open bays rather than tidal streams, or other wetlands or uplands (Figure 28). This large exposure means that areas being actively eroded, plus edge placement error will account for much of the marsh degradation. The tidal regimes tend to be different for these marshes as well, with the tidal ranges being somewhat higher along the ocean coast (Appendix B). The marshes therefore have fewer tidal streams with levees per unit

area, relative to the amount of higher energy tides, than the inland marshes of the bay area.

A close up of the North Carolina coast south of Cape Lookout shows more clearly what is happening in these coastal marshes (Figure 29). The distance from the edge to the center of the largest marsh (center of map) is approximately 800 meters. In fact, the distance from the edge to center of many of these marshes tends to be in the 0.5 to 3 km range. The next range of distances appears to be dominated by some extreme areas in the Great Egg Harbor area.

Conclusion

The hypothesis is supported for the bay area, but is rejected for the Atlantic Coastal area. This may be related to the fact that the Atlantic Coast marshes are substantially different from the Chesapeake and Delaware marshes in size, tidal creek development and exposure to edge erosion.

Hypothesis 3. (Distance upstream as a cause of loss)

The probability of a parcel being completely open water will be negatively related to the distance the upstream of the marsh system that contains the parcel. This hypothesis, resting on the assumption that sea level rise is driving coastal marsh loss, is well supported in both regions.

Bay Area

Taking the bay area first (Figure 30), there is a general trend toward decreased degradation going from the downstream extreme of each river system to the farthest

reach of estuarine marsh. An overview of the entire area (Figure 31) shows that the pattern is followed closely in areas near to the shore. The rivers of the Chesapeake Bay, which are much longer than those of the Delaware Bay, show a repeated fluctuation in degradation with increased distance upstream. Certainly, there are fluctuations in every river system; however, that these fluctuations make a consistent pattern, rather than averaging to the mean line, indicates that there is potentially some driver that operates on many river systems, such as where the maximum tidal sediment delivery occurs. Figure 32 compares the conditions at several upstream distances on the Choptank and Nanticoke Rivers.

The wide disparity in river lengths allows the Potomac River to dominate the entire pattern for any distances over about 70 kilometers. In other cases, there is no expectation that there will be real impacts at distances of 70 or more kilometers with many of the effects being studied in this paper. However, in this case the effect is caused by the rivers as they import both tidal water and fresh water to the borders of the wetlands. Therefore, impacts can be reasonably connected to the effect of distance upstream. However, when only one river system is involved, it hardly poses any general effects. Furthermore, as the mean is driven by fewer and fewer actual marsh parcels, the data cease forming a coherent line.

Atlantic Coast

The data for the Atlantic Coast support the hypothesis that distance upstream impacts marsh health (Figure 33). The regression closely resembles the regression for the bay areas. The narrowness of the Atlantic marshes and nearness to sea level,

however, puts most of them in the category of high probability of being open water (Figure 34) based on effect of distance upstream. The marsh systems up some river systems are likely to be healthy based on this factor. Because the barrier islands force Currituck Sound and Chincoteague Bay to be long and narrow, the back-barrier marshes will appear to be upstream from the inlets through the barrier islands. The upstream assessment indicates that marshes that are farther upstream are likely to be healthy.

Conclusion

The hypothesis that marsh health is related to distance upstream is supported for both systems. This conclusion also supports the hypothesis that sea level rise is a driving factor in marsh loss.

Hypothesis 4. (Distance from upland as a cause of loss)

The probability of a parcel being completely open water will be positively related to the distance of the parcel from the upland. For the purposes of this study, although the term upland is used, in actuality it is distance from whatever is in the "other" (see map legends) class that could be anything except for the wetland type under consideration. Much of the estuarine marsh in BNWR borders on forested swampland. This will be different from upland, but it will provide two of the effects of upland that are postulated here to benefit marshes. First, swamps can act as a source of freshwater to the downstream marsh. Secondly, as the swamp substrate is solid enough to support trees, it must be reasonably stable. The distance to the nearest upland could have been calculated using the uplands and measuring across the

freshwater swamps and marshes, but this study was more interested in what was happening in the estuarine marshes. Therefore, the bounds of the data in the Coastal Marsh Project were used as the marsh boundaries.

Bay Area

There is a strong regression of ln(probability of being open water) on ln(distance from an upland area. The first point (Figure 35) probably reflects edge error artifacts, and that point could have been omitted from the regression as an outlier. A cursory glance at Figure 36 shows how clear this effect is. The BNWR, Nanticoke River area, and the marsh islands all stand out in this map, which is correct, as they are hotspots of marsh loss. The marshes along the York River (Figure 37) show that this loss is focused on either the seaward edge or interior of the marsh.

Atlantic Coast

Of the effects examined in this paper, this is one of the most important for the Atlantic Coast (Figure 38). Like the bay area marshes, this effect ends at approximately 3 km, meaning that 3 km is the longest distance you can go in a coastal marsh from an upland area. There is an interesting result at about 500 meters, where the steady increase in deterioration is suddenly reversed briefly. This is especially interesting because it matches a similar feature in Figure 27. This is the distance from the edge to the center of many of the small back barrier marshes and it seems to represent the upper size limit for many of the Atlantic Coast marshes.

In Figure 39, the general location of the most deteriorated marshes can be seen. Besides the usual locations at Great Egg Harbor and near Cape Lookout, there

is a major area of deterioration north of Cape Charles. Close examination of this marsh system (Figure 40) shows that any point there has a very high probability of being open water. The very high probability value of -0.000042 likely reflects the tip of a single marsh that is heavily degraded.

Conclusion

The hypothesis that distance from upland is strongly correlated with marsh loss is strongly supported for both systems.

Hypothesis 5:

The probability of a parcel being completely open water will be negatively related to the size of the marsh parcel containing the grid cell.

Bay Area

The regression here is much less clear (5-27). The data clearly suggests that there is a little trend up to about e10 meters or 22 hectares, after which the trend is toward more deterioration with increasing size. This is likely driven by interior ponding, which increases as the marsh interior gets farther from the edge.

The distribution of these marshes around the bay area is much different from for the other effects (Figure 42). The previous effects tended to show up in bands. The large tract of marsh south of BNWR is assessed as very healthy, which it is, and the peninsula between the Nanticoke River and Fishing Bay is assessed to be moderately deteriorated, which is same assessment as made by the Coastal Marsh Project data, although parts of it are heavily degraded.

Atlantic Coast

The Atlantic Coast shows a more pronounced shift from low probability of deterioration, to a high level at mid-sized marshes (162 hectares) and then drops precipitously again (Figure 43).

In contrast to the Bay area marshes, most of the Atlantic marshes fall in the low probability of deterioration category (Figure 44). Notable exceptions are the area north of Cape May and the area near Cape Lookout and Cape Hatteras. These areas seem to show up relatively often.

Conclusion**

The hypothesis that probability of being open water will decrease with increasing marsh size is clearly not supported. This hypothesis, however, was included to test whether studies done in one size of a marsh would be applicable to marshes of different sizes. These data would indicate that there are other factors that are more critical in determining whether results of work in one marsh are transferable to another.

Comparison of Effects

The five effects have been examined in isolation. Before moving to creating a model, it is useful to know how the models relate to each other. In examining Figure 45 and Figure 46, a few caveats are in order. The five effects measured here are grouping broad areas of the study area together and calculating an expected value for the entire category. Although some places may be expected to have similar probabilities of being open water under different effects, the likelihood that there will

be an exact correspondence is low. Second, although all the scales run from low probability to high probability, the maximum and minimum for each effect is unique, so an actual equal probability of deterioration may be colored differently for different effects. In addition, not every area of marsh is connected to a road. Areas that are not directly connected to a road will not be represented on the map showing road effects.

The data for each study area is arranged in 6 windows. The first window is the Coastal Marsh Project data reduced to a categorization of either totally degraded (magenta) or not totally degraded (green). This is the data on which all the rest of the analysis in this chapter is based. Each of the other windows has a key word to identify the effect being represented and they are arranged (left to right, top to bottom) in the same sequence as in the preceding discussion.

Bay Area

The maps (Figure 45) are focused on the area including BNWR and the Nanticoke River. Common features include peninsula west of the Nanticoke River being classified as moderately likely to be degraded. The area in BNWR that features a large number of degraded points in the CMP map is consistently classified as degraded. The Wingate area has a variety of classifications, but in most cases it is classified as less likely to be degraded than the area of BNWR. Similarly, the area west of BNWR has a variety of classifications, but is consistently healthier than BNWR and is about the same as Wingate.

Atlantic Coast

This area of the outer banks (Figure 46) is shown in fine detail. The areas labeled A, B, and C tend to be the focus of degradation, although the exact pattern varies. The marsh at C is clearly highly degraded, but only shows up in some scenes. The south end of marsh B is also highly degraded (as shown by the concentration of magenta points in the CMP frame) and is consistently assessed to be degraded in the other views. The water effect is clearly not consistent with the other map views, because the model shows degradation around the water's edge of all these marshes, whether or not the marsh shows deterioration overall.

Conclusion

The evidence given in the preceding sections supports the data in Table 7. This kind of signal processing technique clearly produces regressions that indicate that most of the effects studied have consistent, demonstrable influences on coastal marshes, whether in the major bays or on the Atlantic Coast. This does not, however, make them particularly good assessors individually because there is too much variability introduced by the other factors. Having shown that there are individual influences, the next step is to combine them into a model. The effects as studied here cannot, however, be put directly into a model because the response variable is calculated by zones defined by the test variable. Therefore, each response variable is unique to its test and they cannot be combined. In Chapter 6, a model will be discussed that does use a single response variable.

Table 7. Results of Hypothesis Tests			
Area	Hypothesis	Correlation	Conclusion
Bay	Distance from Roads	Negative	Rejected
Atlantic		Negative	Rejected
Bay	Distance from Tidal Creeks	Positive	Not rejected
Atlantic		Positive	Rejected
Bay	Distan		
Atlantic			
Bay	Distan		
Atlantic			
Bay	Area		
Atlantic			

Figure 14. Health Status of Mars

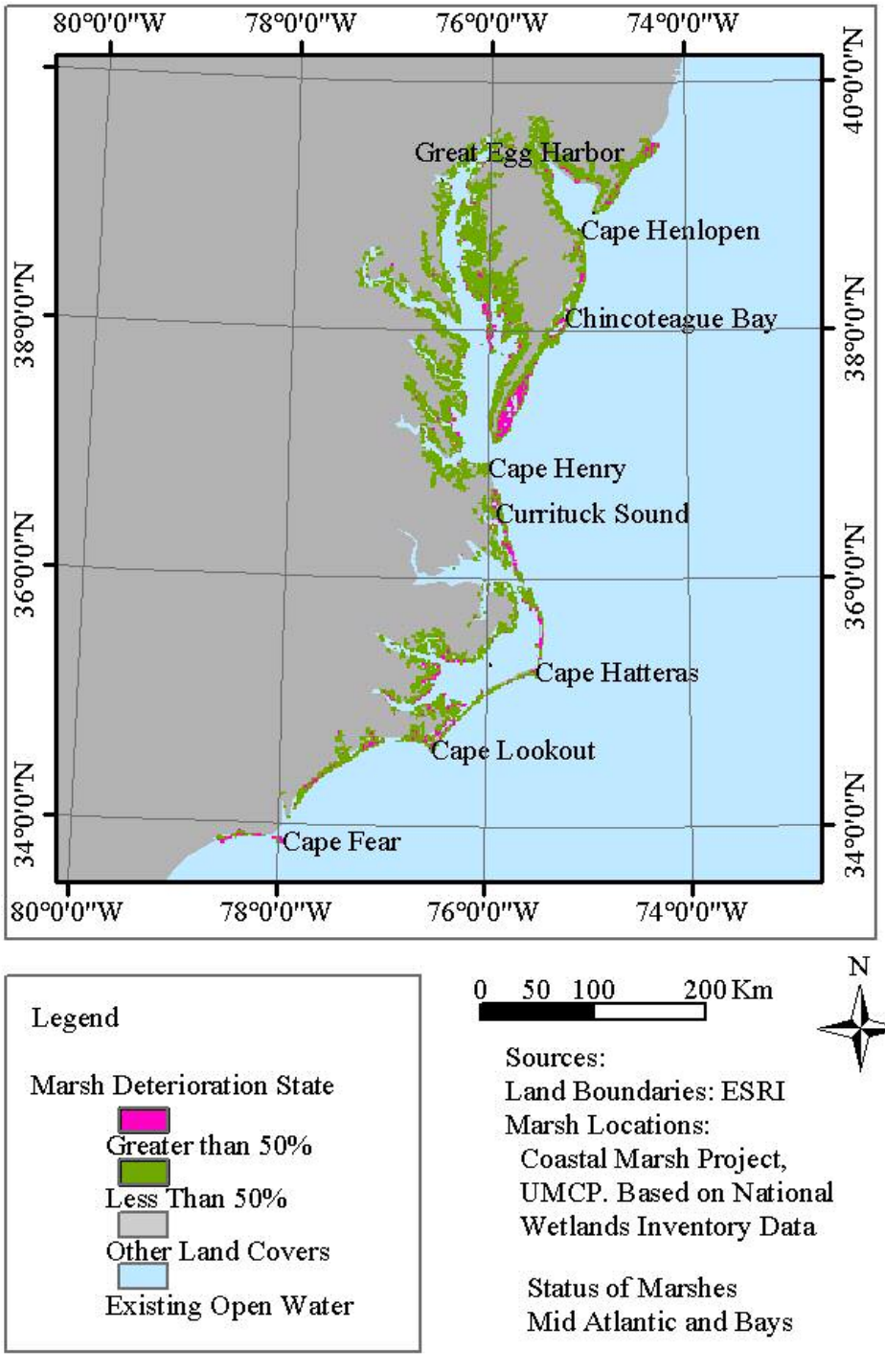

hes in the MidAtlantic Region

Marsh health status based on Coastal Marsh Project data, but reduced to two categories. This categorization is the basis for the data in this chapter.

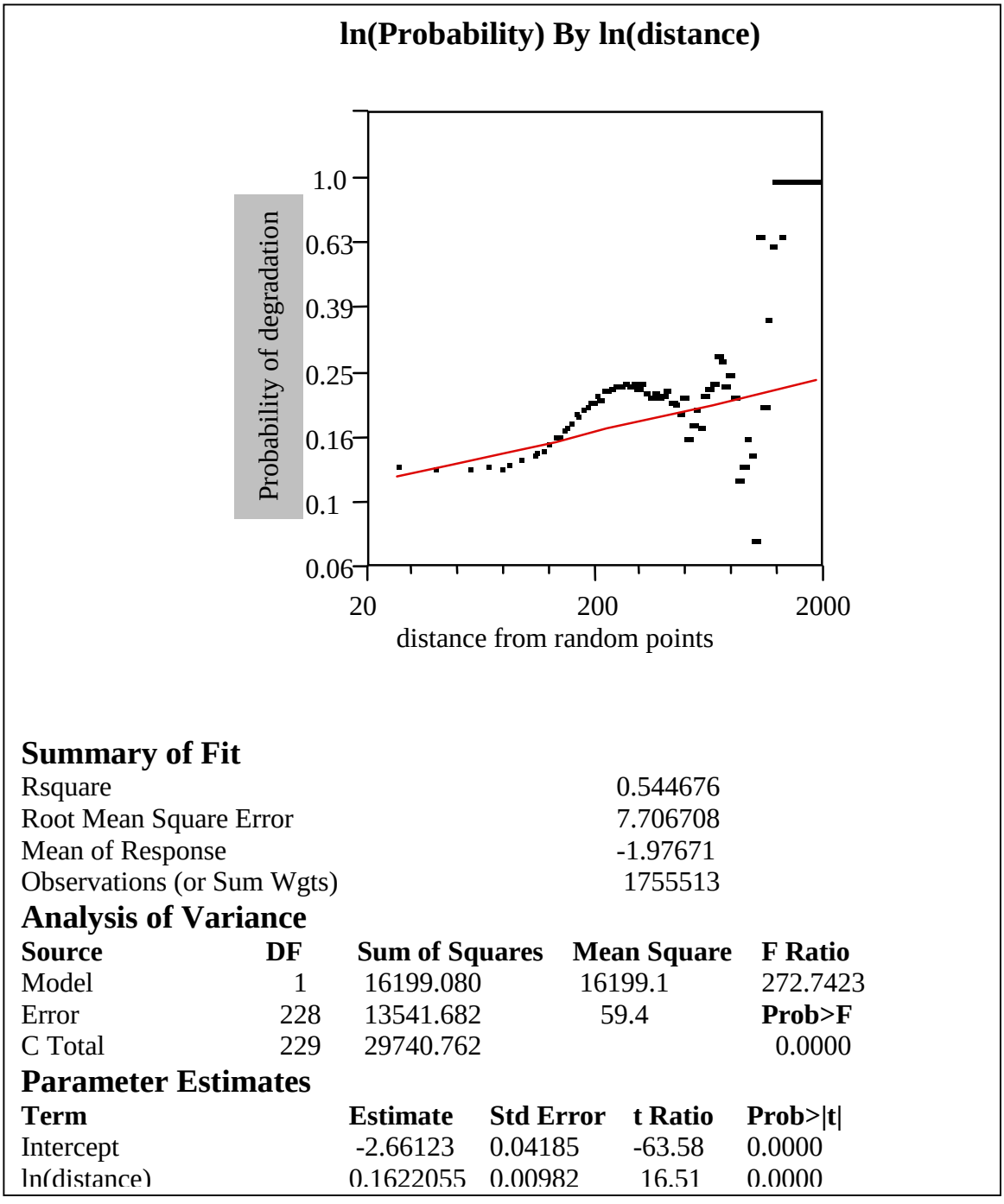

Summary of Fit

Rsquare	0.544676
Root Mean Square Error	7.706708
Mean of Response	-1.97671
Observations (or Sum Wgts)	1755513

Analysis of Variance

Source	DF	Sum of Squares	Mean Square	F Ratio
Model	1	16199.080	16199.1	272.7423
Error	228	13541.682	59.4	**Prob>F**
C Total	229	29740.762		0.0000

Parameter Estimates

Term	Estimate	Std Error	t Ratio	Prob>|t|
Intercept	-2.66123	0.04185	-63.58	0.0000
ln(distance)	0.1622055	0.00982	16.51	0.0000

Figure 15. Effect of non-random distribution of degraded areas in the Atlantic Coast marshes.

This graph shows the increase in probability of degradation with distance from a set of randomly selected points in the marshes.

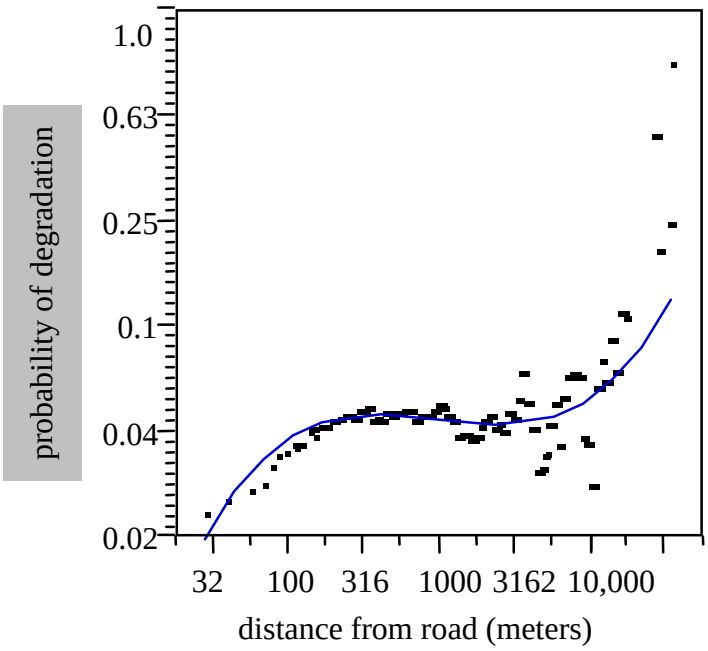

Polynomial Fit, degree=3

Summary of Fit

Rsquare	0.419392
Root Mean Square Error	8.360856
Mean of Response	-3.11847
Observations (or Sum Wgts)	1505282

Analysis of Variance

Source	DF	Sum of Squares	Mean Square	F Ratio
Model	3	26357.824	8785.94	125.6860
Error	522	36489.845	69.90	Prob>F
C Total	525	62847.669		0.0000

Parameter Estimates

Term	Estimate	Std Error	t Ratio	Prob>|t|
Intercept	-12.16941	0.51021	-23.85	0.0000
ln(distance)	4.0891227	0.24125	16.95	0.0000
ln(distance)^2	-0.602365	0.03703	-16.26	0.0000
ln(distance)^3	0.0290202	0.00185	15.69	0.0000

Figure 16. Distance from Roads vs. Marsh Loss in the Bays.

This graph shows the increase in probability of degradation with distance from the nearest road.

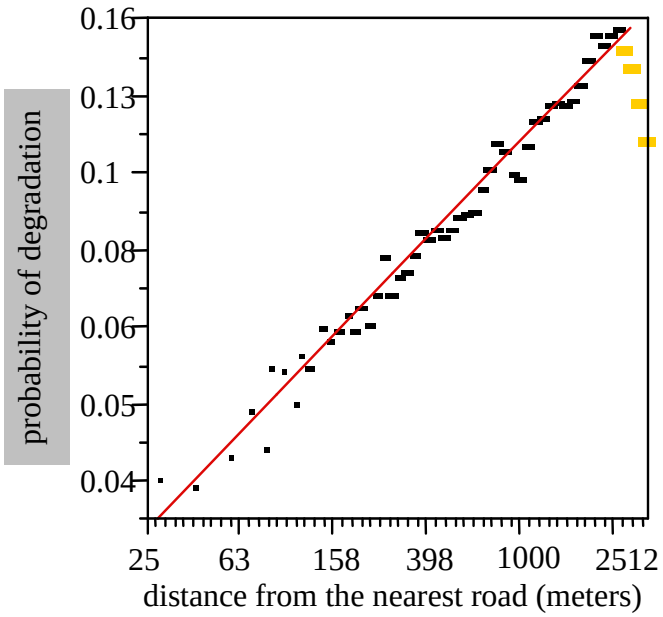

Summary of Fit

Rsquare	0.97685
Root Mean Square Error	2.321977
Mean of Response	-2.31912
Observations (or Sum Wgts)	688896

Analysis of Variance

Source	DF	Sum of Squares	Mean Square	F Ratio
Model	1	66658.045	66658.0	12363.37
Error	293	1579.732	5.4	Prob>F
C Total	294	68237.777		0.0000

Parameter Estimates

Term	Estimate	Std Error	t Ratio	Prob>|t|
Intercept	-4.403214	0.01895	-232.3	0.0000
ln(distance)	0.3143178	0.00283	111.19	0.0000

Figure 17. Distance from Roads vs. Marsh Loss on the Atlantic Coast.

This figure shows the regression of probability of marsh loss on distance from the nearest point on a road in the marsh to a point in the marsh. Only the black points are used in the regression.

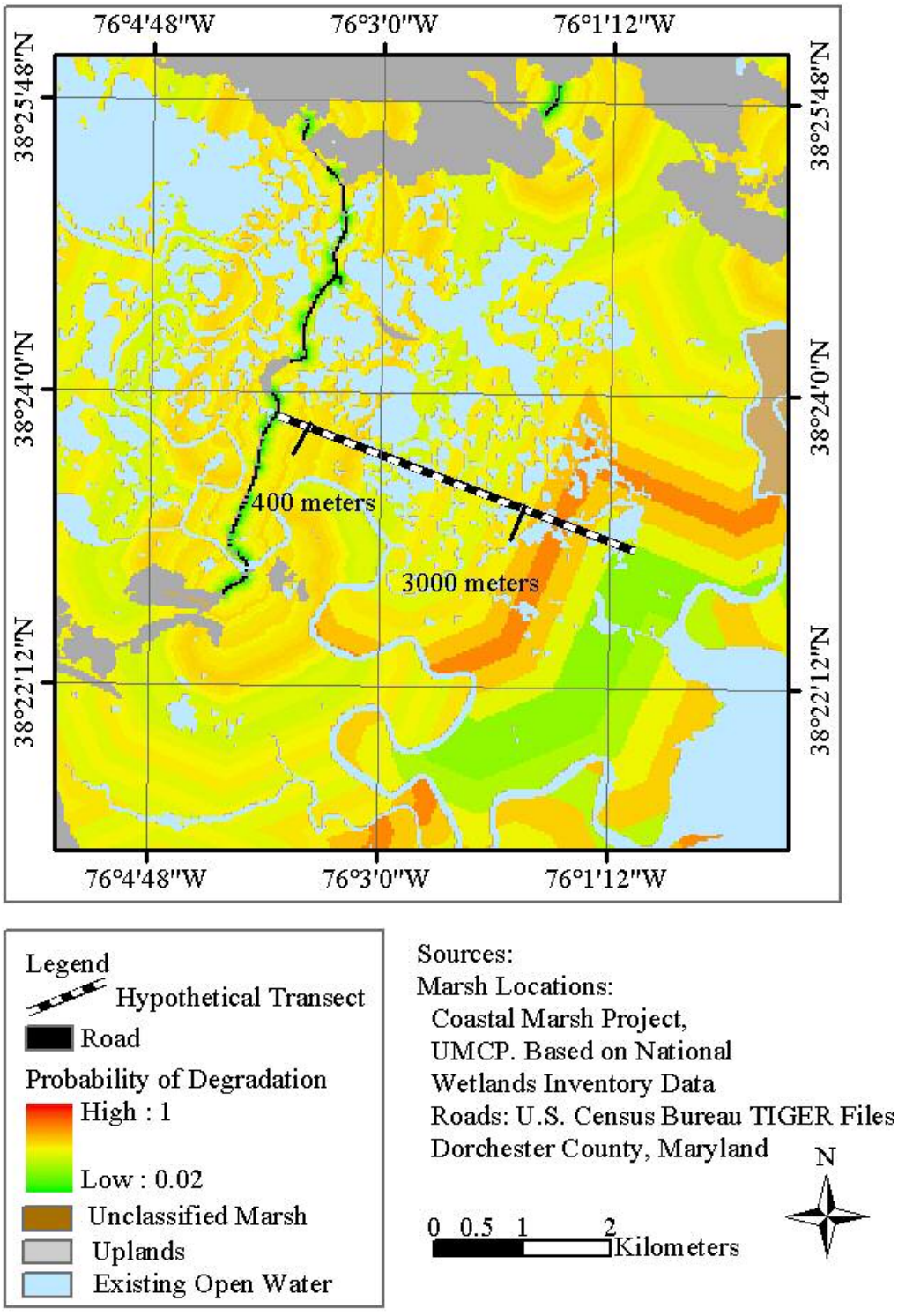

Figure 18. Expected Marsh Loss in BNWR as a Function of Distance from the Nearest Road

The colored bands represent the probability of loss in each distance zone.

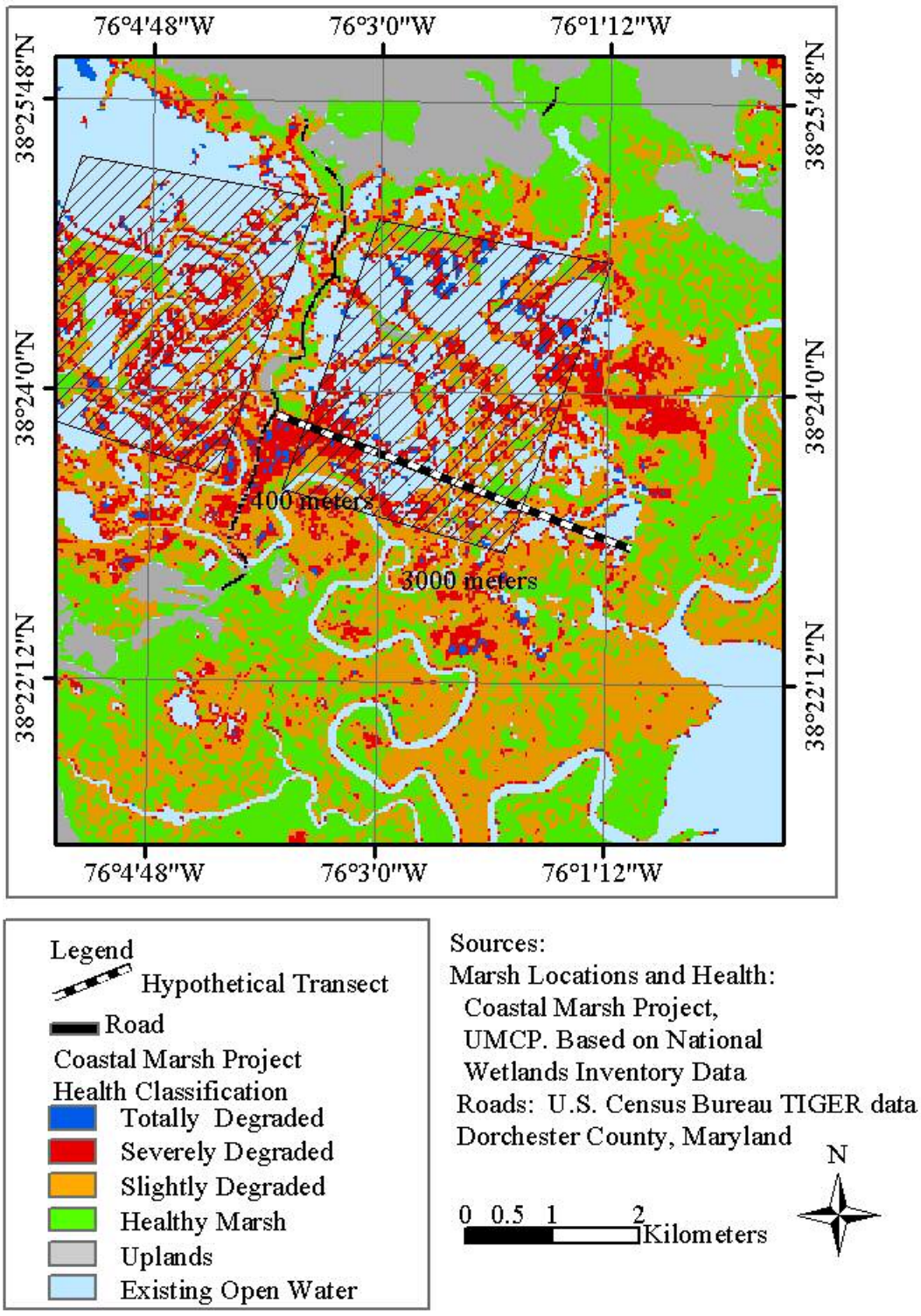

Figure 19. Marsh loss in BNWR as estimated by the Coastal Marsh Project.

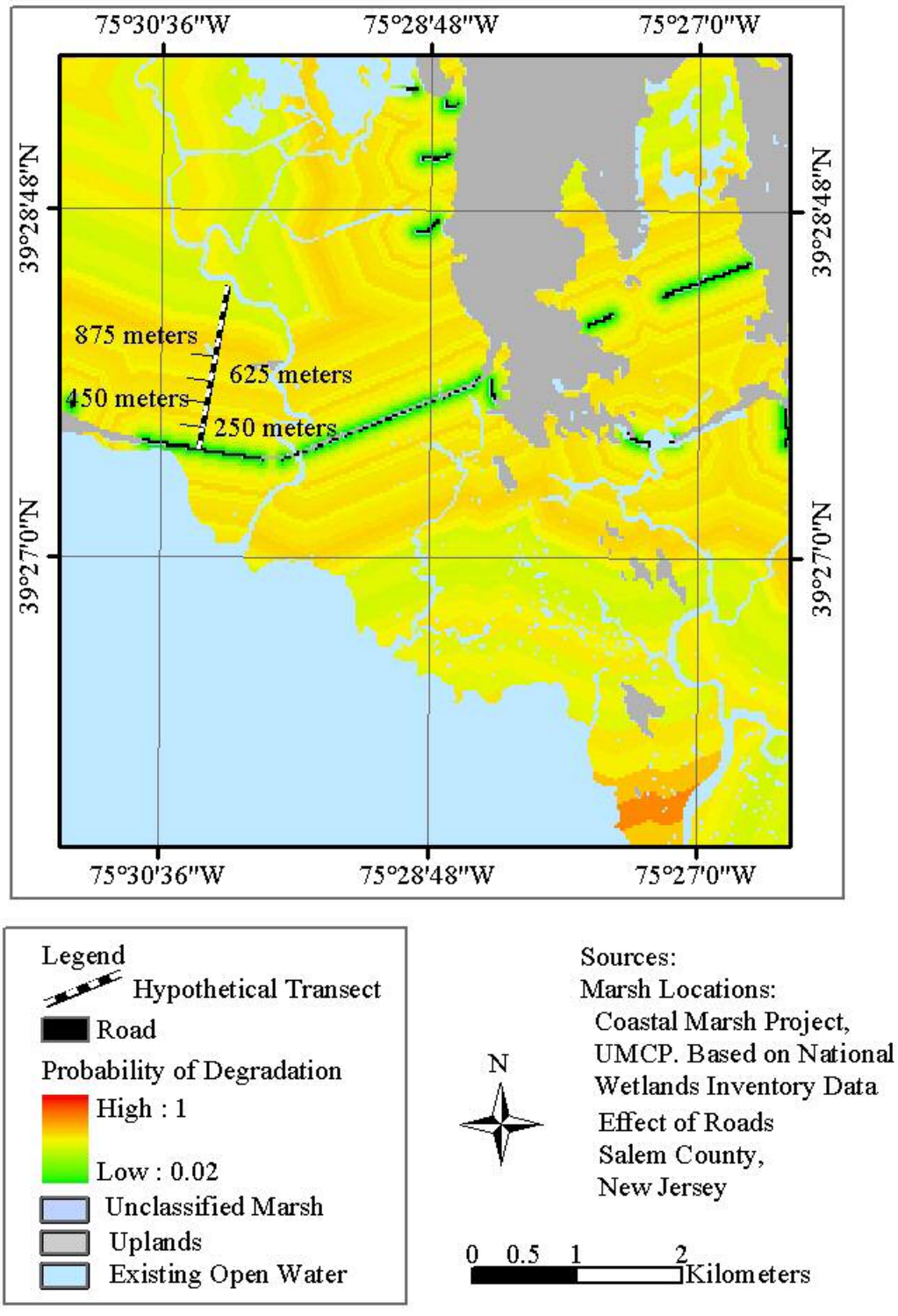

Figure 20. Expected marsh loss related to distance from the nearest road.

This figure shows the probability of marsh loss in various distance zones from the roads on the New Jersey coast.

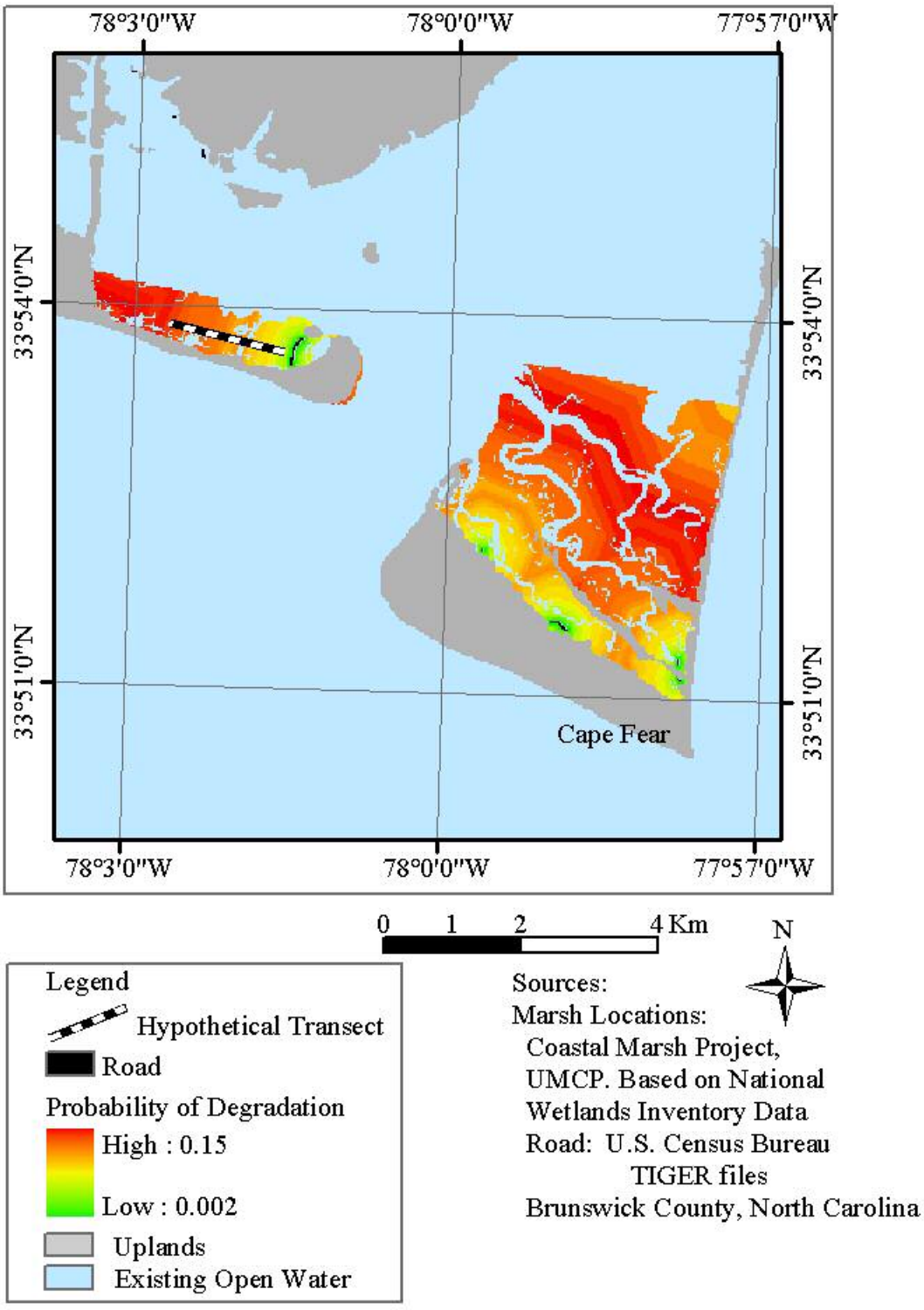

Figure 21. Expected marsh loss related to distance from the nearest road.

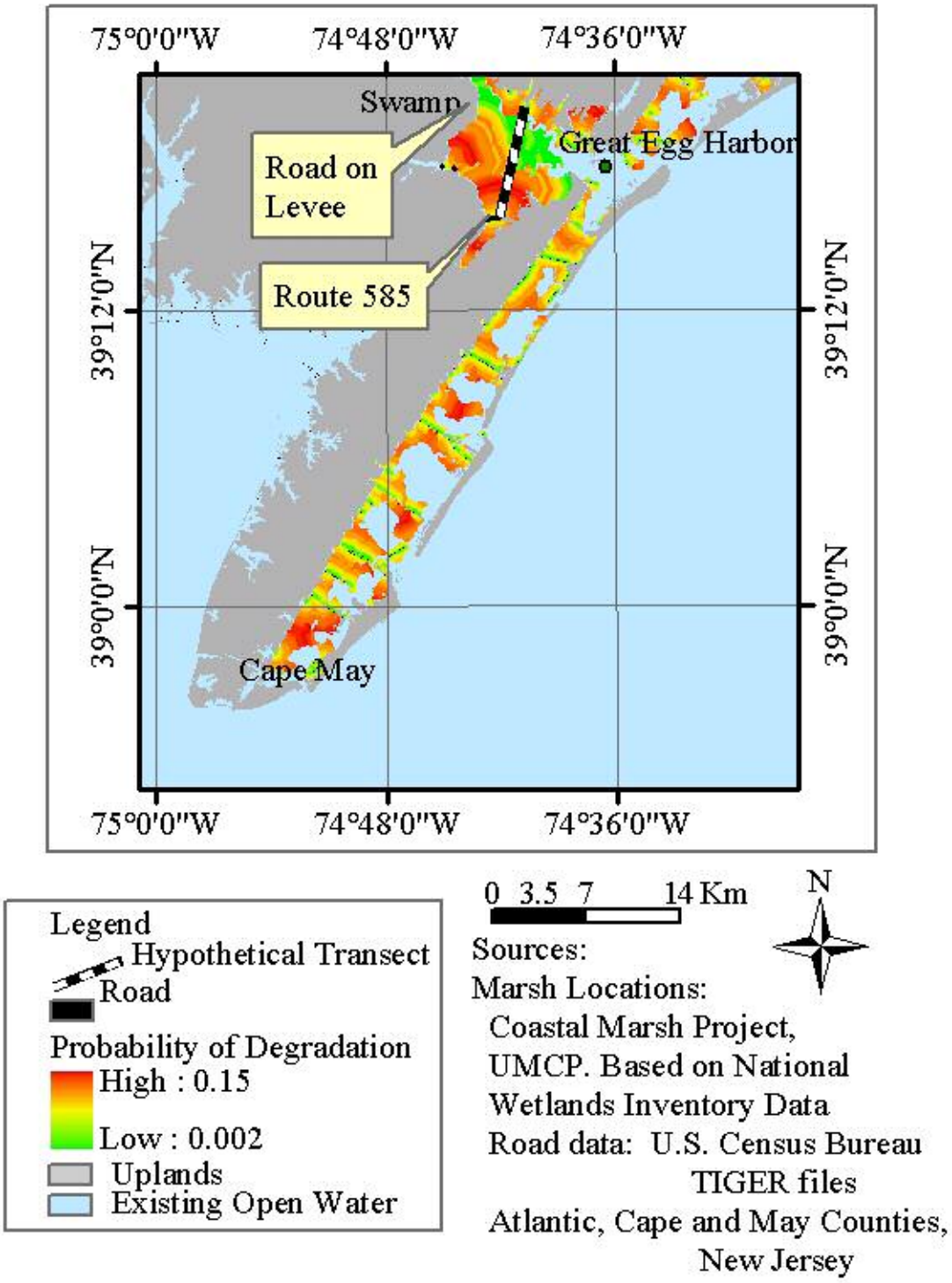

Figure 22. Expected marsh loss related to distance from the nearest road.

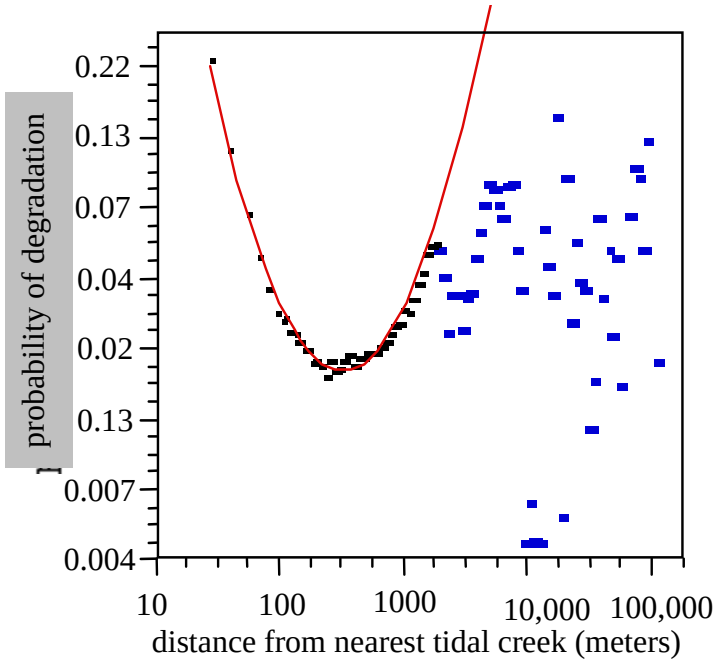

Polynomial Fit, degree=2

Summary of Fit

Rsquare	0.990931
Root Mean Square Error	2.465099
Mean of Response	-1.46827
Observations (or Sum Wgts)	1761712

Analysis of Variance

Source	DF	Sum of Squares	Mean Square	F Ratio
Model	2	161342.89	80671.4	13275.5
Error	243	1476.64	6.1	Prob>F
C Total	245	162819.54		0.0000

Parameter Estimates

Term	Estimate	Std Error	t Ratio	Prob>|t|
Intercept	4.1717618	0.03692	112.98	0.0000
log10(distance)	-4.663207	0.03226	-144.6	0.0000
log10(distance)^2	0.9210766	0.0068	135.51	0.0000

Figure 23. Effect of tidal creeks in the Chesapeake and Delaware Bays

Only the black points were used in the regression. The figure shows that from 100 – 1000 meters from the creek the marsh health deteriorates.

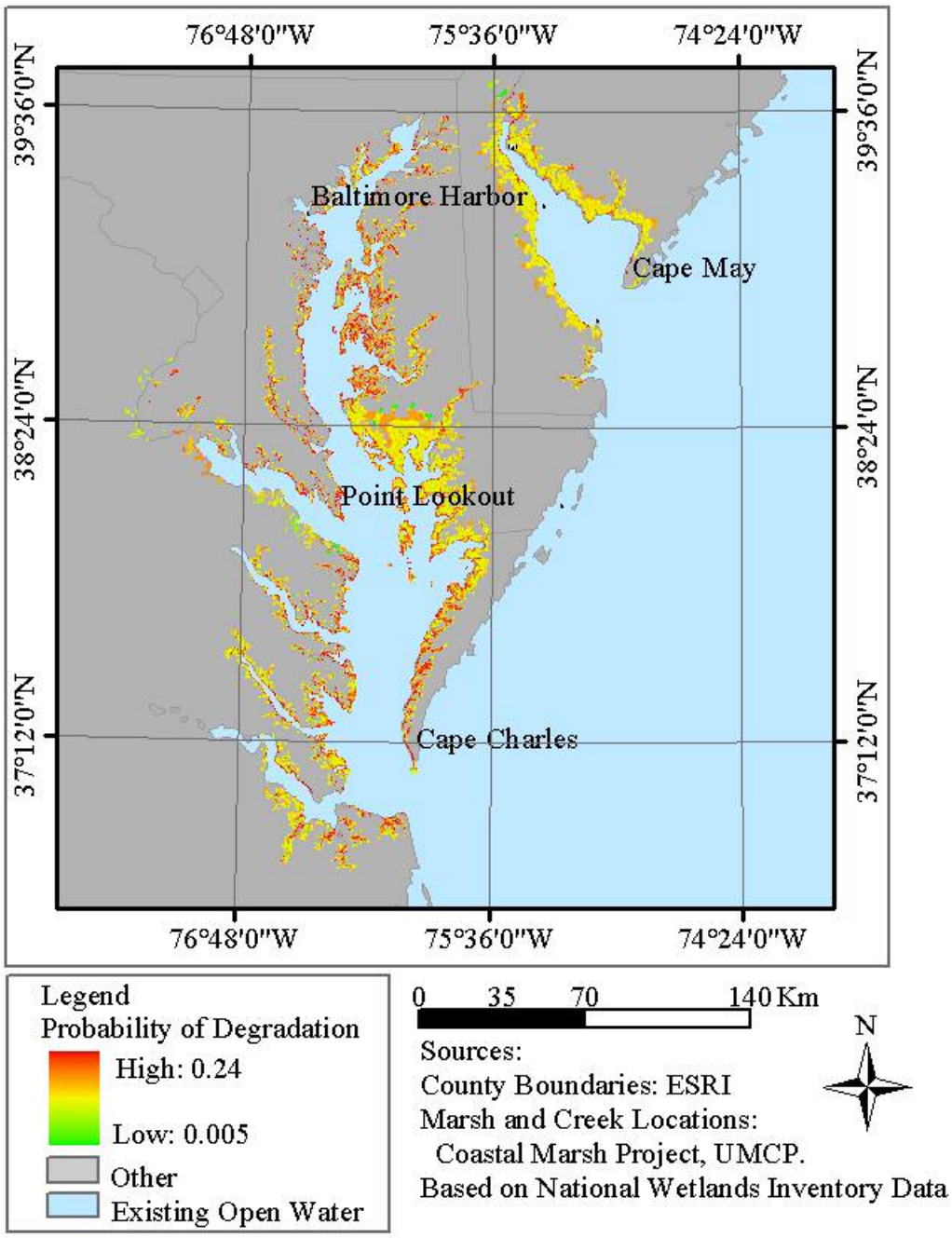

Figure 24. Probability of marsh loss as a function of distance from the nearest tidal creek in the Chesapeake and Delaware Bay area.

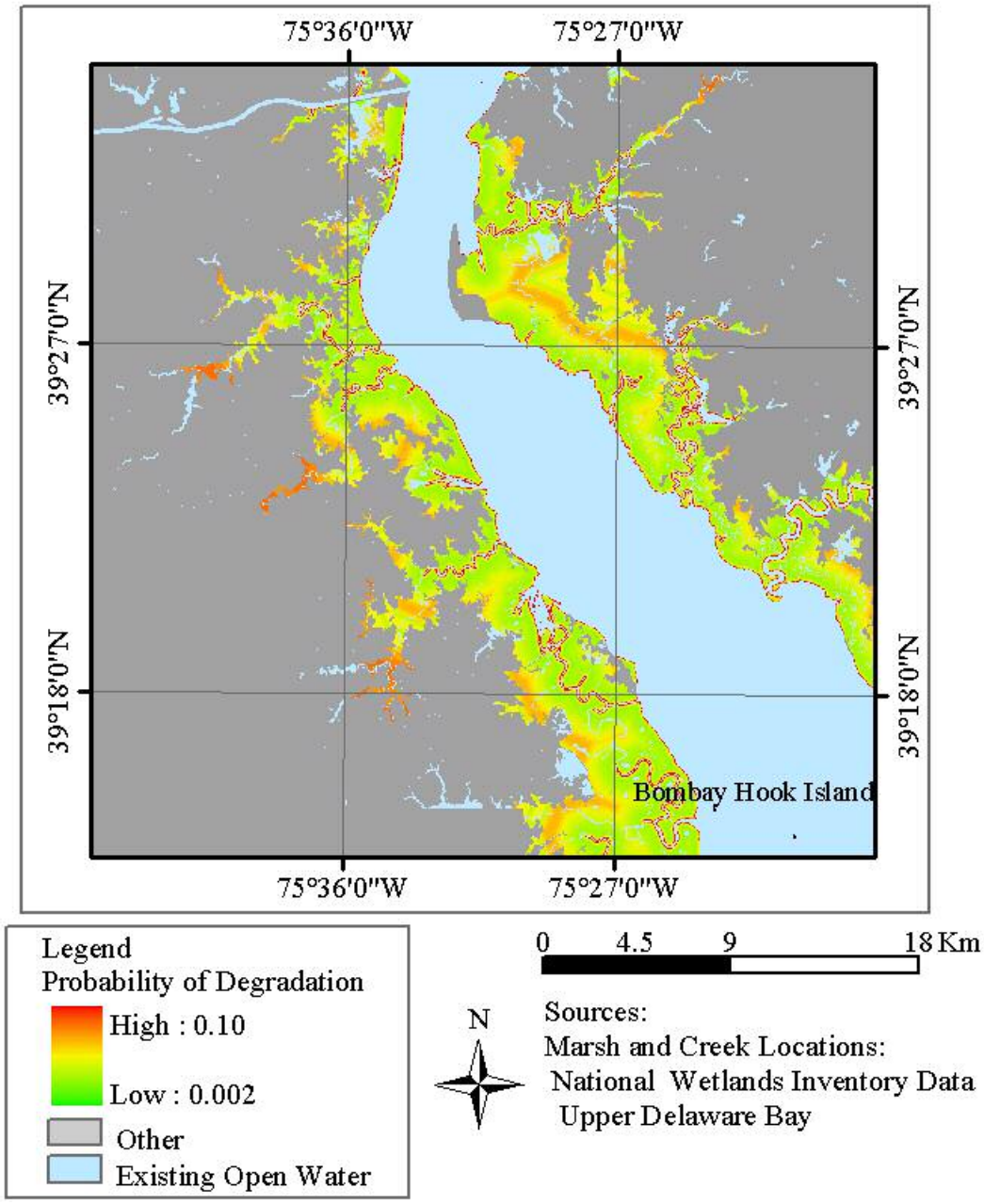

Figure 25. Probability of marsh loss as a function of distance from the nearest tidal creek in upper Delaware Bay marshes.

This is calculated as specified in Chapter 4.

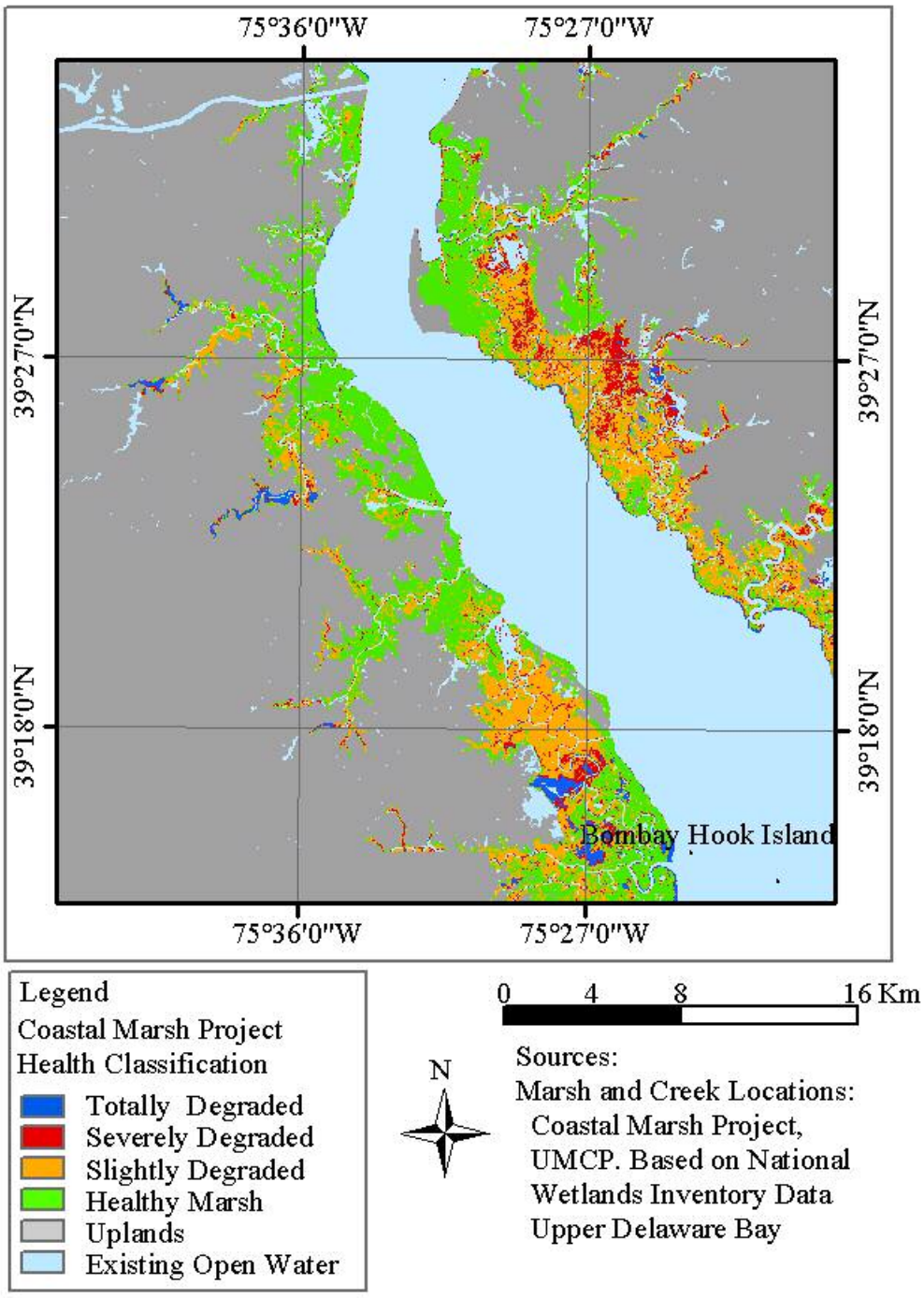

Figure 26. Marsh loss calculated from Thematic Mapper imagery for the upper Delaware Bay marshes.

Data was calculated by the Coastal Marsh Project as discussed in Chapters 3 and 4.

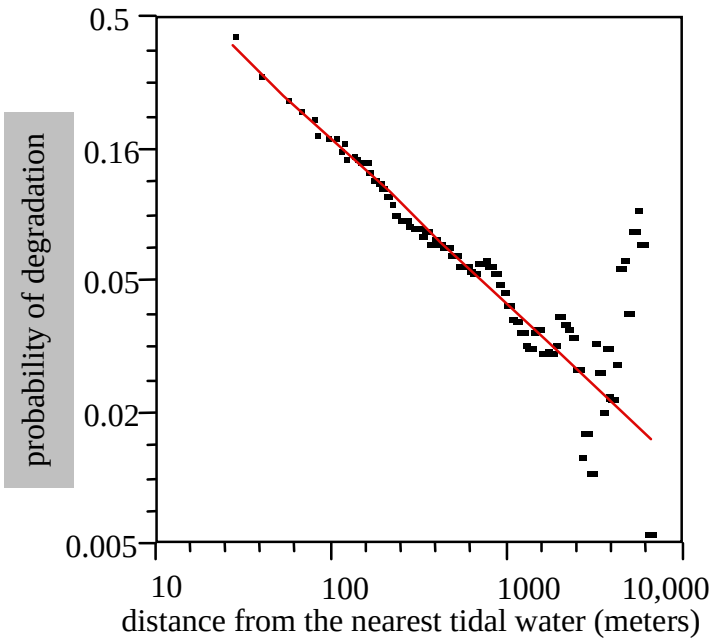

Linear Fit

Summary of Fit

Rsquare	0.971589
Root Mean Square Error	8.718909
Mean of Response	-2.21375
Observations (or Sum Wgts)	1862093

Analysis of Variance

Source	DF	Sum of Squares	Mean Square	F Ratio
Model	1	1029471.9	1029472	13542.23
Error	396	30103.7	76	**Prob>F**
C Total	397	1059575.6		0.0000

Parameter Estimates

Term	Estimate	Std Error	t Ratio	Prob>|t|
Intercept	1.1527794	0.02963	38.91	0.0000

Figure 27. Regression of Probability of Marsh Degradation on Distance from Tidal Creeks on the Atlantic Coast.

The regression shows that the hypothesis of marsh loss increasing away from tidal creeks is not supported for the Atlantic Coast.

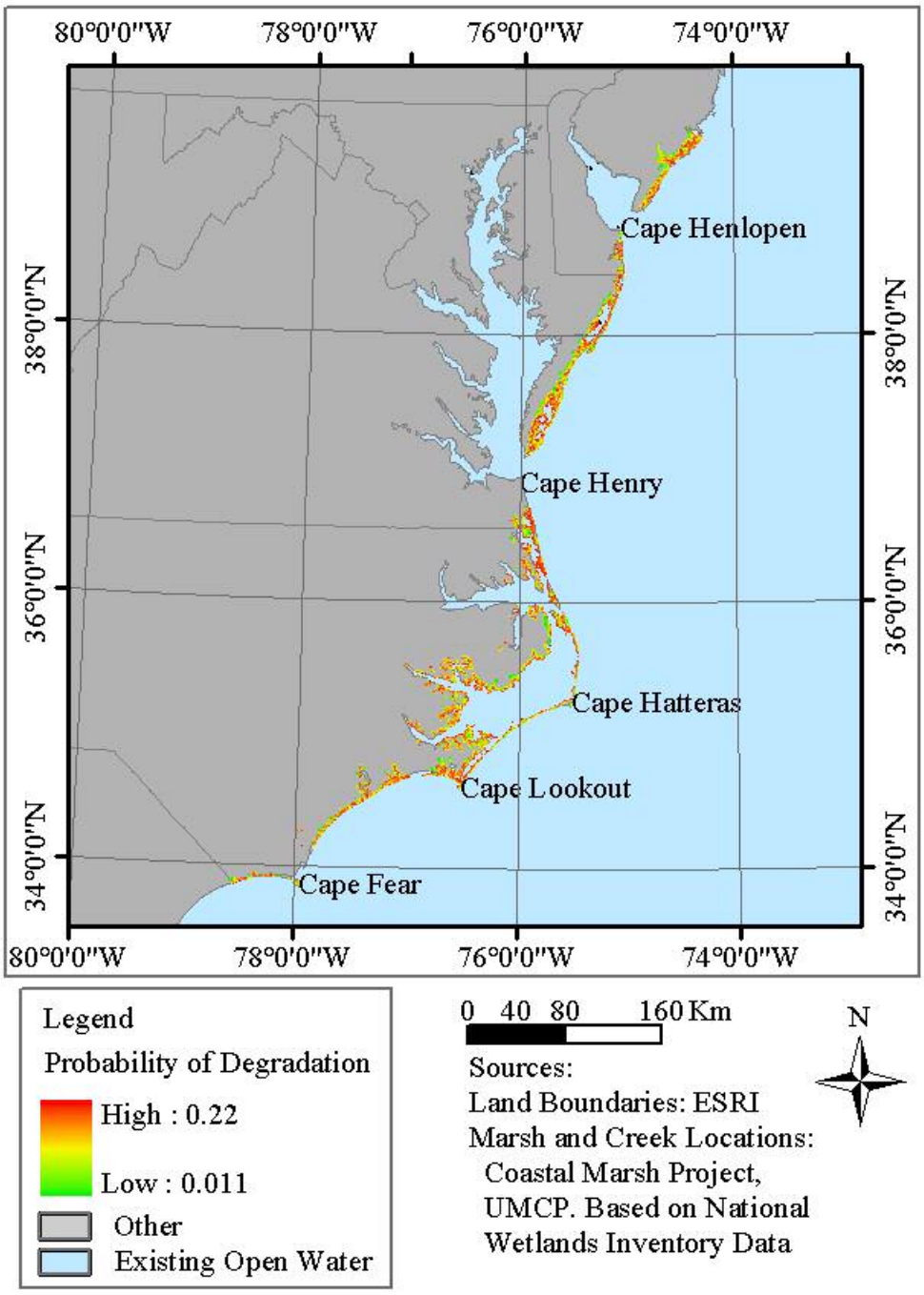

Figure 28. Expected marsh loss as a function of distance from the nearest major water source on the Atlantic Coast.

This is the analog of the distance from tidal creeks in the bays. Loss here seems to be driven more by distance from the ocean shore than by distance from tidal creeks.

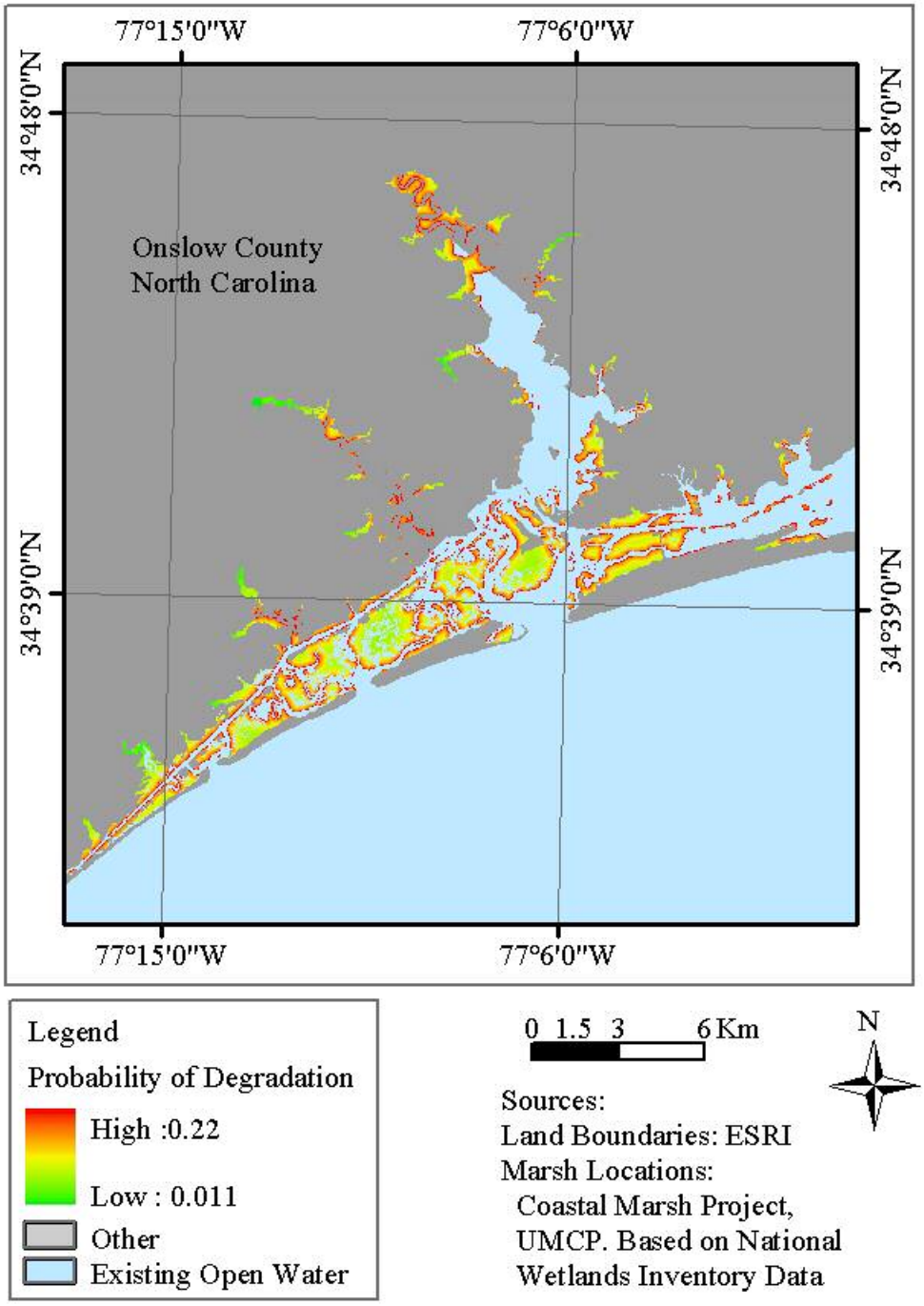

Figure 29. Expected marsh loss as a function of distance from the nearest water in Onslow County, North Carolina.

The expected degradation is focused on the edges of the marsh in this map.

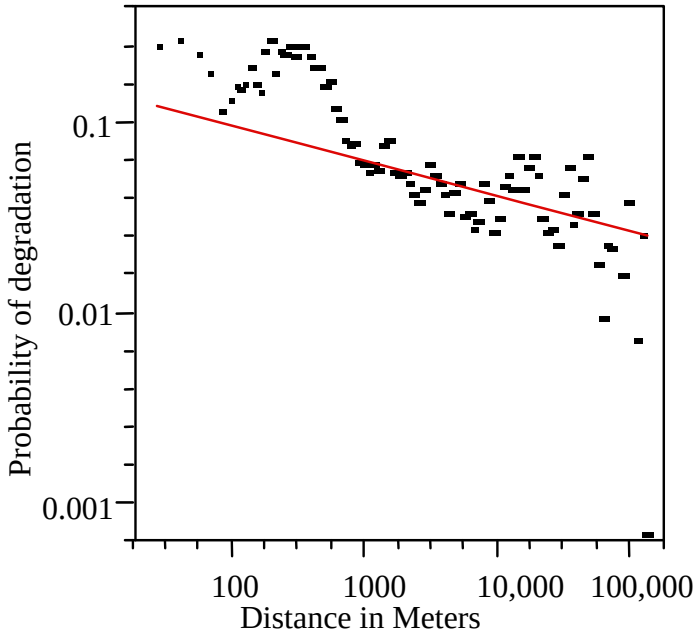

Linear Fit

Summary of Fit

Rsquare	0.264358
Root Mean Square Error	8.528386
Mean of Response	-1.35817
Observations (or Sum Wgts)	2156400

Analysis of Variance

Source	DF	Sum of Squares	Mean Square	F Ratio
Model	1	17773.279	17773.3	244.3621
Error	680	49458.694	72.7	**Prob>F**
C Total	681	67231.973		0.0000

Parameter Estimates

Term	Estimate	Std Error	t Ratio	Prob>|t|
Intercept	-0.653411	0.04546	-14.37	0.0000
log10Distance in Meters	-0.182318	0.01166	-15.63	0.0000

Figure 30. Regression of probability of marsh degradation on distance upstream for the Chesapeake and Delaware Bays area.

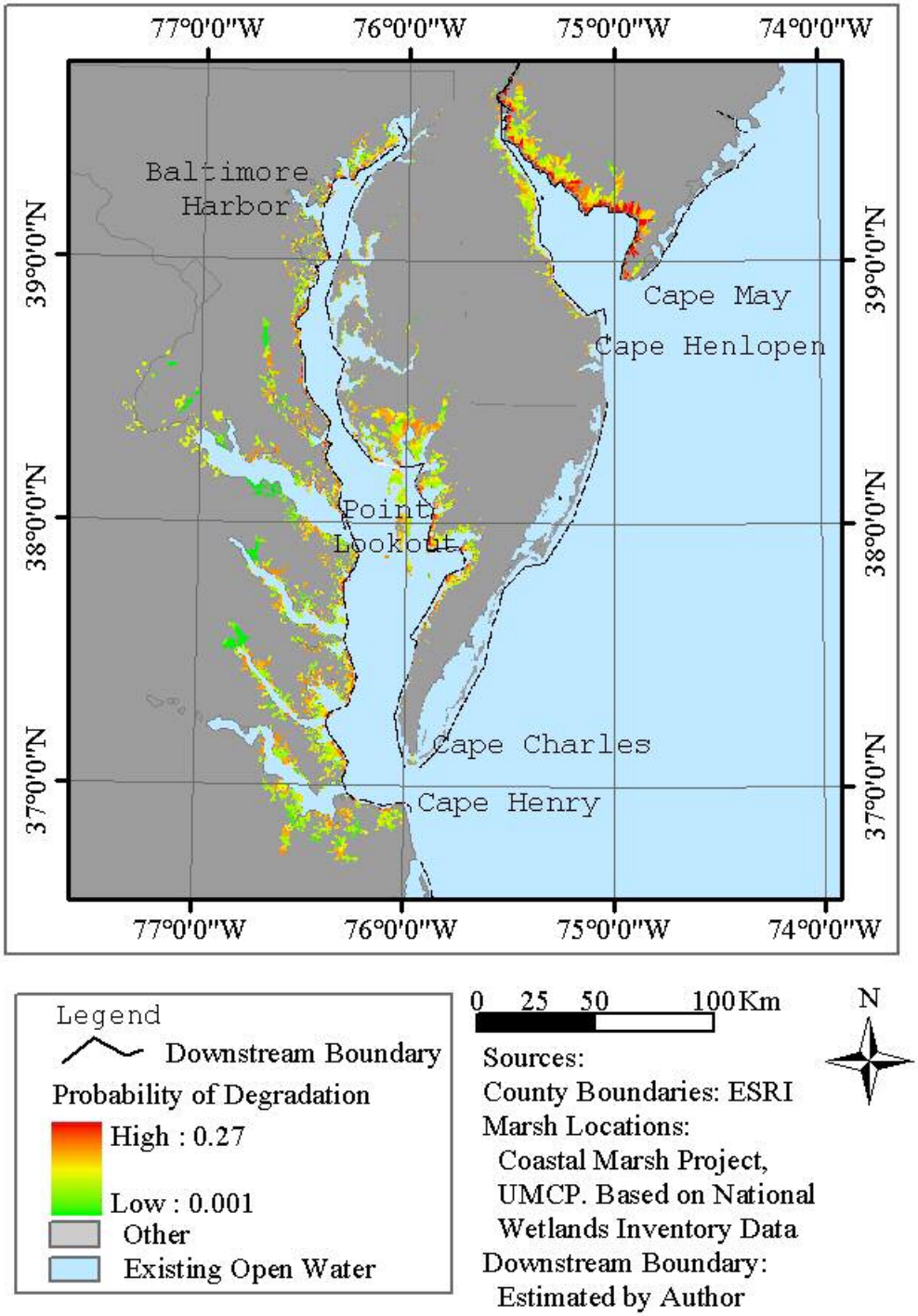

Figure 31. Expected marsh loss as a function of distance upstream in the Chesapeake and Delaware Bay area.

The distance upstream is measured along the major river systems from the downstream boundary.

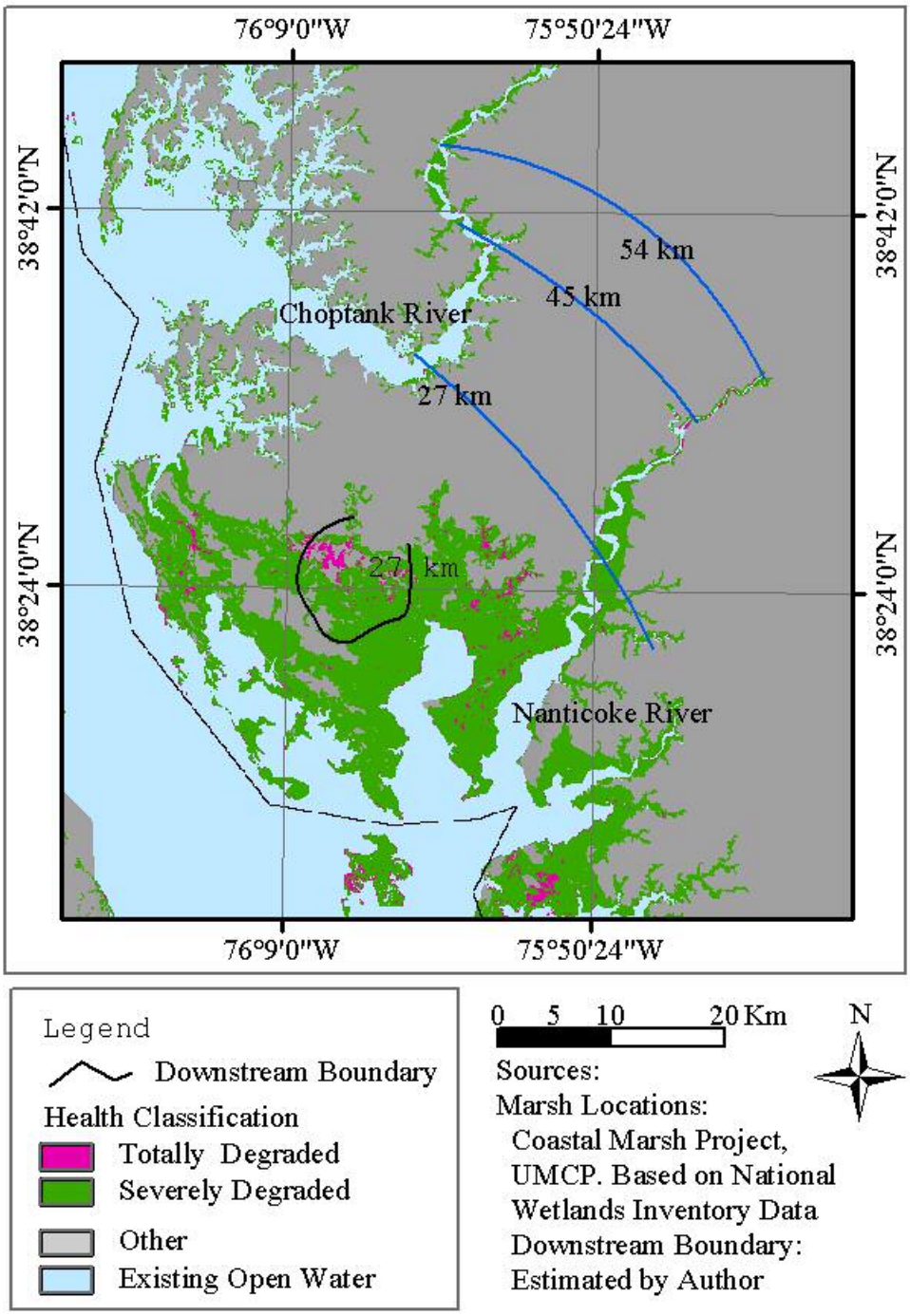

Figure 32. Expected marsh loss as a function of distance upstream on the Eastern Shore of Maryland.

The lines on the marsh are isolines of marsh loss. They are intended to show how the different rivers look at the same distance upstream. There is actually degradation on the Choptank at 45 km, just as on the Nanticoke.

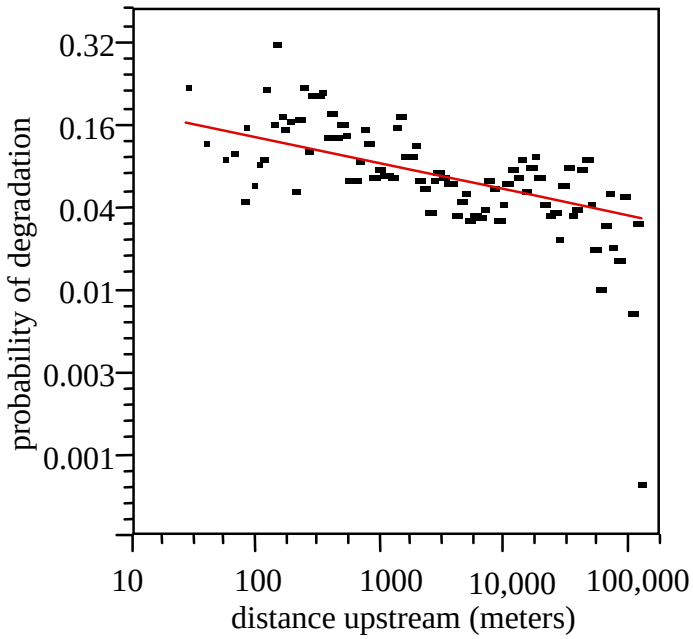

Linear Fit

Summary of Fit

Rsquare	0.237701
Root Mean Square Error	20.18101
Mean of Response	-3.12739
Observations (or Sum Wgts)	2175076

Analysis of Variance

Source	DF	Sum of Squares	Mean Square	F Ratio
Model	1	88516.45	88516.4	217.3393
Error	697	283869.33	407.3	**Prob>F**
C Total	698	372385.78		0.0000

Parameter Estimates

Term	Estimate	Std Error	t Ratio	Prob>|t|
Intercept	-1.723147	0.09623	-17.91	0.0000
ln(Upstream Distance)	-0.158052	0.01072	-14.74	0.0000

Figure 33. Regression of Probability of Marsh Loss on Distance Upstream in Atlantic Coast Marshes

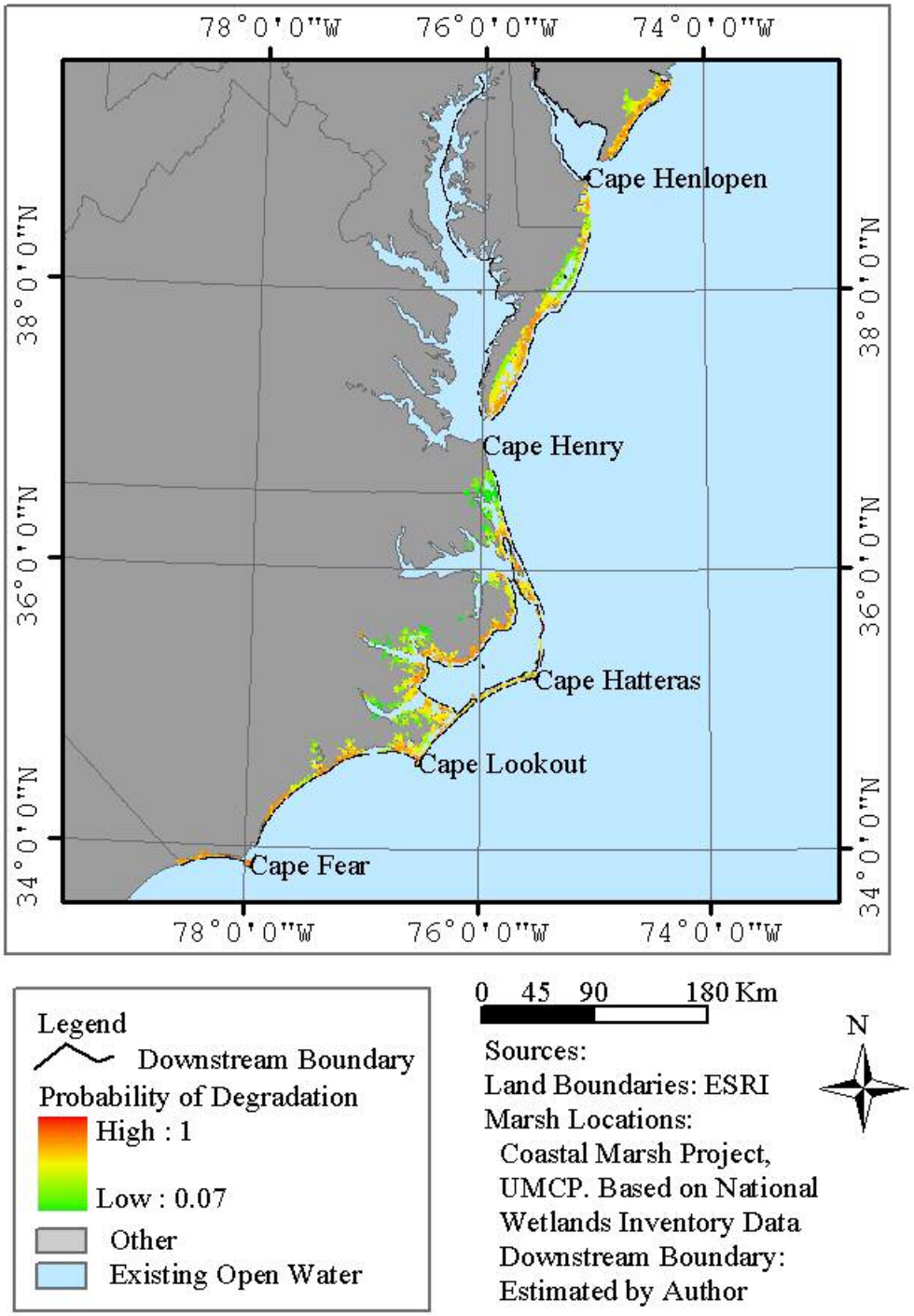

Figure 34. Expected marsh loss as a unction of distance upstream on the Atlantic Coast.

The black boundary line along the Atlantic shoreline and in Pamlico Sound is the downstream limit for measuring distance upstream.

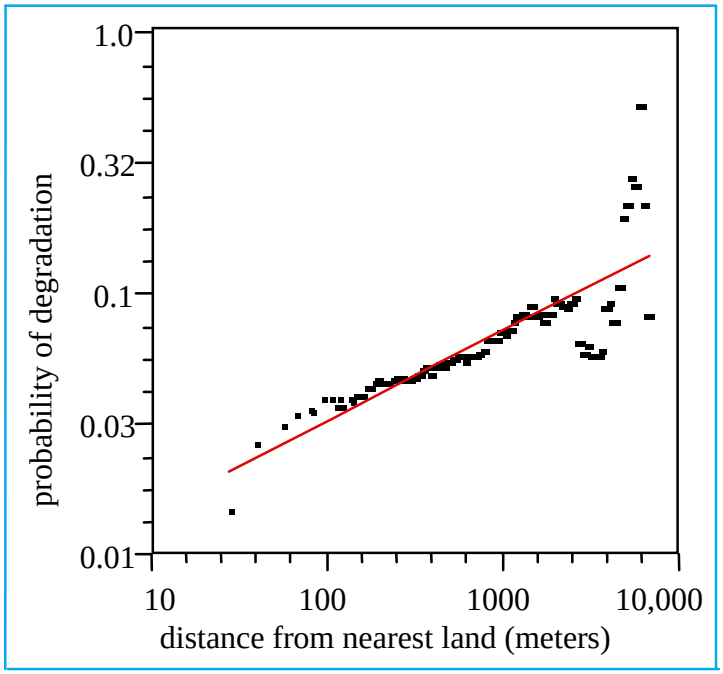

Summary of Fit

Rsquare	0.871136
Root Mean Square Error	13.42716
Mean of Response	-3.15712
Observations (or Sum Wgts)	2178017

Analysis of Variance

Source	DF	Sum of Squares	Mean Square	F Ratio
Model	1	493603.26	493603	2737.851
Error	405	73016.88	180	**Prob>F**
C Total	406	566620.14		0.0000

Parameter Estimates

Term	Estimate	Std Error	t Ratio	Prob>|t|
Intercept	-4.99714	0.03632	-137.6	0.0000
ln(Distance from Land)	0.3437281	0.00657	52.32	0.0000

Figure 35. Regression of probability of degradation on distance from the nearest upland for marshes in the Chesapeake and Delaware Bays

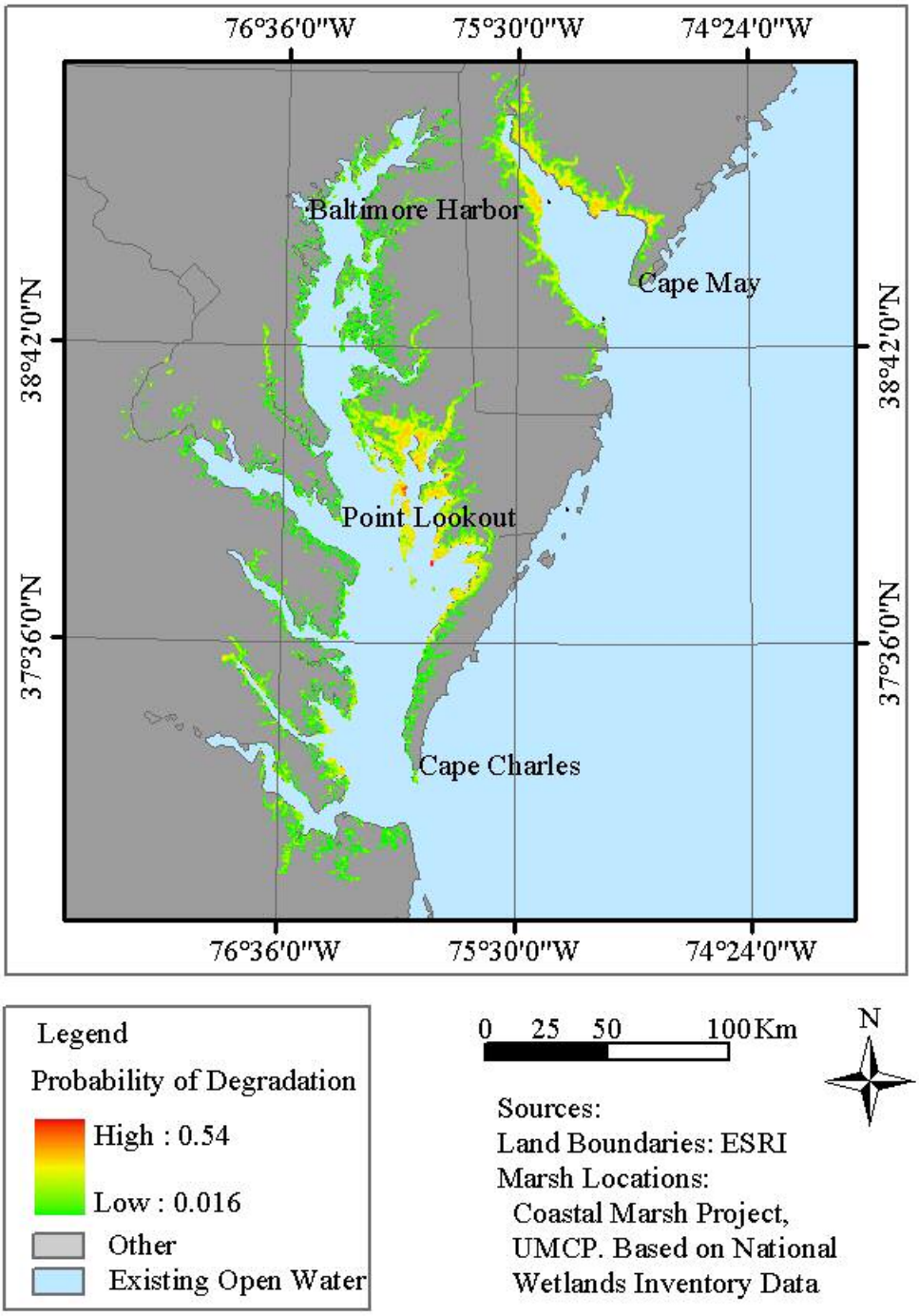

Figure 36. Expected marsh loss as a function of distance from the nearest upland area.

This map depicts the probability of any randomly selected point in the marsh being degraded as calculated based on distance from the upland marsh edge.

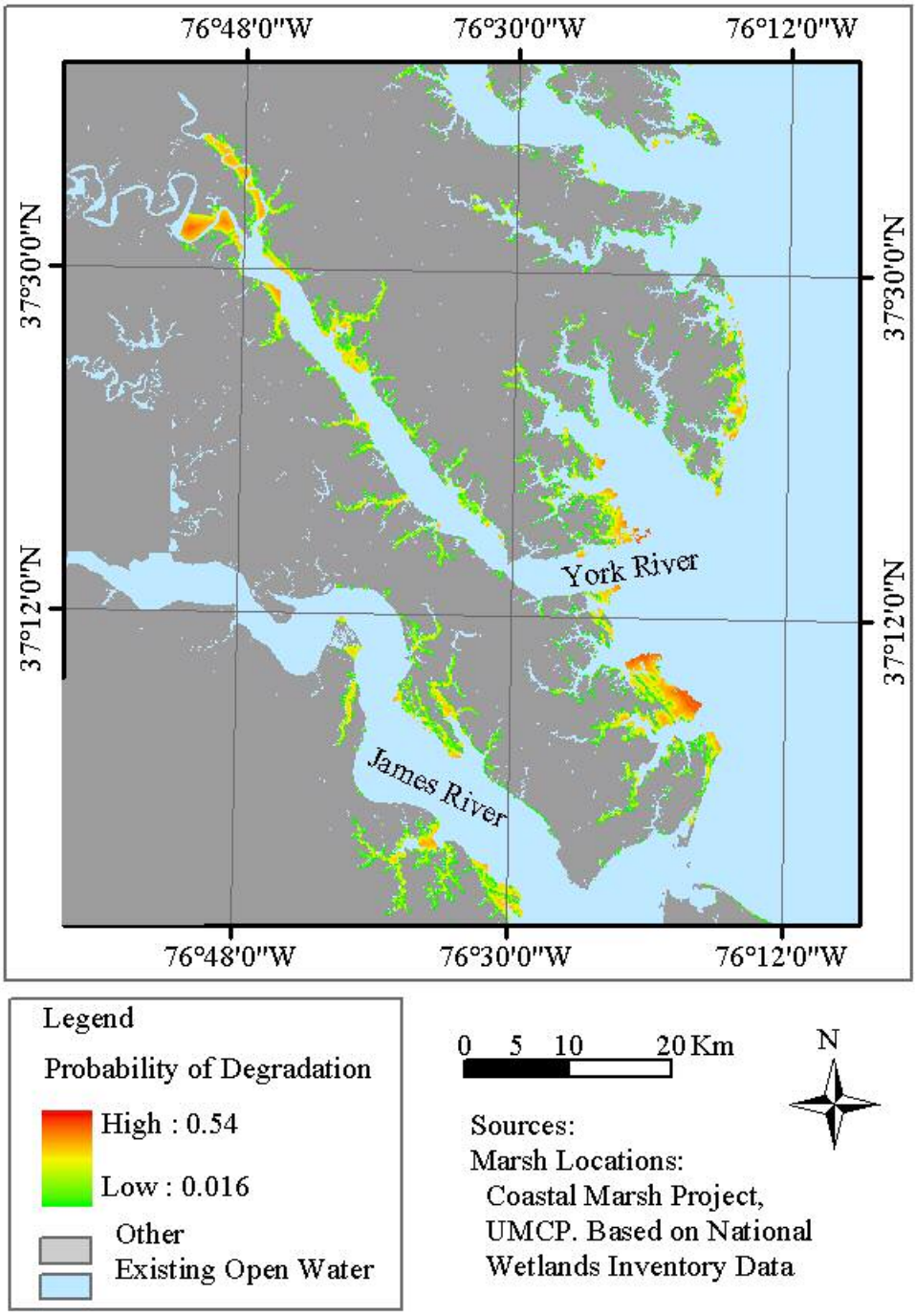

Figure 37. Detail of expected marsh loss as a function of distance from the nearest upland area in the lower Chesapeake.

This map depicts the probability of any randomly selected point in the marsh being degraded as calculated based on distance from the upland marsh edge.

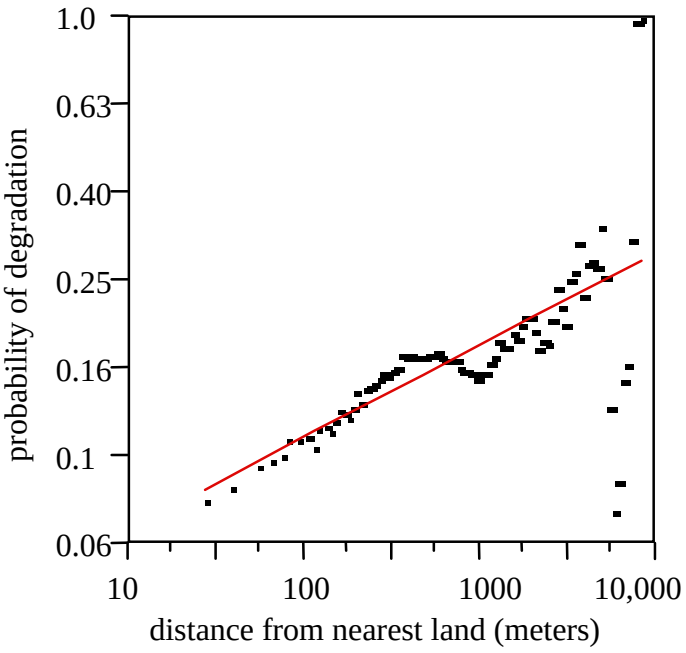

Summary of Fit

Rsquare	0.88531
Root Mean Square Error	6.818498
Mean of Response	-2.00416
Observations (or Sum Wgts)	1884116

Analysis of Variance

Source	DF	Sum of Squares	Mean Square	F Ratio
Model	1	151805.72	151806	3265.207
Error	423	19666.08	46	**Prob>F**
C Total	424	171471.80		0.0000

Parameter Estimates

Term	Estimate	Std Error	t Ratio	Prob>|t|
Intercept	-3.169416	0.02099	-151	0.0000

Figure 38. Regression of probability of degradation on distance from Uplands for Atlantic Coast Marshes

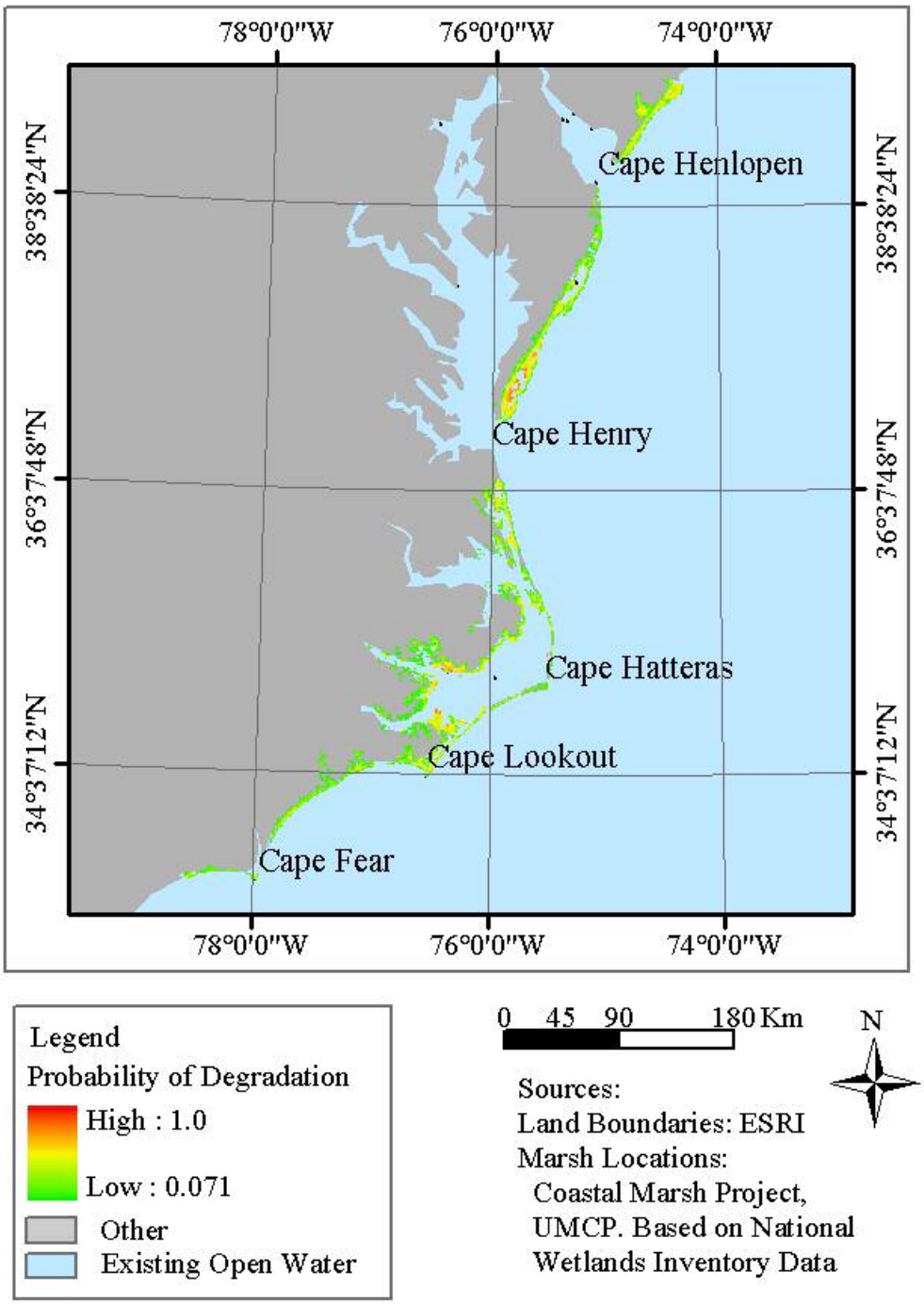

Figure 39. Expected marsh loss as a function of distance from the nearest upland area.

This map depicts the probability of any randomly selected point in the marsh being degraded as calculated based on distance from the upland marsh edge.

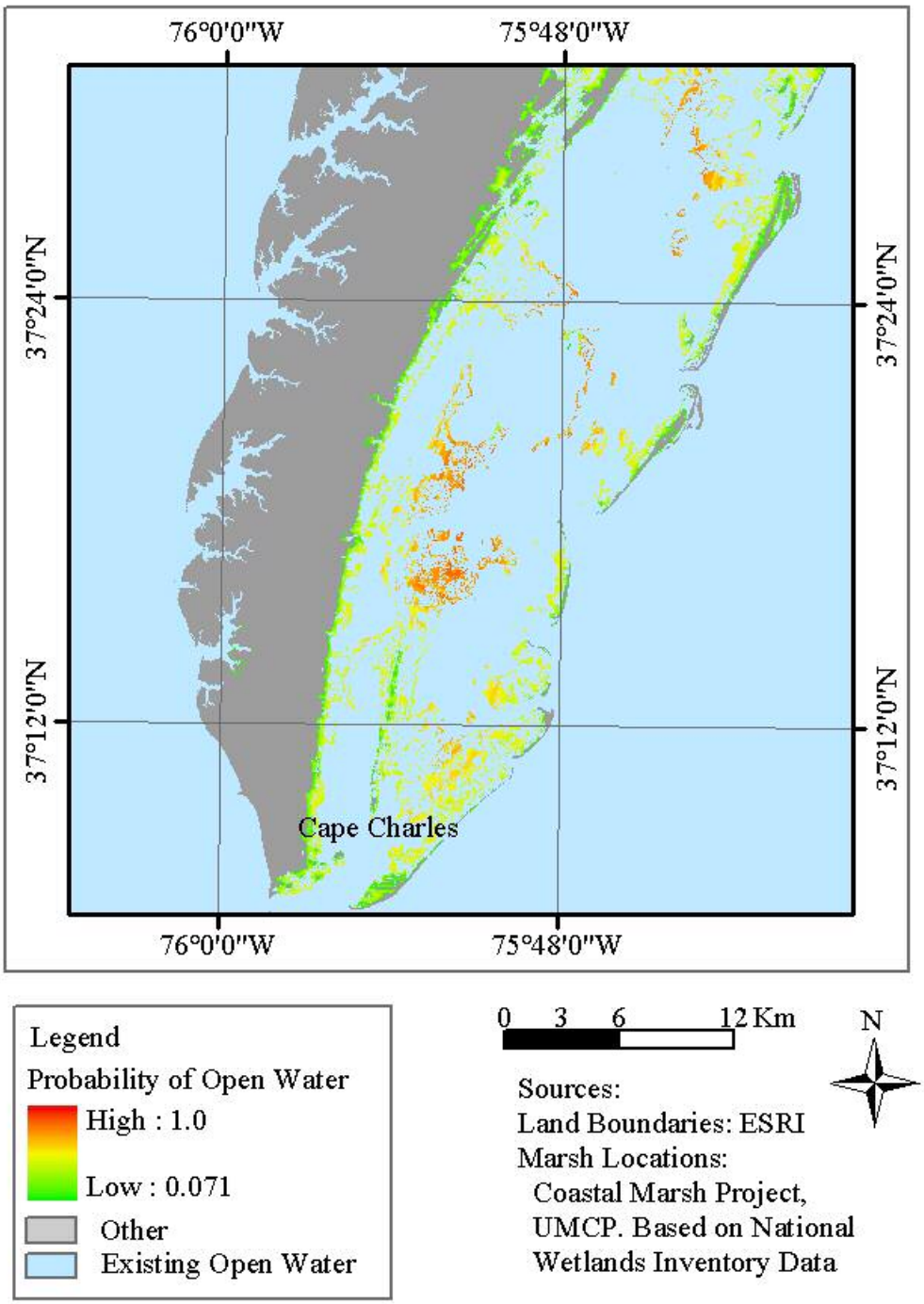

Figure 40. Expected marsh loss as a function of distance from the nearest upland area.

This map depicts the probability of any randomly selected point in the marsh being degraded as calculated based on distance from the upland marsh edge.

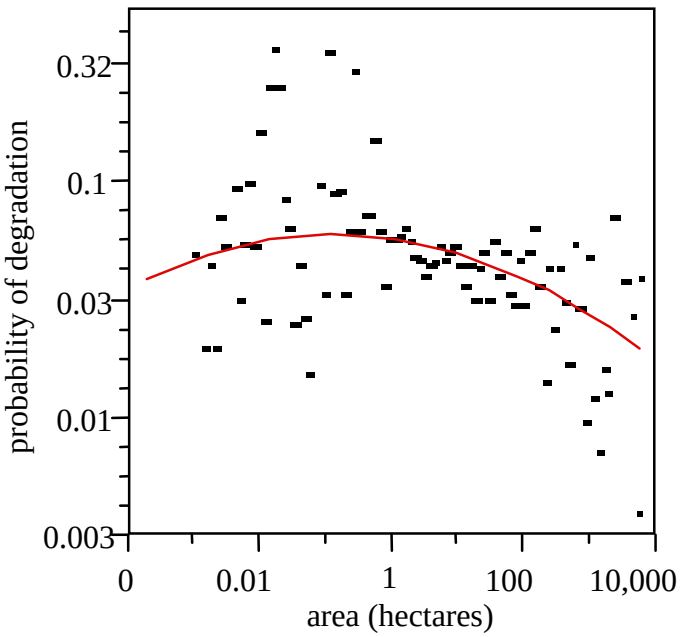

Polynomial Fit, degree=2

Summary of Fit

Rsquare	0.280912
Root Mean Square Error	32.67264
Mean of Response	-3.26635
Observations (or Sum Wgts)	2175155

Analysis of Variance

Source	DF	Sum of Squares	Mean Square	F Ratio
Model	2	350713.7	175357	164.2685
Error	841	897768.7	1068	**Prob>F**
C Total	843	1248482.4		0.0000

Parameter Estimates

Term	Estimate	Std Error	t Ratio	Prob>|t|
Intercept	-3.306989	0.27253	-12.13	0.0000
ln(area)	0.1426084	0.04782	2.98	0.0029
ln(area)^2	-0.00981	0.00193	-5.08	0.0000

Figure 41. Regression of probability of marsh degradation on marsh size in the Chesapeake and Delaware Bays

This figure shows the relationship between the size of a marsh parcel and the probability that any pixel in it will be degraded.

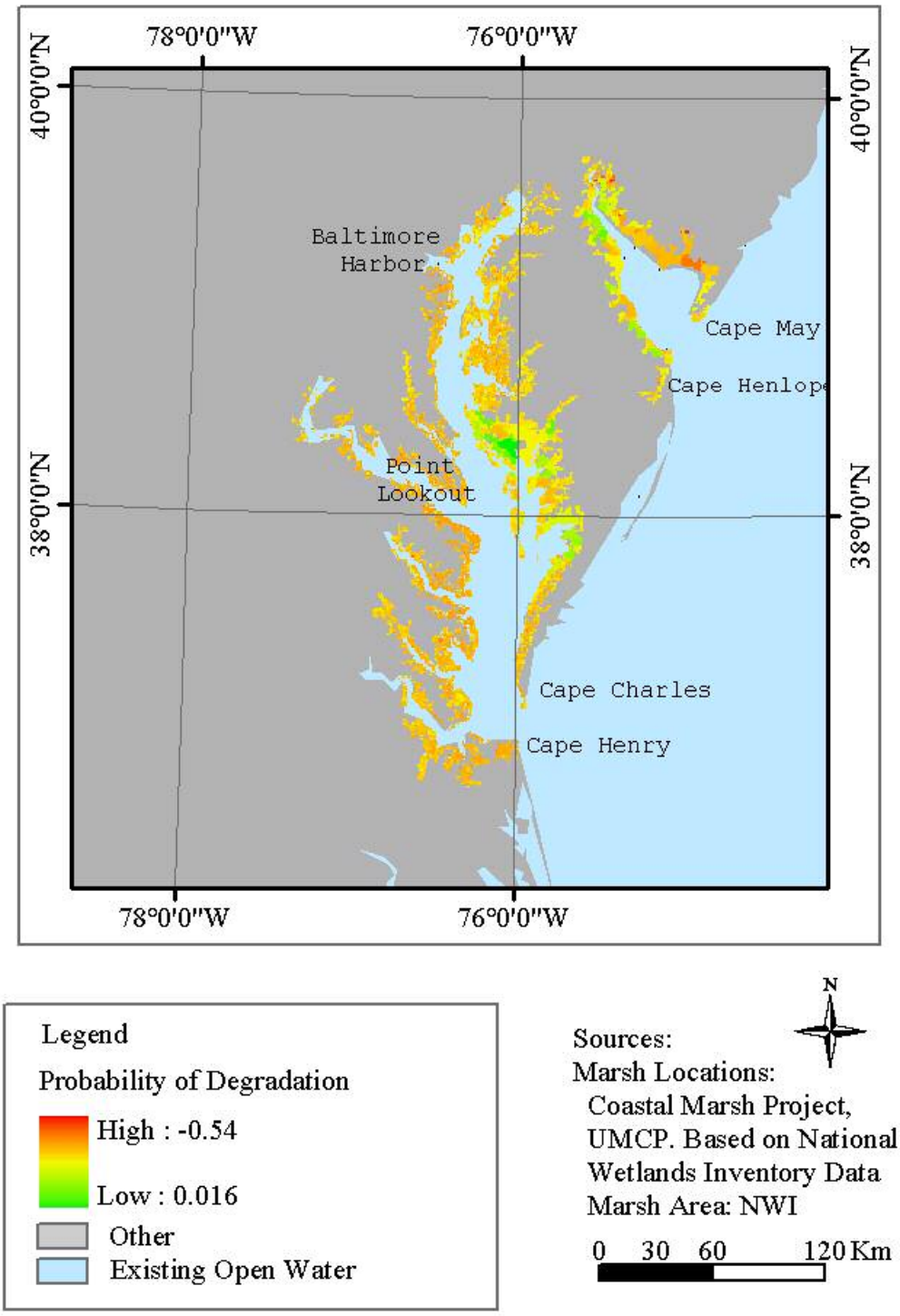

Figure 42. Expected marsh loss as a function of marsh size in Chesapeake and Delaware Bays

This map depicts the probability of any randomly selected point in the marsh being degraded as calculated based on the size of the marsh parcel that contains the point.

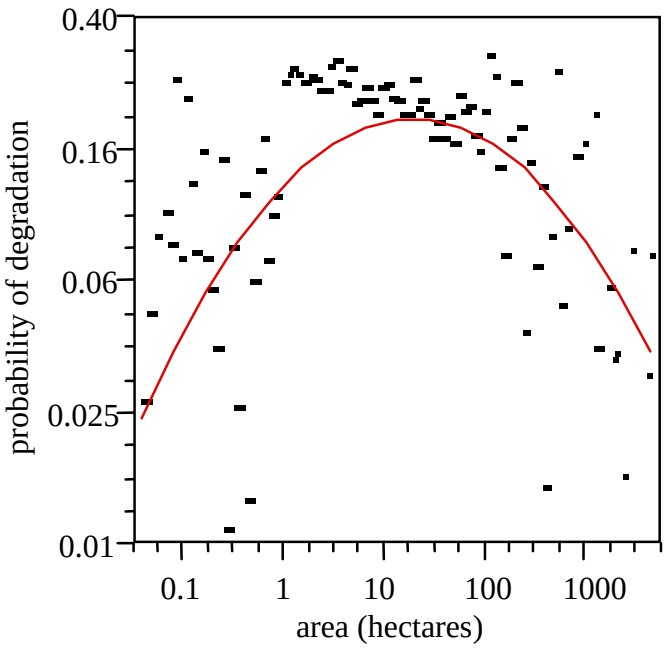

Polynomial Fit, degree=2

Summary of Fit

Rsquare	0.391991
Root Mean Square Error	33.05177
Mean of Response	-2.21751
Observations (or Sum Wgts)	1884171

Analysis of Variance

Source	DF	Sum of Squares	Mean Square	F Ratio
Model	2	516249.5	258125	236.2873
Error	733	800743.3	1092	**Prob>F**
C Total	735	1316992.7		0.0000

Parameter Estimates

Term	Estimate	Std Error	t Ratio	Prob>|t|
Intercept	-9.704339	0.36055	-26.92	0.0000
ln(area)	1.3282013	0.06169	21.53	0.0000

Figure 43. Effect of marsh size on Atlantic Coast Marshes

This figure depicts the probability of any randomly selected point in the marsh being degraded as calculated based on the size of the marsh parcel that contains it.

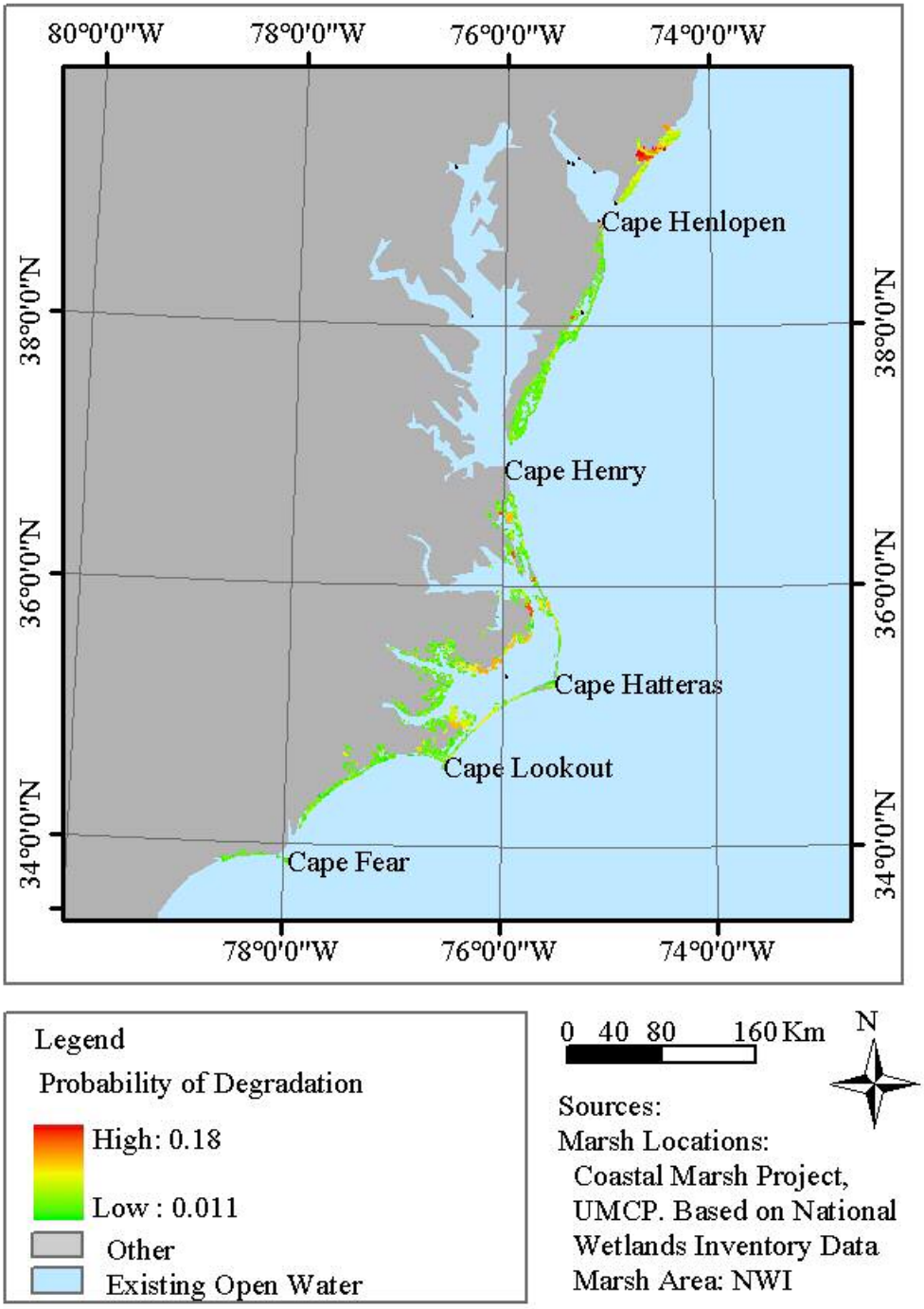

Figure 44. Expected marsh loss as a function of marsh size on the Atlantic Coast

This map depicts the probability of any randomly selected point in the marsh being degraded as calculated based on the size of the marsh parcel that contains it.

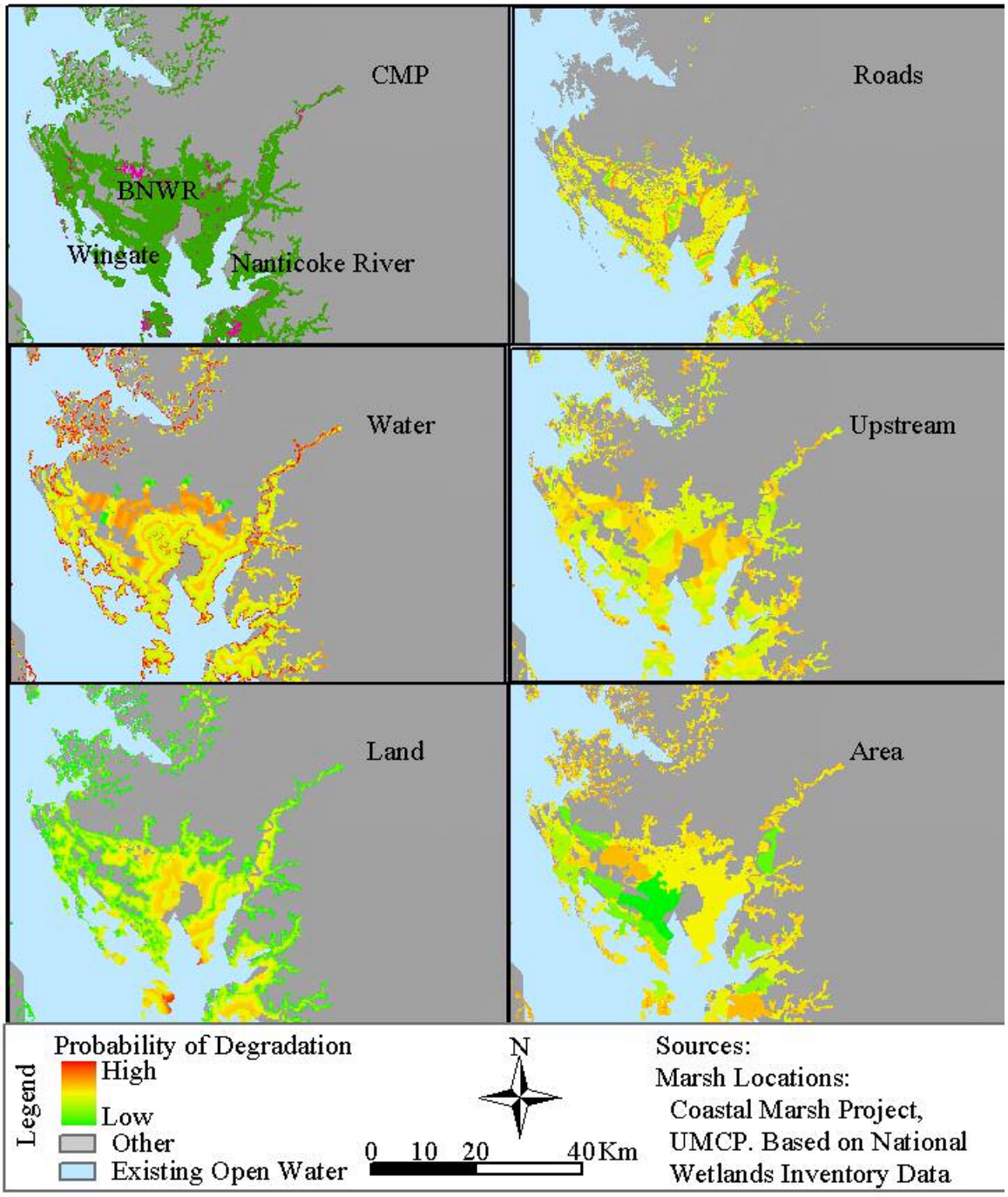

Figure 45. Comparison of Various Effects in Dorchester County, Maryland.

This figure compares the probability of marsh loss calculated by the five different methods in the Chesapeake and Delaware Bays.

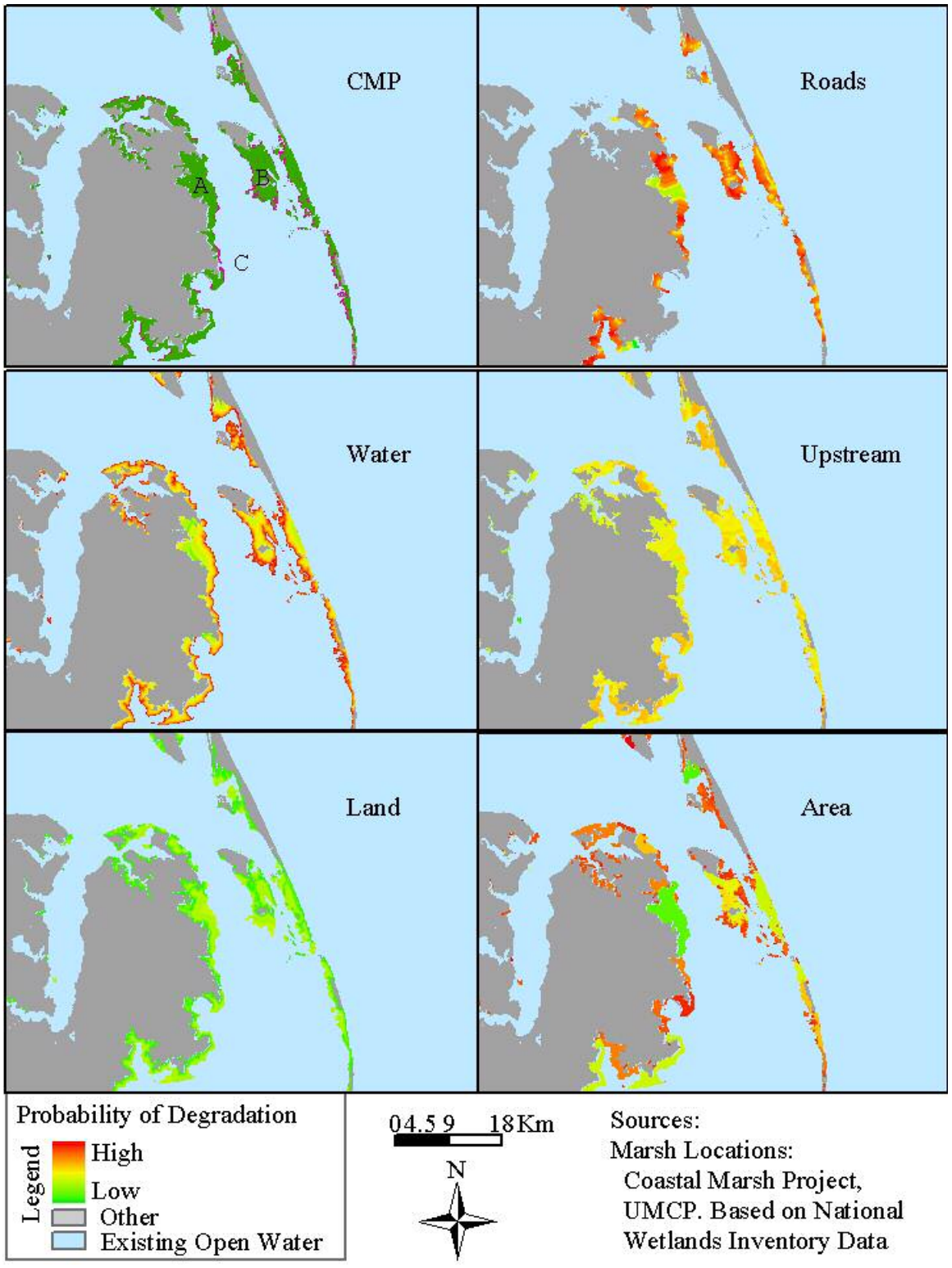

Figure 46. Comparison of analyses for Atlantic Coast Marshes

Chapter 6: Modeling Marsh Loss

Introduction

This section shows the results of a multiple logistic regression model of the various landscape features and other correlates on marsh loss. In this chapter, the landscape model for assessing marsh loss is analyzed using the Coastal Marsh Project (CMP) dataset.

Additional Variables

In this chapter several additional independent variables are introduced – sea level rise, mean tide range, UTM northings and eastings. Relative sea level rise is, of course, one of the factors that would cause marsh loss directly. NOAA records a number of tidal data for various points, but the mean range was chosen because it represents the hydroperiod that most of a marsh will be experience better than other measures. Easting and northing were included as proxies for any environmental conditions that might be keyed to geography such as temperature changes on a north-south axis.

Sea level rise and tides were not formally included in a hypothesis but were included as possible additional factors. However, given the data available, these factors turn out to have only slight relevance (Table 8) for the bay areas. Given the low R^2 values of either factor in the Chesapeake and Delaware Bays in the bay landscape model, they were not used in further analysis. This low correspondence was probably because the tidal and sea level rise data are for the coastal regions, but most of the bay area marshes are upstream and inland. Tides, in particular, are sensitive to many things so that

the coastal tides may not accurately represent local inland tides. Also, the high degree of spatial variation in tidal range may not be well mirrored in the available tide gauge records (Kearney, pers. com.). Similarly, if relative sea level rise is a result of eustatic sea level rise and land subsidence, erosion or accretion, then the sea level rise measured at a certain point may not accurately reflect the relative sea level rise in more inland areas.

Table 8. Regression of Sea Level Rise and Mean Tidal Range on Probability of Marsh Loss

Factor	Area	R2	Slope
Sea Level Rise	Bay Area	0.002	
	Atlantic Coast	0.28	-1.99
Tidal Range	Bay Area	0.002	
	Atlantic Coast	0.1	0.0003

Models

Bay model 1: Land, Water, Roads, Area, Upstream, Northing, Easting.

Bay model 2: Land, Water, Area, Upstream, Northing, Easting.

Atlantic Model: Land, Water, Upstream, Tide, Sea level rise, Northing, Easting.

The regression parameters for all models are listed in Table 9.

Table 9. Landscape model Coefficients and Values				
Coefficient/Value.	Bay with Roads	Bay without Roads	Total Bay Model	Atlantic
β0	-5.227	-7.091	NA	70.511
β1	0.053	0.018	NA	-0.179
β2	0.437	0.372	NA	0.100
β3	-0.213	0.190	NA	0.562
β4	-0.532	0.419	NA	0.516
β5	0.699	0.681	NA	-0.662
β6	-0.493	0.123	NA	0.137
β7	0.057	NA	NA	-0.548
RMS error	0.439	0.440	NA	0.312
Model Chi Square	180.466	214.524	NA	171,166
G adjusted	NA	NA	5206	71,238
Chi Square of Significance	NA	NA	10.828	10.828
Significance Level	NA	NA	0.001	0.001
The β-values are logistic regression coefficients. The chi-square values are very high, in part, due to the fact that the numbers involved are very large.				

Bay Area Model

The Bay Area landscape model had to be constructed in two pieces. The roads are modeled as only having an impact on parcels of marsh that they actually touch. Many areas of marsh are not actually touched by a road. Two separate models were run, one including the road factor and covering a smaller area, and one not including the road factor and covering a larger area. The two were then combined so that any areas not included in the road model would be added from the non-road model. Small areas of marsh were lost from the analysis because the data available at this scale did not show any connection between them and the major bodies of water.

The major contributors to each principal component are shown in Table 10 and 11. The complete loadings and other information about the principal components analysis are in the Appendix D.

These tables show that there is much similarity between the two models. For example, Model 1, PC 6 matches Model 2 PC 1. PC's 3, 4 and 5 in both models are very similar in terms of major loadings. Figure 47 compares the principal component five in each of the two bay models in their full extent. This component is dominated by distance from land. It is not possible to represent faithfully the full detail because smaller features are lost at this resolution. However, it can be seen that for areas that both cover, there is not a great deal of difference, but there are differences.

Figure 48 shows a close up of Blackwater National Wildlife Refuge using the 4th principal component from each model. In this case, Northing was swapped for Roads and three others factors have almost equal input as shown in Table 10 and 11. Again, the models are very similar, but it can be seen that the areas covered by high values are larger in Model 2. Therefore, the distance from roads adds information to the regression.

The results of the combined assessments are shown in Table 12. The results show that the model does identify the areas of degradation in the marsh – but not very accurately. However, considering that only 5% of the marsh is in the degraded category, then only 1.2% of the degraded marsh pixels and 70% of the healthy pixels would be assessed correctly. The results of this landscape model are much better than that. The significance of the model results are shown in Table 9

The global result for the Bay model is shown in Figure 49. The Bay area landscape model is compared with the full range of the CMP model here for several reasons. The CMP model was most developed and most heavily validated in this region. The areas that the landscape model mischaracterizes as being totally lost can also be

interpreted as “predicted to be lost”. As most of the mischaracterization involves pixels that the CMP had designated as partly or severely degraded, this makes sense.

Some of the results can be examined in detail in Figure 50 and Figure 51. In the BNWR area, several areas are mischaracterized by the landscape model. In particular, the tip of the peninsula between Fishing Bay and the Nanticoke River appears much more degraded in the landscape model than in the CMP data, with other mismatched areas scattered over the map. In one sense, these may be errors, but in looking at it as a predictive model, the area by the Nanticoke River (area A) is certainly at high risk. There are numerous creeks and internal ponding already is in progress. In Areas B and C, the same thing is true. Although the CMP data classifies many areas of the marsh as healthy, in among the healthy patches of marsh are distributed many ponds and creeks, which could lead to further deterioration. The same reasoning could apply to the large parts of Area D that are characterized as degraded by the landscape model, but do not look degraded in the CMP data. However, from an overall perspective, given the uncertainties of the model, it is noteworthy most areas are correctly classified by the landscape model.

Table 10. Bay Model 1 Primary Principal Component Loadings

Principal Component				
1	Northing			
2	Upstream	Area		
3	Water	Land		
4	Water	Upstream	Area	Roads
5	Land			
6	Easting			
7	Roads	Area		

In the map of the central Delaware Bay, the same kinds of situations exist. The marsh at Egg Island Point is mostly classified as Severely Degraded by the CMP data, so

the landscape model is not far off in showing it as total loss. On the other hand, Bombay Hook does not appear nearly as degraded by the CMP data, yet is shown as almost totally lost by the landscape model. Between Egg Island Point and Ben Davis Point and on up the eastern side of the Delaware Bay, the whole side is classified as total loss by the landscape model, but shows very high variability in the CMP data. This would suggest that large parts of it are at high risk.

Table 11. Bay Model 2				
Principal Component				
1	Easting			
2	Northing	Upstream		
3	Water	Land		
4	Northing	Water	Upstream	Area
5	Land			
6	Area	Upstream		

Table 12. Accuracy of Bay Area Model

		Actual Pixel Values		Row Totals
		Healthy	Degraded	
Assessed Pixel Values	Healthy	1,497,225	64,829	1,562,054
	Degraded	532,961	37,750	570,711
	Column Totals	2,030,186	102,579	2,132,765
	Percent of pixels assessed correctly			
	Healthy	73.7		
	Degraded	36.8		
	Total	72.0		

Atlantic Model

The Atlantic Coast model did not need to be run in pieces as roads were omitted and all other factors were assumed to be global in nature. These marshes tend to exist in

a relatively narrow band parallel to the coast, therefore assuming that the factors are global in nature is reasonable. This narrowness also may explain why sea level rise and mean tides had a measurable (though still minute) correlation in the Atlantic coastal region but not in the bay area.

The results of the landscape model are compared with the CMP data in Figures Figure 52, Figure 53, Figure 54 and Table 13. These data are not compared with all the categories in the CMP data as the bay data were. The CMP model of marsh evolution was designed for low-energy, protected areas such as the Chesapeake Bay, not for higher energy environments such as Winyah Bay, South Carolina, where the tides can rise 4 meters.

Table 13. Accuracy of Atlantic Model

		Actual Pixel Values		Row Totals
		Healthy	Degraded	
Assessed Pixel Values	Healthy	1,490,005	213,109	1,703,114
	Degraded	22,503	35,201	57,704
	Column Totals	1,512,508	248,310	1,760,818
	Percent of pixels Assessed correctly			
	Healthy	98.5		
	Degraded	14.2		
	Total	86.6		

On the Atlantic Coast, while roughly 14% of the area is degraded, the model only assesses 3% to be degraded. This is more than likely a failure of calibration. It does indicate that the model is working, however. Given 14% and 3%, random chance would result in only 0.4% degraded marsh pixels correctly identified and only 83% of healthy pixels correctly assessed. The model results far exceed both those expectations.

Moreover, of the areas assessed as degraded, 61% are, in fact, degraded and for healthy marsh assessments, 88% are correct. For anyone using this data to work in a marsh, there is a 0.87 probability that when they investigate an area, they will encounter what the model indicates.

The Atlantic Model map (Figure 51) shows the Atlantic study area. Most of the area is in the less than 50% degraded category and is correctly classified. However, the second largest class represents areas that are actually more than 50% water, but are classified as healthy. Much of this area is transitional zones, a mixture of partly degraded areas with totally degraded areas. The areas shown here as greater than 50% open water were classified as intact marsh in the NWI. This means that there is a presumption that the areas classified as totally degraded do in fact represent loss of marsh. However, it cannot be presumed that the partly degraded areas are moving toward total loss because, unlike for the estuarine marshes, there is no model or tested data that concludes that there is a constant progression from healthy to partly deteriorated to completely deteriorated.

In Figure 53, the general pattern can be seen in more detail on the Delmarva Peninsula. Figure 54 shows the area around Pamlico Sound, where there are also areas of complete loss that are characterized correctly.

Conclusion

The logistic regression clearly shows that the elements identified in the five original hypotheses, plus the factors added in this chapter, can model marsh loss to a limited extent. The accuracy is far better than would be expected from chance alone.

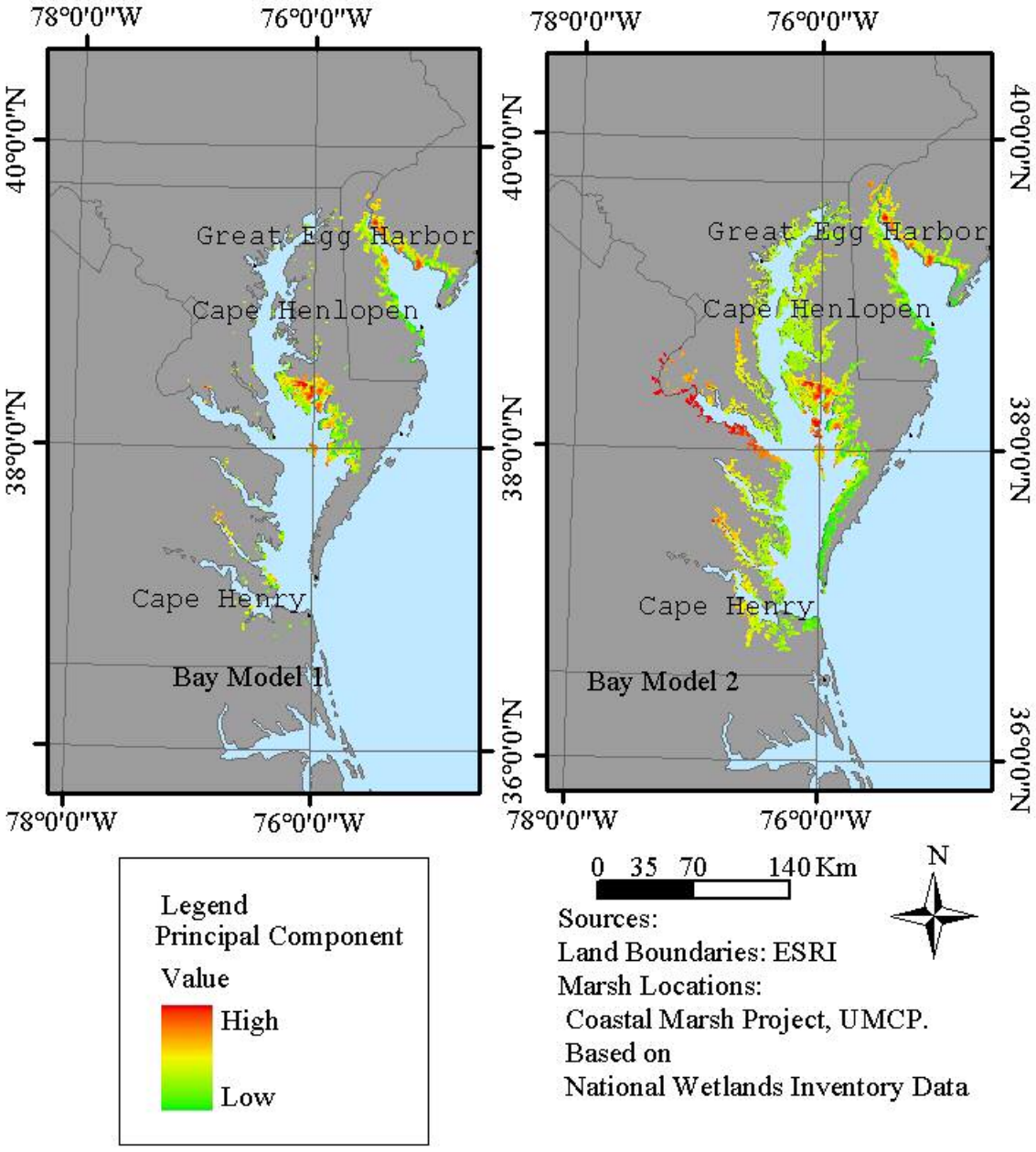

Figure 47. Comparison of eigenvalue 5 for the two different bay models

Bay Model 1 includes roads while Bay Model 2 does not. This figure shows the different areas covered by the two Bay Area models, as well as the fact that they are not identical. Adding the roads does add information.

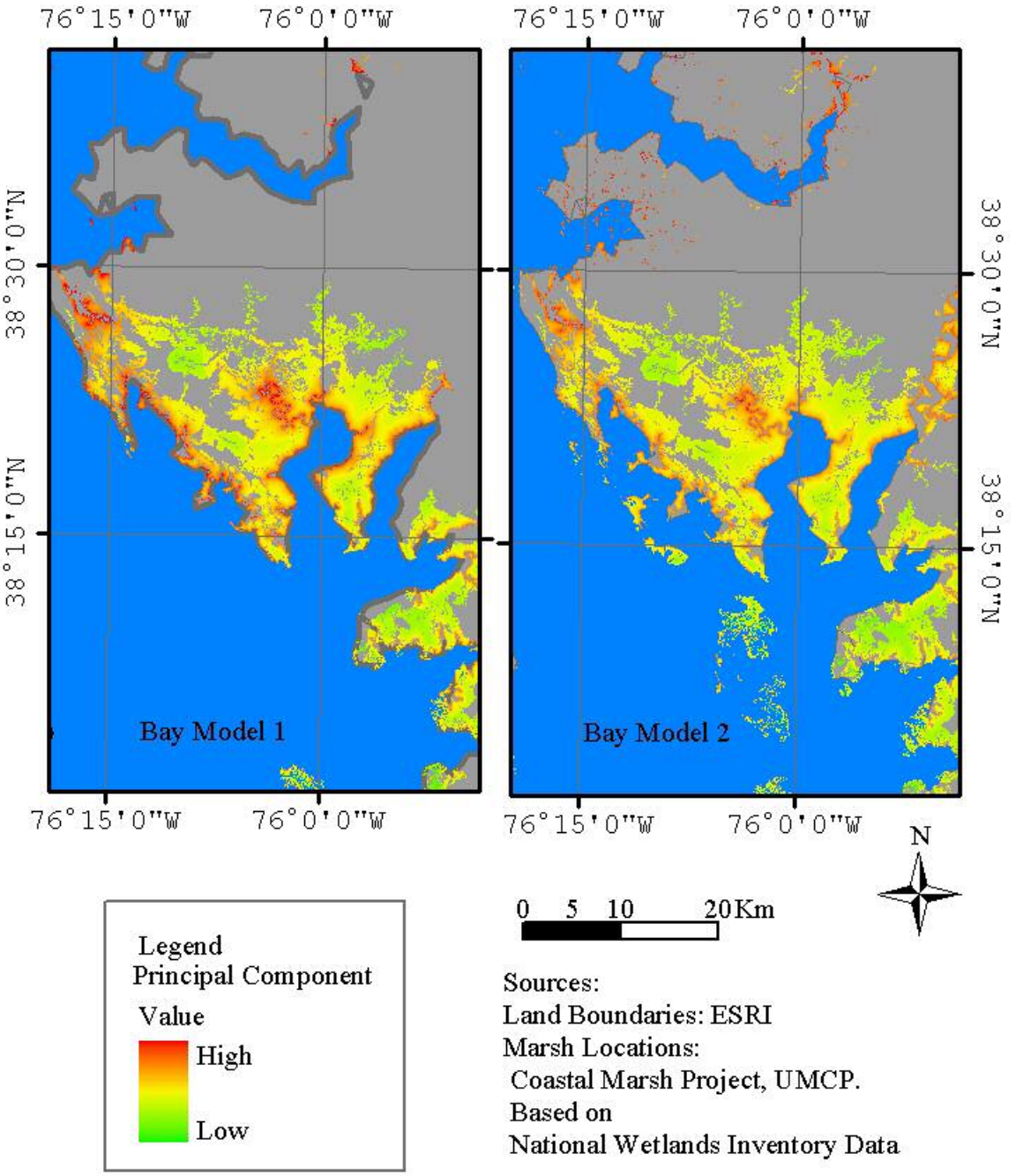

Figure 48. Comparison of eigenvalue 4 for the two different bay models

Bay Model 1 includes roads while Bay Model 2 does not. This figure shows the different results for this eigenvalue based on that difference. Adding the roads does add information.

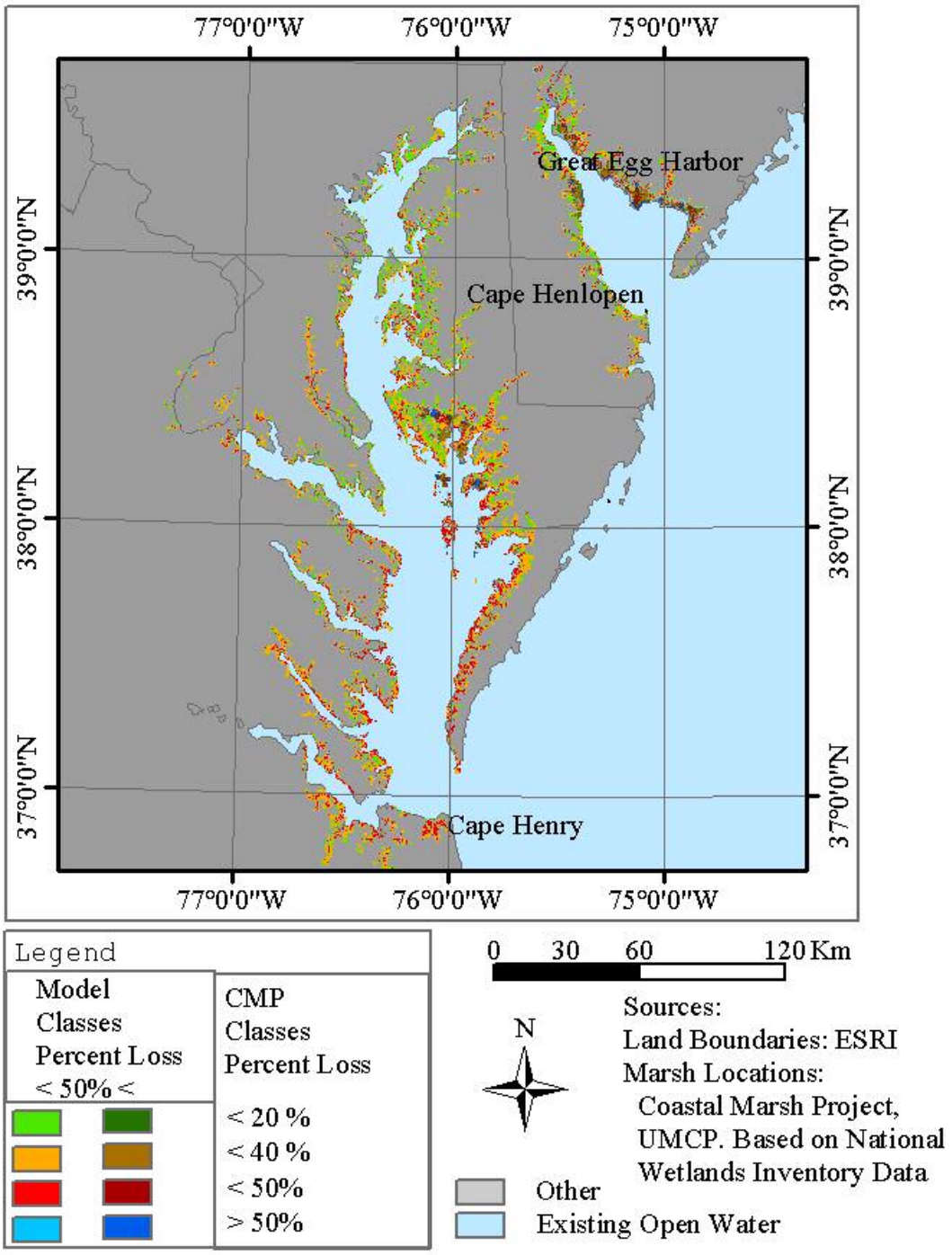

Figure 49. Landscape model results for marsh loss in the Chesapeake and Delaware Bays

This figure shows the predicted marsh loss based on the combination of Bay Models 1 and 2, done by using Bay Model 1 where it exists, and Bay Model 2 everywhere else.

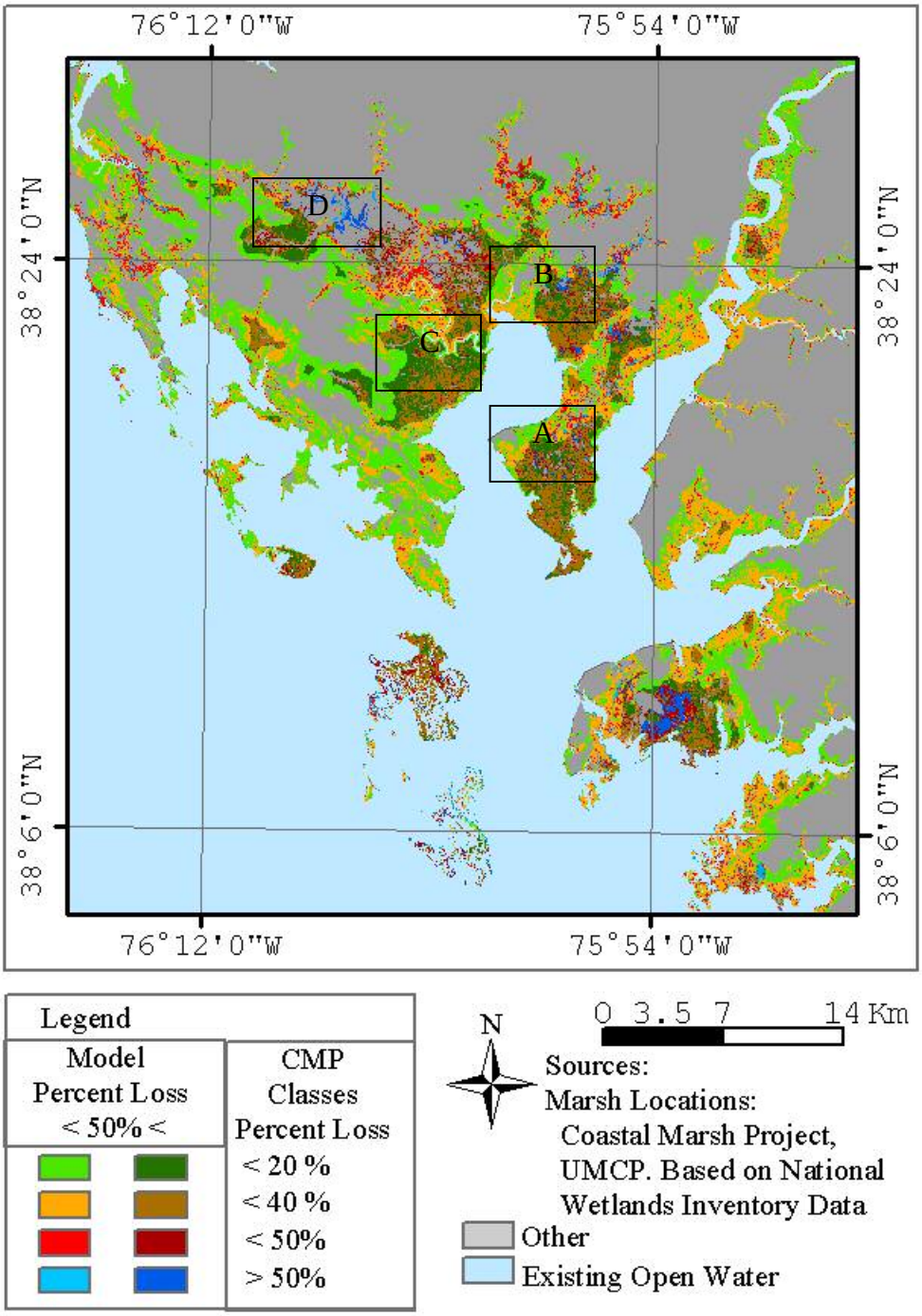

Figure 50. Model of marsh loss in the middle Eastern Shore of Maryland. At A, B, C and D healthy pixels were determined by the Landscape Model to be degraded. However, the healthy pixels are interspersed with degraded areas.

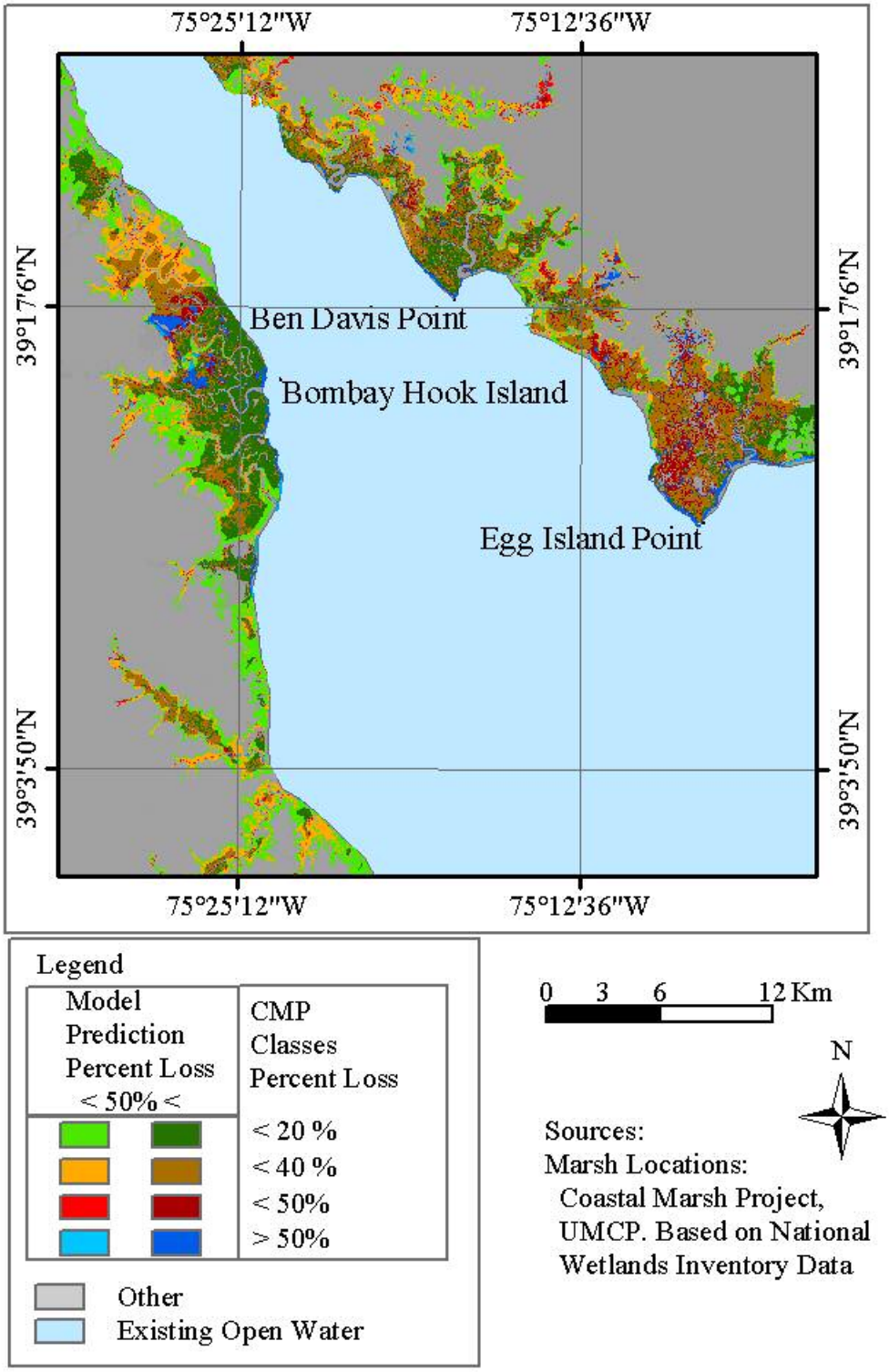

Figure 51. Landscape model validation in Delaware Bay

This figure shows that although the model is not a perfect pixel by pixel classifier, it does pick out areas of high degradation, even if not all the points in it are highly degraded/,

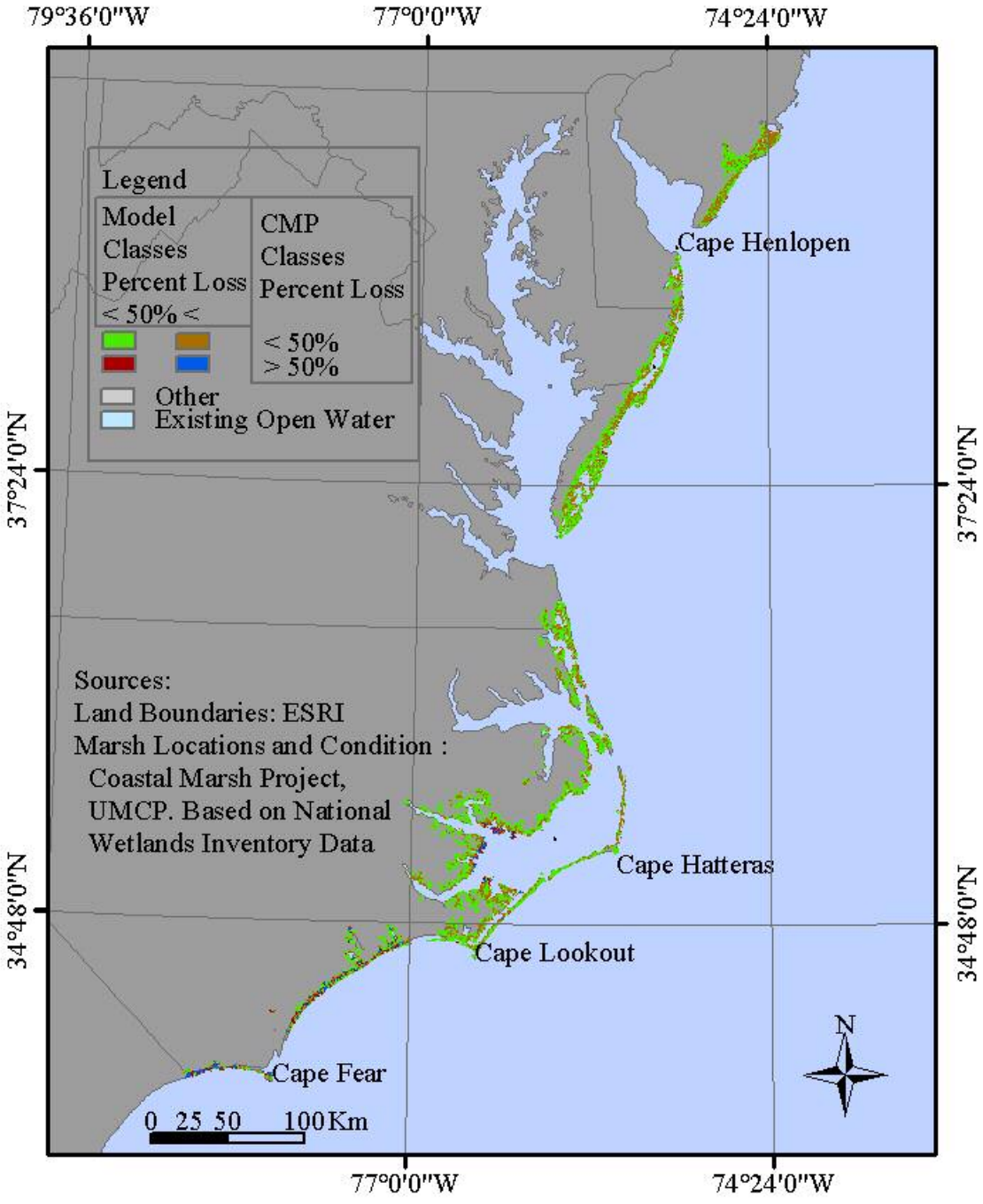

Figure 52. Atlantic Coast marsh loss model showing expected degradation due to all factors except distance from roads.

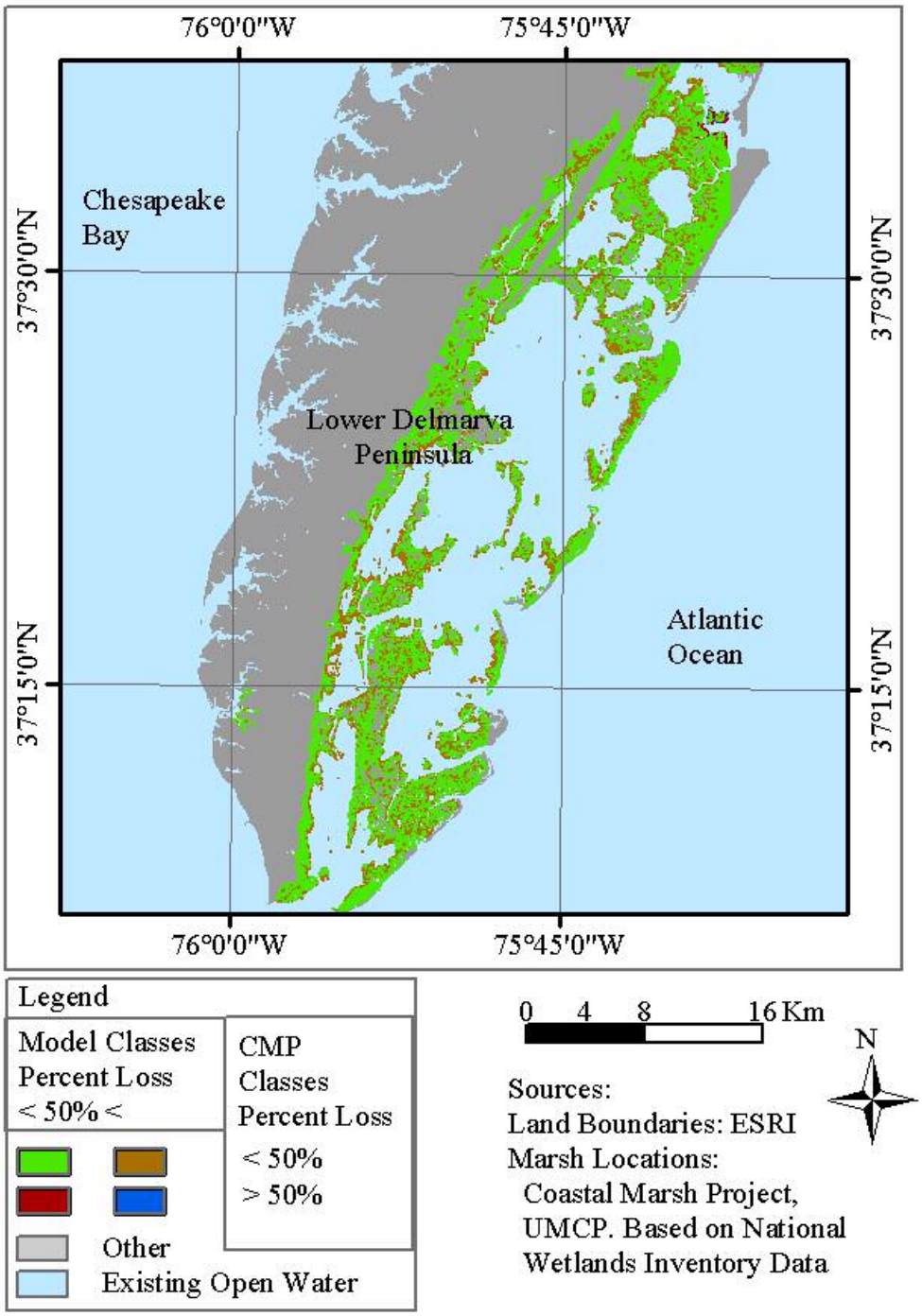

Figure 53. Landscape model validation on the lower Delmarva Peninsula

This figure shows the relative accuracy of the model in this particular area. The green areas are healthy areas that were predicted by the model to be healthy.

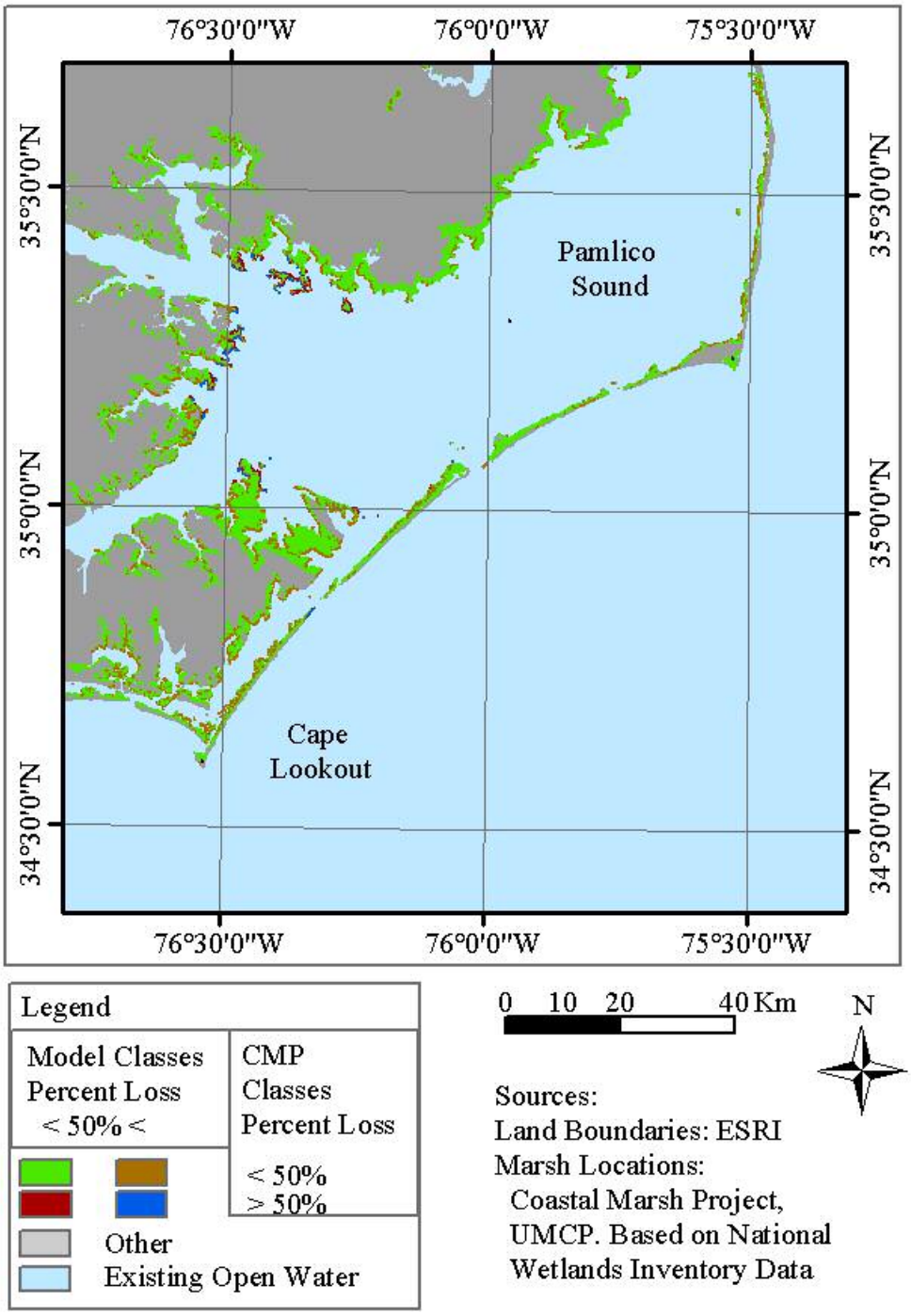

Figure 54. Landscape model validation on the Outer Banks

Chapter 7: Discussion and conclusion

Significance of results

The starting point for this research is the hypothesis that the probability of a parcel of marsh being open water is directly related to its position in the landscape. This proposition was broken into five specific hypotheses, briefly restated below. Although the null hypothesis for the original hypothesis is that: "The conversion of marsh surface to open water is a completely stochastic process, and it is not possible to infer that ponds are more or less likely to form in certain places based on position in the landscape" each of the tested hypothesis was stated as a one-tailed test. Had they been stated as two-tailed tests, virtually all could have been accepted. The actual results with R^2 values are shown in Table 14 below. The results in Chapter 5 indicate that there is a very strong signal exerted upon marsh loss by some of the five landscape factors examined. When combined, these same factors model the marsh loss reasonably well. While it is not a surprise that landscape factors impact marsh development and loss, these particular measures are of some interest.

The work of the Coastal Marsh Loss project was based on the Marsh Surface Condition Index, which was based on studies of the Nanticoke River estuary and other marshes on the Chesapeake Bay. These microtidal systems are different from the meso and macrotidal regions of the Atlantic Coast. The MSCI may not be meaningful in these areas. The Coastal Marsh Project data used here are affected by this. Although the remote sensing algorithm was shown to be accurate (Stevens, 1997), it is not clear what the amount of water on the marsh surface means in some areas. For example, the

categories were determined to be accurately assessed for microtidal areas because the tide never got high enough to make healthy areas of the marsh look degraded. This is clearly not the case for areas where the tidal range is in excess of a meter and can cover short plants such as Wilmington, North Carolina. In these areas a presumption has to be made that most of the area was not at high tide during the time of acquisition.

Review of the Hypotheses

An additional hypothesis was tested, that degradation in the marsh should have no relation to distance from randomly selected points. The results from this test show that degradation is a rare event and clumped. It also gives a picture to compare or contrast with the other hypotheses. In particular, the marsh loss from roads in the Bay areas looks very similar to the pattern related to random points. The others do not. Also, most results that shared the same positive slope have much higher R^2. The random hypothesis was only tested for the Atlantic Coast, but the result may have been similar for the Bay areas. This hypothesis was only to test whether or not other unmeasured factors could influence the regression and, if so, how.

Hypothesis 1 states that the probability of a parcel being completely open water will be negatively related to the distance of the parcel from a road. The hypothesis that roads had a correlation with marsh loss on the Atlantic Coast marshes was rejected because it seemed to be more confounded with upland effects. The roads in the bay areas, on the other hand, are not so strongly tied to upland areas, because they are often built in submerging landscapes (i.e., Dorchester, Somerset and Wicomico counties in Maryland).

The regressions involving the other factors all support the general hypothesis, even if the particular one-tailed tests failed. The results with distance from tidal creeks are a good example. Hypothesis 2 states that the probability of a parcel being completely open water will be positively related to the distance the parcel is from the nearest tidal creek or man-made ditch (e.g. mosquito ditches). For the Bay areas, the regression at short distances actually did not support the hypothesis. However, measured deterioration immediately adjacent to creeks is probably as much due to misregistration as it is to any actual losses on the ground. This may be augmented by the fact that in some locations, Bloodsworth Island, for example (Downs et al., 1994) , shoreline erosion is an important process. From about 150 meters to 2 km, there is a very strong trend (0.92 R^2 for that region) and the tendency toward increasing degradation continues to about 5 km, with some variations. This provides general support to the concept that the interiors of marshes are more degraded than the areas adjacent to tidal creeks or shores.

The slope of this regression for the Atlantic Coast was diametrically opposed to the prediction. This may be related to the fact that the Atlantic Coast marshes tended to be smaller and, therefore, had less developed tidal creek systems that could bring nutrients into the interior of the marsh. Also, fully degraded areas tend to cluster along the coast. This could indicate that either the marshes in this system are eroding at the edge more than deteriorating at the center due to interior ponding. This would have some implications for comparing results of studies done in marshes in different coastal environments. For the Atlantic Coast shoreline erosion seems to be the only significant process indicated by this hypothesis test, and this seems to be a key difference between these systems.

Hypothesis 3 states that the probability of a parcel being completely open water will be negatively related to the distance the marsh system containing the parcel is upstream. The regressions for upstream distance vs. degradation are not very strong, and the variations clearly have a cyclical component. However, this cyclicity may be a result of tidal flooding, which can be higher upstream than downstream. There is a fair amount of scatter, which may be related to the grossness of the measurement. The distance upstream was only measured for major rivers and creeks, and part of the presumption is that where freshwater meets brackish water, sediment will precipitate. This can occur anywhere along a river or major creek, where a smaller stream joins. However, the general trend supports the hypothesis in both regions.

For the distance upstream, Hypothesis 3 was based, in part, on the fact that plant communities change with distance upstream and that relative sea level rise will alter marshes along a river by drowning the downstream marshes and killing species that are less tolerant to salt and anaerobic conditions further upstream. Because seawater is a source of sulfate ions, the seaward marshes on a river would tend to have high sulfide content, as anaerobic bacteria convert sulfate to sulfide, although high sulfide can occur in other areas. As both high salinity and high sulfide concentrations are generally toxic to plants (Koch et al., 1990), this would reduce the number of species able to survive in the more saline and high sulfide conditions at the seaward end of a river. In addition, anoxic conditions can limit plant growth (Anastasiou and Brooks, 2003). Coupled with higher inputs of sediment for the marshes closest to fresh water, this makes a coherent picture of the relationship seen between distance upstream and probability of marsh loss.

Hypothesis 4 states that the probability of a parcel being completely open water will be positively related to the distance of the parcel from the upland. This hypothesis was strongly supported for both areas. Distance from uplands obviously, like the other variables, is a stand in for some other factors. One these factors may simply be elevation. If so, the distance from upland is a more useful measurement than elevation for studying large areas of wetlands. Elevation is extremely time consuming and difficult to measure for a sufficient number of points to build a good model of a marsh. Upland boundaries are mapped already, and only require mapping a single line at the edge of each marsh if a new datum is required. There are likely other factors involved as well, including sediment and nutrient supply, and freshwater runoff to reduce salinity.

Hypothesis 5 states that the probability of a parcel being completely open water will be negatively related to the size of the marsh parcel containing the grid cell. This is naturally potentially confounded with hypotheses 2 and 4 as either upland or a creek will be the boundary of most marsh parcels. The results here are similar for both study areas, and there is a relationship between marsh loss and the size of the parcel. The relationship is a little hard to understand, however. If edge erosion, either shoreline or tidal creek bank, were the primary process, a regression with small parcels being at the most risk would be expected. This is because the ratio of edge to marsh area could be expected to decrease as parcel size increases, if the parcel is convex. If interior ponding is the primary mechanism of loss, then a regression showing large parcels as the most at risk would be expected because the ratio of area available for loss compared to the total size diminishes as the overall parcel size drops. If these two mechanisms operate together, it might be anticipated that large and small parcels would be the most at risk. However, in

actuality the regression shows that for both study areas, the mid-size parcels are the most at risk. The midsize parcels at the most risk are about 2.2 hectares for the Bay Areas and 16.3 hectares for the Atlantic Coast. One possible explanation is that marsh loss probability as a function of interior ponding and the loss as a function of edge to interior ratio overlap.

Table 14. Results of Hypothesis Tests Revisited

Area	Hypothesis	Predicted Correlation	R-Square	Degree	Conclusion
Atlantic	Distance from Random	none	0.544676	1st	Not Rejected
Bay	Distance from Roads	Negative	0.419392	3rd	Rejected
Atlantic		Negative	0.97685	1st. for 100 meters – 1000 meters	Rejected
Bay	Distance from Tidal Creeks	Positive	0.990931	2nd	Not rejected
Atlantic		Positive	0.971589	1st	Rejected
Bay	Distance Upstream	Negative	0.264358	1st	Not rejected
Atlantic		Negative	0.237701	1st	Not rejected
Bay	Distance from Upland	Positive	0.871136	1st	Not rejected
Atlantic		Positive	0.88531	1st	Not rejected
Bay	Area	Negative	0.280912	2nd	Rejected
Atlantic		Negative	0.391991	2nd	Rejected

Primary drivers in marsh loss

The fact that the hypotheses are supported across landscapes and marsh types indicates that there is a great deal of consistency across these marshes. For example, the same primary factors – distance from land and distance upstream - impact both Atlantic

Coast marshes and Chesapeake and Delaware Bay marshes, although the distances involved are different. This would indicate that the same drivers apply in both systems.

These results raise several interesting questions. One question is in the area of defining the primary drivers in marsh loss. If the primary drivers are factors that are related to landscape position, then altering the plant and animal species present at a given location may not have much impact on marsh longevity. On the other hand, if landscape topography merely sets conditions that make an area susceptible to loss (assuming other factors are present such as *Nutria*), then altering the biota of an area will clearly have a positive impact on marsh longevity. Money is spent on wetland mitigation banks, for example, where the local topography is changed and desirable species are planted. If the general topography of a site will eventually override the local changes, then the money may not be well spent and the environment may be poorly served if the created or restructured wetlands are only required to be kept in order for five years.

Management

The main result of this research is to show that marsh processes are influenced by events happening at the landscape scale. As noted previously, most marsh studies take place on very small scales. This may not be appropriate to understanding the function of salt and brackish marshes. The landscape model presented here cannot identify exact points of marsh loss. However, it may be possible to better identify where disintegration of a marsh will start, or which direction it will move using landscape parameters than local measurements of fluctuating sediment height.

Some crucial management questions can be addressed with this model. Evers (1998) showed that in the absence of *Nutria* marshes will regrow. It would be useful to attempt to predict if this regeneration is likely to be long-term or short-lived. If marsh loss is mainly driven by its position in the landscape, then it may be preferable to build exclosures or take other measures to reduce *Nutria* impacts in areas where degradation is not predicted to occur for landscape reasons. If the landscape drivers only predispose an area to loss given the action of some other impact, then removing *Nutria* would be useful in preserving high-risk areas.

For the Bay, the overall accuracy in correctly identifying pixels is 72%, with 37% of the degraded pixels correctly identified. On the flip side, of the pixels predicted to be degraded, only 7% were actually degraded. This means that a manager or researcher looking for degraded points in the marsh may have difficulty using these data, except that, as shown in Figure 50, the model tends to pick areas where degradation is occurring. Given this, the results would help in identifying areas of future loss.

For the Atlantic Coast, the results are somewhat different. The model correctly identifies 14% of the degraded pixels. On the other hand, 60% of the pixels identified as degraded are, in fact, degraded. This means that the same manager going into an Atlantic Coast marsh looking for degraded pixels has a very high likelihood of finding one based on these data. The problem is reversed from the Bay area. On the Atlantic Coast, the problem would be finding more than a small percentage of the degraded pixels. The clumpiness of degradation would help with this, however. Because marsh loss is more likely in some places than others, finding some degraded points will lead the manager to associated degraded areas.

The Bay area marshes seem to be impacted by the presence of roads, but this is not as strong a correlation as hoped. There are several possible reasons for this. One is that the effect is too localized. A second is that the marsh areas where roads are built may have been chosen because they were more stable areas to begin with and may be maintained by anthropological inputs of material and energy. In addition, some roads have culverts under them to allow drainage from one side to the other. Lastly, much of the damage in areas like BNWR was apparently done before the NWI data were collected, so that the major historical component of damage from roads was missed. The only other source of marsh loss examined here that is arguably anthropogenic in nature is sea level rise. Though it is difficult to know how much of sea level rise is actually anthropological in nature and how much has other causes, there is a growing consensus that the acceleration in the sea level rise since the early decades of the 20th century reflected anthropogenic global warming.

This does not alleviate the need for understanding, monitoring and modifying human impacts on coastal marsh systems. As with biology, there is no way to know if localized human impacts -- ranging from management techniques to pollution or reduction of freshwater and sediment inputs -- are able to drive the large scale processes leading to marsh loss. Nor is there is any real way to determine if they merely amplify landscape drivers in marsh loss, while having minimal impact where the landscape and other natural mechanisms encourage marsh development and sustainability. Direct impacts such as filling a marsh, of course, have impacts on the marsh destroyed. From the fact that uplands tend to make the marshes next to them more stable, it would be useful to see what happens to neighboring marsh parcels when one area is filled.

Assuming no further human encroachment occurs, this would likely reduce erosion and supply nutrients to the areas adjacent to the fill. However, it might also precipitate penetration of the marsh by invasive species such as *Typhus* sp. or *P. australis*.

Questions for further study

What resolution of imagery would be best for both the Coastal Marsh Project analysis and the landscape analysis? Would finer resolution data (like Ikonos) give a clearer understanding on such a large scale? For example, in order to differentiate tidal creeks that are sources of tidal water and sediment from those that are loci of marsh loss, would it be appropriate to use imagery of sufficient detail to see where creek bank slumping was occurring? On a project of this scale, that level of detail might overwhelm the resources available to analyze them. Similarly, if mapped at a higher resolution, the impact of different plant species on the longevity of the marsh could be assessed statistically.

An uncontrolled factor was allowed into the analysis by not differentiating between different types of land cover that border the marsh. As long as the land covers were not estuarine intertidal marsh, they were considered upland. Presumably, it makes a difference if the neighboring land cover is palustrine marsh, a swamp, an old sand dune, or a hill. Uplands were hypothesized to have an impact on the marsh both through hydrology and by providing stability. The amount of water flowing into a marsh from its landward edge may be more a result of climate than whatever land cover exists there, although the sediment and nutrient load and rate variability will be affected However, the stability provided will be less if the intervening non-estuarine wetland is large. This

provides some degree of uncertainty in the results. However, adding in other cover types would have simply expanded the number of factors, but not necessarily added more information.

Once done, most of the hard work of developing this model for an area does not need to be repeated. Additional factors could be added as new geographic layers at the resolution of 28.5 meters. For example, *Nutria* population density could be added and the statistical tests performed to determine the impact of this factor.

One good question, especially from the management point of view, would be rates. Knowing that two areas are at equal risk of loss does not help much if the expected rates of loss are unknown. This research, ultimately based on the NWI, which is a variable starting point, does not have the possibility of giving rates. However, multiple images taken over 5 to ten year intervals, for example, 1984, 1989, 1994, 1999, and 2004 would give an excellent time series from which to derive rates. This would help with smoothing out errors caused by tidal fluctuations and weather events that can make an area look more degraded than it is. In Moreover, to accomplish this end, multiple scenes should be collected each year during the growing season.

A decision tree approach might have produced more useful results and be easier to update. One way to go about this would be to start with marsh parcel size. This would allow a manager to see directly how different factors related to marsh health. For the type of decision tree shown in Figure 55 the data must be broken into categories. This process would help clarify the inputs and outputs. For example, the probability of degradation based on size of the marsh parcel can be divided into two groups. For the Atlantic Coast, those marsh pixels in a parcel that is between 1 and 500 hectares, have an

approximately 0.16 probability of being degraded. Pixels in marsh parcels that are not in that size range have a much smaller likelihood of being degraded. Dividing the distance from upland into three categories yields the tree in the figure. From this it is very easy to see that areas within 100 meters of an upland that are in a small or large parcel are much less likely to be degraded than an area more than 1000 meters from the upland in a parcel between 1 and 500 hectares in size.

.

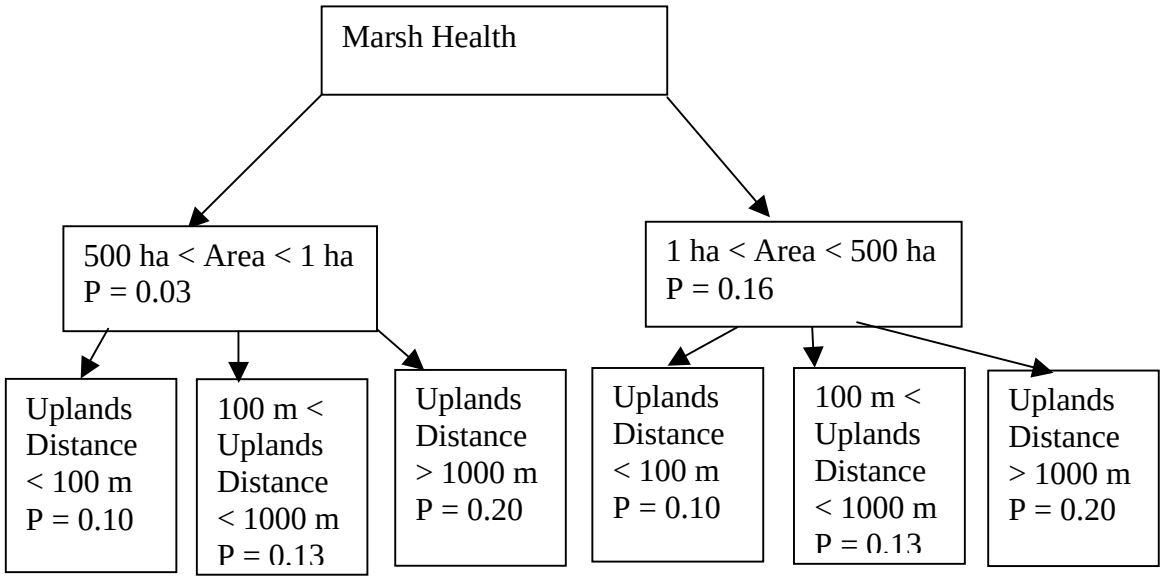

Figure 55. Simplified Model Decision Tree for Analysis of Marsh Health

P is the probability of degradation given the conditions described in the box.

Appendices

Appendix A (Rogers unpublished data)

This was done as a research project for Dr. Andrew Baldwin's Wetlands course in 1999, titled "Impact of Position in the Landscape on the Health of Wetlands" The investigators were Andy Rogers, Deanna Guerieri, Nicole Hale, and Chris Rogers.

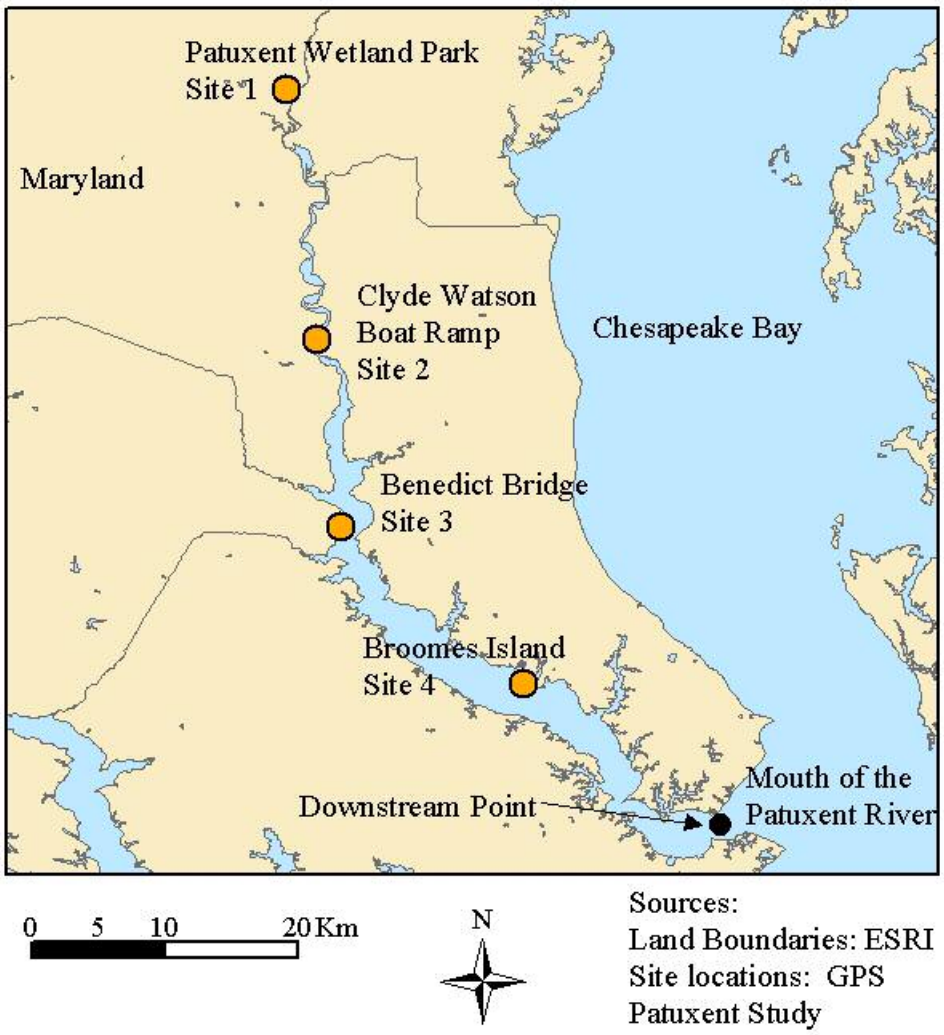

Figure 56. Transect locations for study done by Rogers et al., 1999.

Table 15. Data Collected for the Patuxent Study

Site	Distance Upstream (m)	Distance Inland (m)	Fraction Bare	Species Richness	Salinity	REDOX (mV)
1	74624	0	15	2	2	-273
1	74624	0	0	5	3	64.2
1	74624	15	15	3	1	-205.75
1	74624	15	97.5	4	0.5	-181
1	74624	30	3	4	1	-281
1	74624	30	62.5	3	1.5	-221
2	50072	0	37.5	1	7	-195.5
2	50072	0	62.5	1	7	-206.25
2	50072	15	15	1	8	-346
2	50072	15	3	1	7	-196.5
2	50072	30	85	1	7	-203
2	50072	30	85	2	8	-181
3	34948	0	62.5	2	14	38.5
3	34948	0	62.5	1	16	
3	34948	15	37.5	3	15	-211.5
3	34948	15	0.5	2	16	-106.5
3	34948	30	37.5	4	15	-214.25
3	34948	30	15	3	15	-188.25
4	18870	0	15	2	16	156.33
4	18870	0	15	1	15	162.75
4	18870	15	15	2	17	9.25
4	18870	15	37.5	2	16	28.25
4	18870	30	15	2	17	105
4	18870	30	0.5	3	17	64.75

Appendix B Tide and Sea Level Rise Data

Table 16. Data for Tide and Sea Level Rise Calculations

Station Name	Latitude	Longitude	Date Established	Mean Range (feet)	Sea Level Rise
Annapolis MD	38.98333333	-76.48	Sep 14 1978	0.97	3.53
Atlantic City NJ	39.355	-74.41833333	Aug 15 1911	4.02	3.98
Baltimore MD	39.26666667	-76.57833333	Jul 1 1902	1.14	3.12
Beaufort NC	34.72	-76.67	Jun 4 1964	3.11	3.71
Brandywine Shoal Light DE	38.98666667	-75.11333333	Mar 18 1984	4.73	
Burlington Delaware Rive NJ	40.08	-74.87333333	Feb 21 1977	7.3	
Cambridge MD	38.57333333	-76.06833333	Oct 21 1980	1.62	3.52
Cape Hatteras Fishing Pie NC	35.22333333	-75.635	May 24 1973	2.99	
Cape May NJ	38.96833333	-74.96	Oct 25 1965	4.85	3.88
Chesapeake Bay Bridge Tun VA	36.96666667	-76.11333333	Jan 26 1975	2.55	7.01
Colonial Beach VA	38.25166667	-76.96	Jan 7 1972	1.63	5.27
Delaware City DE	39.58166667	-75.58833333	Oct 8 2001	5.28	
Duck NC	36.18333333	-75.74666667	Dec 1 1977	3.22	
Gloucester Point VA	37.24666667	-76.5	May 16 1950	2.38	3.95
Kiptopeke VA	37.16666667	-75.98833333	Aug 22 1951	2.6	3.59
Lewes DE	38.78166667	-75.12	Jan 14 1919	4.08	3.16
Lewisetta VA	37.995	-76.465	Oct 20 1970	1.24	4.85
Money Point	36.77833333	-76.30166667	Dec 17 1997	2.86	

VA					
Ocean City Inlet MD	38.32833333	-75.09166667	Jun 5 1978	2.19	
Oregon Inlet Marina NC	35.795	-75.54833333	Aug 14 1974	0.89	
Reedy Point DE	39.55833333	-75.57333333	Jul 30 1956	5.34	
Sandy Hook NJ	40.46666667	-74.01	Jan 7 1910	4.7	3.88
Sewells Point VA	36.94666667	-76.33	Jul 1 1927	2.43	4.42
Ship John Shoal NJ	39.305	-75.375	Oct 30 1997	5.6	
Solomons Island MD	38.31666667	-76.45166667	Nov 5 1937	1.17	3.29
Springmaid Pier SC	33.655	-78.91833333	Sep 28 1976	5.02	
Tacony-Palmyra Bridge NJ	40.01166667	-75.04333333	May 7 2002	6.5	
Tolchester Beach MD	39.21333333	-76.245	Jun 24 1971	1.2	
Wachapreague VA	37.60666667	-75.68666667	Jun 28 1978	4.02	
Wilmington NC	34.22666667	-77.95333333	Jan 1 1908	4.28	2.22
Windmill Point VA	37.615	-76.29	Jun 24 1970	1.16	

Appendix C Arc Macro Language Scripts

AMLS

This comprises all the amls actually used in processing the data for this project. Numbers in the titles, such as streammask2.aml are design numbers. Streammask1 was not used in the final output. Some of these amls are bare-bones scripts, a few are full implementations including subroutines to cleanup temporary files, usage statements that are printed when incomplete command lines are typed. In most, the line "&severity &error &ignore" is used at the beginning, usually followed later by a "&severity &error &fail." These tell the routine what to do when it encounters an error. The ignore option is used when the routine is removing files that may or may not have been left behind by a previous run of the same program, or when one of the first commands is "grid". If the aml was run from grid, encountering the "grid" command or attempting to delete a file that is not there will cause it to fail unnecessarily.

Eucdist_proc.aml

```
/* this aml takes in the water data produced by combining all
/* the water data from NWI and clips off all the
/* streams that are less than 3 pixel wide.  It then uses these
/* major streams to calculate how far upstream a given parcel of marsh is.
/* Inputs required
/*  wetmask (watermask of area) in first line after initial cleanup
/*  downstreamg  (boundary marking downstream limit)
```

```
&args wetmask downstreamg parms:res
&if [NULL %downstreamg%] &then
  &call usage
&else
  &call water_process
&return
&routine water_process
&call cleanup
&severity &error &ignore
kill eucdistance all
grid
&severity &error &routine terminate
setcell %wetmask%
keeptmp = focalsum(%wetmask%,rectangle,3,3,data)
if(keeptmp > 4 & %wetmask% == 1)
streamcliptmp = 1
else
streamcliptmp = 0
endif
&type "Just made streamcliptmp"
streamclip = setnull(streamcliptmp <> 1,streamcliptmp)
/* kill streamcliptmp all
updist = costdistance(%downstreamg%,streamclip)
```

```
/* kill streamclip all
updistint = int(updist)
kill updist all
/* Eucdistance is the upstream distance required for
/* analysis of effects from being upstream from low tide
eucdistance = eucallocation(updistint)
&return
/*****************************************************************
/*****************************************************************
&routine cleanup
/*****************************************************************
/*****************************************************************
&severity &error &ignore
/* This removes files left over if the program
/* crashed on its previous run
kill backlink all
kill backlink2 all
kill creeks all
kill dorcmars2 all
kill dorcmars3 all
kill dorcmask all
kill dorcnotwater all
kill dorcnotwater2 all
```

kill eucdistance all

kill fc3max all

kill fc3min all

kill flowdir all

kill flowlen all

kill flowlen2 all

kill fmax all

kill fmin all

kill keeptmp all

kill keeptmp2 all

kill keeptmp3 all

kill keeptmp4 all

kill keeptmp5 all

kill majority all

kill majstreams all

kill maxwidth all

kill narrow_water all

kill outgrid all

kill outgrid2 all

kill outgridave all

kill outgridb all

kill outgridb2 all

kill outgridc all

```
kill streamclip all
kill streamcliptmp all
kill streamclptmp2 all
kill tmpcreeks all
kill updist all
kill updist2 all
kill updistint all
kill upstreamcrk2 all
kill upstreamcrks all
kill upstreamdist all
kill upstreamdist1 all
kill upstreamtmp all
kill width all
&severity &error &fail
&return
/*****************************************************************
/*****************************************************************
&routine terminate
/*****************************************************************
/*****************************************************************

q
&return &error
```

&routine usage

&type USAGE: water_process wetmask downstreamg

&return
==========

mask.aml

```
/* This file creates stream, road and land masks to do
/* costdistance calculations with.
/* updated 10/8/01 so that kernels for stripping out roads are defined on left
/* and right or top and bottom halves, and each half must contain an upland
/* value to remove the road.
/* The wetmasks were replaced by the output from streammask2.aml
&args health streams roads parms:rest
&call cleanup
&severity &error &ignore
kill roadmask all
kill wetmask all
kill landmask all
&severity &error &fail
&call road
&call cleanup
&return
&routine road
grid
if(isnull(%health%))
jm = %health%
else if(%health% == 6)
```

```
jm = 1
else if(%health% == 7)
jm = 9
else
jm = 4
endif
&type Passed first grid
landmask = setnull(jm ^= 9,1)
&type Passed landmask
if(isnull(%streams%))
jm2 = jm
else
jm2 = 1
endif
wetmask = setnull(jm2 ^= 1, 1)
if(isnull(%roads%))
jm3 = jm2
else
jm3 = 2
endif
/* strip out roads across dry land in one direction.
/* possible values for jm4 are 1,2,9,4
/* 4 = marsh
```

```
/* 2 = road
/* 9 = upland
/* 1 = open water
jm4 = focalmax(jm3,irregular,../kernels/kernel1x5r,DATA)
jm41 = focalmax(jm3,irregular,../kernels/kernel1x5l,DATA)
jm42 = focalmax(jm3,irregular,../kernels/kernel5x1t,DATA)
jm43 = focalmax(jm3,irregular,../kernels/kernel5x1b,DATA)
if(jm4 == 9 & jm41 == 9)
jm5 = jm2
else if(jm42 == 9 & jm43 == 9)
jm5 = jm2
else if(jm42 == 4 & jm43 == 4)
jm5 = jm3
else if(jm4 == 4 & jm41 == 4)
jm5 = jm3
else if(jm4 == 9 | jm41 == 9 | jm42 == 9 | jm3 == 9)
jm5 = jm2
else
jm5 = jm3
endif
roadmask = setnull(jm5 ^= 2, 1)
q
&return
```

```
/* End of routine land
/*****************************************************************
/*****************************************************************
&routine cleanup
/*****************************************************************
/*****************************************************************
&severity &error &ignore
kill jm all
kill jm2 all
kill jm3 all
kill jm4 all
kill jm41 all
kill jm42 all
kill jm43 all
kill jm5 all
&severity &error &fail
&return
/*****************************************************************
```

prjtiger.aml

```
/* This aml reprojects TIGER line files from geographic to UTM NAD83
&args cover parms:rest
project cover %cover% %cover%p
input
```

projection geographic

datum nad83

units dd

parameters

output

projection utm

datum nad83

units meters

zone 18

parameters

end

/**********

probability2.aml

```
/* Inputs:
&args distance_file input_prob output_probability parms:res
/* distance_file is any of the various distance files
/* input_prob is simply the MSCI marsh coverage from the Coastal Marsh Project
/* Output_probability is the name of the grid being created.
/* This file normalizes the distances into 100 integer units.
/* It then calculates the probability of a marsh pixel being totally degraded
    /* in each zone.
/* It then converts both the input distance file and the out_probability file
/* into natural logarithms
&if [NULL %output_probability%] &then
  &call usage
&else
  &call process
&return
&routine process
&call cleanup
kill %output_probability% all
grid
&severity &error &fail
/* The describe command puts all of the data about the coverage
```

```
/* into variables in memory that can be accessed in the script.
/* In this case, the minimum and maximum values are of interest.
&describe %distance_file%
ingrid = setnull(isnull(%input_prob%),%distance_file%)
tmpgrd1 = ((ingrid - %GRD$ZMIN%) * 100)/(%GRD$ZMAX% -
%GRD$ZMIN%) + 0
/* zonal functions only work on integer grids
tmpgrdint = int(tmpgrd1)
kill tmpgrd1 all
/* calculate the area of each zone
tmpzonalarea = zonalarea(tmpgrdint)
/* convert the input marsh grid into 1's or 0's.
tmpprob = con(%input_prob% == 4,1,0)
/* calculate the total number of totally degraded cells in each zone.
tmpprob1 = zonalsum(tmpgrdint,tmpprob)
/* calculate the zonal probability of a square meter being totally
/*  degraded and convert to natural logarithm.
%output_probability% = ln(28.5 * 28.5 * tmpprob1 / tmpzonalarea)
/* calculate natural logarithm of input file
%distance_file%ln = ln(%distance_file%)
q
&call cleanup
&severity &error &fail
```

```
        &return
        &routine usage


        &type USAGE: distance input_probability (marsh surface index 1 - 4)
output_probability_file_name
        &return
        &routine cleanup
        &severity &error &ignore
        kill tmpgrd0 all
        kill tmpgrd1 all
        kill tmpgrdint all
        kill tmpprob all
        kill tmp_prob0 all
        kill tmpprob1 all
        kill ingrid all
        kill tmpzonalarea all
        &return
```

putfile0.aml

```
/* creates a new file and populates it with lines from another file
&args cover output parms:rest
ae
ec %cover%
ef arc
select all
put %output%
q
```

putfile.aml

```
/* combines two line coverages, by adding lines from the cover to the output.
&args cover output parms:rest
ae
ec %cover%
ef arc
select all
put %output%
y
q
```

putpoly.aml

```
/* combines two polygon coverages.
```

```
&args cover output parms:rest

ae

ec %cover%

ef poly

select all

put %output%
```

road_process.aml

```
/* This aml improves the initial roadmask made by eliminating roads on upland
/* borders and incorporating stream data.  This script additionally calculates
/* whether a given road segment impedes by determining if the difference
/* in the distance required for water to flow to points on opposite sides of
/* the road is greater than expected for parallel flows on each side.
/* Inputs required
    &args wetmask downstreamg roadmask landmask parms:res
/* Remove any temporaty files left by previous runs
&call cleanup
&severity &error &ignore
kill roadout3 all
grid
&severity &error &routine exit
setcell %roadmask%
/* Determine whether roads that match up with upland areas
/* are roads across the marsh or more likely roads on a narrow strip
/* of upland.
&type "Performing width calculations"
if(isnull(%landmask%))
 tlandmask = 0
```

```
else
 tlandmask = %landmask%
endif
if(tlandmask == 0)
 notland = 1
else
 notland = 0
endif
notland2 = setnull(notland == 0,1)
/* This just creates a background layer of all 1's
/* that defines the extent and cost in the cost
/* distance function
if(isnull(%roadmask%))
 troadmask = 0
 else
 troadmask = %roadmask%
endif
if(troadmask == 0)
 tmpmask = 1
else
 tmpmask = 1
endif
landwidth = costdistance(notland2,tmpmask)
```

```
kill notland all
kill notland2 all
maxwidth = focalmax(landwidth,rectangle,7,7,data)
kill landwidth all
&type "Completing width calculation"
/* This sets non road areas to null as well as areas
/* of roads that are on broad expanses of land
/* and codes the remaining road segments as 1
/* 255 is used here similary to NULL or zero in other places
if((troadmask == 0) | (maxwidth > 75))
 roadout = 255
else
 roadout = 1
endif
&type "calculated maxwidth"
kill maxwidth all
/* use a wetmask to run the distance calculation on.
/* It will supercede roads where they cross.
/* roads and uplands will be combined to provide
/* a boundary otherwise distance will flow up from
/* the downstream boundary too far
/* This sets road values to 255 (inpenetrable) and
/* all else to 100 restricted flow)
```

```
/* one implies road is present
if(troadmask == 1)
 tmp1 = 255
else
 tmp1 = 100
endif
&type "calculated tmp1"
/* This sets all land pixels to 255 and brings over the
/* road values (assumes that a value of 1 in landmask =
/* land is present and that there are no NULL values
if(tlandmask == 1)
 tmp2 = 255
else
 tmp2 = tmp1
endif
kill tmp1 all
&type "calculated tmp2"
/* This sets any non-water pixel to the value
/* of the previous set, either 255 or 100
/* Water pixels are assigned a resistance of 1
if(%wetmask% == 0)
 tmp3 = tmp2
else
```

```
 tmp3 = 1
endif
kill tmp2 all
&type "calculated tmp3"
tmp4 = setnull(tmp3 == 255, tmp3)
&type "calculated tmp4"
kill tmp3 all
/* the following just thickens road lines making them
/* more impervious to being crossed at thin points
/* by the cost function
tmp5 = focalmajority(tmp4,nodata)
kill tmp4 all
&type "calculated tmp5"
distance = costdistance(%downstreamg%,tmp5)
kill tmp5 all
&type "calculated distance"
tmp1 = con(isnull(distance),0,distance)
kill distance all
&type "calculated tmp1"
downstreammin = focalmin(tmp1,rectangle,5,5,data)
downstreammax = focalmax(tmp1,rectangle,5,5,data)
&type "calculated downstreammax"
kill tmp1 all
```

```
if(((downstreammax - downstreammin) > 13000) & (roadout == 1))
 roadout3 = 1
else if(roadout == 1)
 roadout3 = 2
else
 roadout3 = 255
endif
&type "calculated roadout3"
kill roadout all
kill downstreammin all
kill downstreammax all
q
&return
/*****************************************************************
/*****************************************************************
&routine cleanup
/*****************************************************************
/*****************************************************************
&severity &error &ignore
/* This removes files left over if the program
/* crashed on its previous run
kill tlandmask all
kill troadmask all
```

```
kill notland all
kill notland2 all
kill tmpmask all
kill maxwidth all
kill landwidth all
kill roadout all
kill roadout2 all
kill roadout3 all
kill downstreammin all
kill downstreammax all
kill dorcnwigmax all
kill tmp1 all
kill tmp2 all
kill tmp3 all
kill tmp4 all
kill tmp5 all
kill distance all
kill downstreammin all
kill downstreammax all
kill roadout all
&severity &error &fail
&return
/*************************************************************
```

```
/*****************************************************************
&routine exit
/*****************************************************************
/*****************************************************************
q
&return &error
```

Streammask2.aml

```
/* This aml converts a set of road and marsh water grids into
/* a single mask suitable for calculating distance
&severity &error &ignore
/* remove previous temp files
kill jm all
kill jm3 all
kill jm4 all
&args water roads outmask parms:rest
/* remove the previous output
kill %outmask% all
&severity &error &fail
grid
/* if the marsh coverage, which is the water input, is 1,2 or 3
/* it represents marsh land.
if(%water% > 0 and %water% < 4)
jm = 4
/* a marsh code of 7 = upland
else if(%water% == 7)
jm = 10
else
```

```
/* values 4 or 6 represent open water
jm = 9
endif
/* take a look at the road grid.  If it has a null value, just use the value calculated
above.
if(isnull(%roads%))
jm3 = jm
/* otherwise, if a road is present, assign it to class 10, not marsh and
/* not water.
else
jm3 = 10
endif
/* replace road pixels with water pixels if they intersect
jm4 = min(jm,jm3)
/* this creates a mask that is null, 4,9 or 10
%outmask% = jm4
/* The water_process routine requires a mask that is null or 1.
if(%outmask% == 9)
  %outmask%_proc = 1
else
  %outmask%_proc = 0
endif
q
```

kill jm all

kill jm3 all

kill jm4 all

==========

water_dist.aml

```
/* This aml uses the output of water_process and calculates the distance from each point in the marsh to the nearest stream.
&type need allcreeks and roadout3
grid
ALLCREEKSZERO = CON (ISNULL(ALLCREEKS),0,allcreeks)
TMPWETCOST = CON (ALLCREEKSZERO == 0,1,1)
TMPCOST = CON (ISNULL(LANDMASK),1,roadout3)
tmpcost = con(isnull(landmask),1,roadmask5) or
wetcost = setnull(tmpcost == 255,tmpwetcost)
allcreeks is output from water_process.aml
allcreeksnull = setnull(allcreeks == 0, allcreeks)
waterdist = costdistance(allcreeksnull,wetcost)
q
```

water_process.aml

```
/* this aml takes in the water data produced by combining all
/* the water data from NWI and clips off all the
/* streams that are less than 1 pixels wide.
/* Inputs required
/*  wetmask (watermask of area) in first line after initial cleanup
/*  downstreamg  (boundary marking downstream limit)
&args wetmask downstreamg landmask parms:res
&call cleanup
&severity &error &ignore
kill allcreeks all
kill upstreamdist2 all
&severity &error &fail
grid
setcell %wetmask%
keeptmp = focalsum(%wetmask%,rectangle,3,3,data)
/* restrict water mask to water bodies that occupy
/* more than half of a moving five x five window.
if(keeptmp > 4 & %wetmask% == 1)
  streamcliptmp = 1
else
  streamcliptmp = 0
```

```
endif
&type "Just made streamcliptmp"
/* set non-water pixels to NULL
streamclip = setnull(streamcliptmp <> 1,streamcliptmp)
kill streamcliptmp all
/* Calculate the distance upstream for every point on the connected water bodies
updist = costdistance(%downstreamg%,streamclip)
kill streamclip all
/* This step just reduces data storage issues.  Occasionally,
/* the program ran out of disk space doing this set of calculations.
updistint = int(updist)
kill updist all
/* allocate the value of the nearest water pixel to each marsh pixel
eucdistance = eucallocation(updistint)
/* If the stream is connected to the Bay or ocean directly
/* give it a value of 1, else 0
if(updistint > 0 )
  majstreams = 1
else
  majstreams = 0
endif
&type "Performing width calculations"
/* Created an inverted water mask
```

```
if(%wetmask% == 0)
  dorcnotwater = 1
else
  dorcnotwater = 0
endif
/* Now set the non water pixels to null and all else to 0.
dorcnotwater2 = setnull(dorcnotwater == 1,0)
/* This just creates a background layer of all 1's
/* that defines the extent and cost in the cost
/* distance function
if(%wetmask% == 0)
  dorcmask = 1
else
  dorcmask = 1
endif
kill dorcnotwater all
/* using the watermask, this essentially calculates the half-width of a body
/* of water by calculating the shortest distance to a shoreline.
/* Backlink gives a value for the current cell which shows the previous cell
/* in the least cost path.
width = costdistance(dorcnotwater2,dorcmask,backlink)
/* This just saves disk space
tmp = int(width)
```

```
kill width all
rename tmp width
kill dorcmask all
kill dorcnotwater2 all
/* These steps extract the directions of least cost paths from a block
/* of pixels.
fmax = focalmax(backlink,rectangle,3,3)
fmin = focalmin(backlink,rectangle,3,3)
fc3max = focalmax(backlink,irregular,../kernels/kernel_circle_3)
fc3min = focalmin(backlink,irregular,../kernels/kernel_circle_3)
/* For a 3x3 rectangle, assigns the maximum width calculated to the center cell.
maxwidth = focalmax(width)
tmp = int(maxwidth)
kill maxwidth all
rename tmp maxwidth
/* Used to call flow.aml
&type "Running flow calculation"
flowdir = flowdirection(width)
/* upstream is a keyword in the command below, not a file name
flowlen = flowlength(flowdir,%wetmask%,upstream)
kill flowdir all
/* used to call width2
```

```
&type "Completing width calculation"
/* If the water body is < 3 pixels wide, assign the width value to the output,
/* otherwise assign 0.
if((fmin == 0) & (maxwidth < 60))
  outgrid = width
else
  outgrid = 0
endif
kill maxwidth all
/* This was designed to deal with some issues in the way
/* backlink represents neighboring cells.  IN particular, the numbers go
/* continuously around the cell from 1 – 8. but there is a disconuity
/* at the juncture of 8 and 1.
if((backlink == 8) & (fc3min > 6))
  outgridb = 0
else if((backlink == 8) & (fc3max == 1))
  outgridb = 0
else if((backlink == 1) & (fc3max < 3))
  outgridb = 0
else if((backlink == 1) & (fc3min == 8))
  outgridb = 0
else if((fmax - fmin) < 2)
 outgridb = 0
```

```
else
outgridb = width
endif
kill backlink all
kill fmax all
kill fmin all
kill fc3max all
kill fc3min all
kill width all
/* eliminate null values
if(isnull(outgridb))
  outgridb2 = 0
else
  outgridb2 = outgridb
endif
kill outgridb all
if(outgrid > 0)
  outgridc = outgrid
else
  outgridc = outgridb2
endif
kill outgrid all
kill outgridb2 all
```

```
        outgridave = focalmean(outgridc)
        kill outgridc all
        outgrid2 = setnull(outgridave == 0, outgridave)
        kill outgridave all
        &type "Calculating creeks"
        narrow_water = setnull(outgrid2 > 50,outgrid2)
        kill outgrid2 all
        creeks = setnull(isnull(narrow_water) | (%wetmask% == 0) | (flowlen < 50)
,narrow_water)
        kill narrow_water all
        kill flowlen all
        if(isnull(creeks))
          tmpcreeks = 0
        else
          tmpcreeks = creeks
        endif
        kill creeks all
        upstreamcrks = setnull((tmpcreeks + majstreams) == 0, 1)
        kill majstreams all
        kill tmpcreeks all
        if(isnull(%downstreamg%))
          upstreamcrk2 = upstreamcrks
        else
```

```
  upstreamcrk2 = 1
endif
&type "Calculating distance updist2"
updist2 = costdistance(%downstreamg%,upstreamcrk2)
kill upstreamcrk2 all
if(updist2 > 0)
 allcreeks = 1
else
 allcreeks = 0
endif
q
&return
/*****************************************************************
/*****************************************************************
&routine cleanup
/*****************************************************************
/*****************************************************************
&severity &error &ignore
/* This removes files left over if the program
/* crashed on its previous run
kill backlink all
kill backlink2 all
kill creeks all
```

kill dorcmars2 all

kill dorcmars3 all

kill dorcmask all

kill dorcnotwater all

kill dorcnotwater2 all

kill eucdistance all

kill fc3max all

kill fc3min all

kill flowdir all

kill flowlen all

kill flowlen2 all

kill fmax all

kill fmin all

kill keeptmp all

kill keeptmp2 all

kill keeptmp3 all

kill keeptmp4 all

kill keeptmp5 all

kill majority all

kill majstreams all

kill maxwidth all

kill narrow_water all

kill outgrid all

```
kill outgrid2 all
kill outgridave all
kill outgridb all
kill outgridb2 all
kill outgridc all
kill streamclip all
kill streamcliptmp all
kill streamclptmp2 all
kill tmpcreeks all
kill updist all
kill updist2 all
kill updistint all
kill upstreamcrk2 all
kill upstreamcrks all
kill upstreamdist all
kill upstreamdist1 all
kill upstreamtmp all
kill width all
&severity &error &fail
&return
============================================================
===============
```

A.1 Processing Steps for All Input Grids

A.1.1 Upstream Distance

1. eucdistance (upstream distance) comes directly out of the water processing aml or can be generated by the eucdistance_proj.aml.

A.1.2 Distance from Water

2. waterdist = costdistance(allcreeksnull,wetcost)
    a. allcreeksnull = setnull(allcreeks == 0, allcreeks)
        i. allcreeks is output from water_process.aml
    b. wetcost = setnull(tmpcost == 255,tmpwetcost)
        i. tmpcost = con(isnull(landmask),1,roadmask5) or
        ii. TMPCOST = CON (ISNULL(LANDMASK),1,roadout3)
        iii. TMPWETCOST = CON (ALLCREEKSZERO == 0,1,1)
            1. ALLCREEKSZERO = CON (ISNULL(ALLCREEKS),0,allcreeks)
3. ROADDIST = costdistance(roadmask5,roadcost2)
    a. ROADCOST2 = CON (ISNULL(DORCMARS),roadcost,1)
        i. dorcmars is the marsh coverage in 4 categories, leaving out existing open water
        ii. ROADCOST = setnull(tmproadcost2 == 1,1)
            1. tmproadcost2 = con(wetshoremax == 0,tmproadcost,wetshoremax)
                a. tmproadcost = con(isnull(landmask2),0,1)

i. landmask2 = setnull(focalmax(roadmask4,data) == 1,landmask)

ii. roadmsk4 (see below)

b. wetshoremax = focalmax(wetshoremask)

i. wetshoremask = con(isnull(dorcshorepg),0,dorcshorepg == 0,0,1)

1. polygrid dorcshorep dorcshorepg grid-code
2. build dorcshorep
3. project cover dorcshore dorcshorep utmproj
4. clip mdshore dorchclip dorcshore
5. import cover mdshore mdshore

b. ROADMASK5 = setnull(roadmask4 == 0,roadmask4)

i. ROADMASK4 = CON (ROADMASK3 == 1 or roadmask3 == 2,1,0)

1. ROADMASK3 = CON (ISNULL(REMOVE-ROADSG),roadout3,0)
2. roadout3 is product of road_process.aml
3. remove-roadsg is hand-created coverage to remove residual undesirable roads.

4. LANDDIST = costdistance(landmask,landcost)

a. rename dorclandmask landmask

i. DORCLANDMASK = SELECTPOLYGON(../delmarva/landmask, dorchclip)

ii. LANDCOST = con(isnull(landmask),1,1)

5. dorcareaint = int(dorcareanorm + 0.5)
    a. dorcareanorm = datanormalization dorcarealn
        i. dorcarealn = ln(dorcareainv)
            1. dorcareainv = 1 / dorcareatru2
                a. dorcareatru2 = setnull(isnull(marsh),dorcareatrue)
                    i. dorcareatrue = con(dorcarea > 600000000,0,dorcarea)
                        1. DORCAREA = polygrid(dorcnwidis,area,#,#,28.5)

A.2 Calculating the Probabilities

/* indicates a comment

%xxx% indicates a variable grid name, either the inputs or outputs.

tmpxxx are grids used only in these calculations which are then discarded.

/* First convert the distance file to natural logs

%distance_file%ln = ln(%distance_file%)

/* convert the logarithms to 100 categories 1 - 100.

tmpgrd1 = ((%distance_file%ln - distanceMIN) * (99))/(distanceMAX -

```
distanceMIN) + 1

/* round the converted logs to the nearest integer to actually create
categories.
tmpgrdint = int(tmpgrd1)

/* Calculate the total area of each zone
tmpzonalarea = zonalarea(tmpgrdint)

/* calculate the total number of pixels that are open water in each zone
tmpprob1 = zonalsum(tmpgrdint,%input_prob%,data)

/* calculate the probability of a square meter being open water.
/* Since the zonal area is in meters and the probability is in pixels,
/* the number of pixels has to be multiplied by the pixel size in meters.
%output_probability%ln = ln(28.5 * 28.5 * tmpprob1 / tmpzonalarea)

To create the graphs, the numbers are processed by.
tmp = int(100 * lndistance)
sampeffectbay = sample(tmp,effectprobbayln)
kill tmp all
```

Appendix D Landscape Model Eigenvalue Loadings

Bay Model 1

Table 17. Bay Model 1 Covariance Matrix

Layer	Land	Water	Roads	Area	Upstream	Northing	Easting
Land	0.02986	-0.00245	-0.00525	0.00857	0.00554	0.02195	0.00476
Water	-0.00245	0.03624	0.00143	0.00675	0.00949	0.01808	-0.00091
Roads	-0.00525	0.00143	0.02534	-0.02242	-0.01691	0.01745	0.00173
Area	0.00857	0.00675	-0.02242	0.05555	0.04639	-0.01045	-0.00335
Upstream	0.00554	0.00949	-0.01691	0.04639	0.08635	-0.02395	-0.00661
Northing	0.02195	0.01808	0.01745	-0.01045	-0.02395	0.23746	0.01364
Easting	0.00476	-0.00091	0.00173	-0.00335	-0.00661	0.01364	0.01496

Table 18. Bay Model 1 Correlation Matrix

Layer	Land	Water	Roads	Area	Upstream	Northing	Easting
Land	1.00000	-0.07447	-0.19078	0.21051	0.10917	0.26063	0.22512
Water	-0.07447	1.00000	0.04720	0.15041	0.16959	0.19486	-0.03924
Roads	-0.19078	0.04720	1.00000	-0.59742	-0.36154	0.22493	0.08874
Area	0.21051	0.15041	-0.59742	1.00000	0.66979	-0.09100	-0.11637
Upstream	0.10917	0.16959	-0.36154	0.66979	1.00000	-0.16725	-0.18404
Northing	0.26063	0.19486	0.22493	-0.09100	-0.16725	1.00000	0.22890
Easting	0.22512	-0.03924	0.08874	-0.11637	-0.18404	0.22890	1.00000

Table 19. Bay Model 1 Eigenvalues and Eigenvectors

Layer	1	2	3	4	5	6	7
Eigenvalues	0.24890	0.12471	0.03931	0.02734	0.02190	0.01263	0.01096
Eigenvectors							
Land	0.08661	0.14624	-0.52566	-0.15062	0.76104	-0.28574	0.10626
Water	0.07037	0.15472	0.72227	-0.56817	0.34443	-0.04090	-0.07943
Roads	0.09776	-0.22561	0.31670	0.40139	0.27143	0.12808	0.76685
Area	-0.10077	0.57091	-0.20127	-0.40551	-0.33203	0.17149	0.56507
Upstream	-0.17677	0.73389	0.20266	0.56439	0.16822	0.02383	-0.20419
Northing	0.96559	0.19481	-0.01195	0.07958	-0.14245	-0.02484	-0.04794
Easting	0.06496	-0.03597	-0.14137	-0.06393	0.26397	0.93257	-0.17621

Bay Model 2

Table 20. Bay Model 2 Covariance Matrix						
Layer	Land	Water	Area	Upstream	Northing	Easting
Land	0.02986	-0.00245	-0.00525	0.00857	0.00554	0.02195
Water	-0.00245	0.03624	0.00143	0.00675	0.00949	0.01808
Area	-0.00525	0.00143	0.02534	-0.02242	-0.01691	0.01745
Upstream	0.00857	0.00675	-0.02242	0.05555	0.04639	-0.01045
Northing	0.00554	0.00949	-0.01691	0.04639	0.08635	-0.02395
Easting	0.02195	0.01808	0.01745	-0.01045	-0.02395	0.23746

Table 21. Bay Model 2 Correlation Matrix						
Layer	Land	Water	Area	Upstream	Northing	Easting
Land	1.00000	-0.07447	-0.19078	0.21051	0.10917	0.26063
Water	-0.07447	1.00000	0.04720	0.15041	0.16959	0.19486
Area	-0.19078	0.04720	1.00000	-0.59742	-0.36154	0.22493
Upstream	0.21051	0.15041	-0.59742	1.00000	0.66979	-0.09100
Northing	0.10917	0.16959	-0.36154	0.66979	1.00000	-0.16725
Easting	0.26063	0.19486	0.22493	-0.09100	-0.16725	1.00000

Table 22. Bay Model 2 Eigenvalues and Eigenvectors						
Layer	1	2	3	4	5	6
Eigenvalues	0.24791	0.12457	0.03879	0.02728	0.02122	0.01102
Eigenvectors						
Land	0.08590	0.14750	-0.51332	-0.13978	0.82726	0.05894
Water	0.07130	0.15384	0.74234	-0.54587	0.33950	-0.08339
Area	0.09772	-0.22652	0.31914	0.41512	0.24295	0.77842
Upstream	-0.09993	0.57195	-0.19963	-0.41642	-0.32752	0.58512
Northing	-0.17530	0.73474	0.20771	0.57583	0.12736	-0.19617
Easting	0.96813	0.19052	-0.02433	0.07198	-0.13367	-0.05278

Atlantic Model

Table 23. Atlantic Model Covariance Matrix							
	Upstream	Land	SLR	Tide	Easting	Northing	Water
Upstream	5.50e-3	-8.57e-4	-2.32e-5	-3.13e-4	1.86e-4	6.78e-5	1.71e-3
Land	-8.57e-4	9.80e-3	1.08e-4	-1.38e-3	1.44e-4	1.82e-3	2.12e-3
SLR	-2.32e-5	1.08e-4	1.81e-1	5.93e-5	-2.51e-4	1.15e-3	4.66e-4
Tide	-3.13e-4	-1.38e-3	5.93e-5	7.42e-3	-1.10e-4	1.00e-3	8.42e-4
Easting	1.861e-4	1.44e-4	-2.51e-4	-1.10e-4	5.59e-4	5.03e-5	1.20e-3
Northing	6.781e-5	1.82e-3	1.15e-3	1.00e-3	5.03e-5	2.23e-2	2.94e-2
Water	1.711e-3	2.12e-3	4.66e-4	8.42e-4	1.20e-3	2.94e-2	5.60e-2

Table 24. Atlantic Model Correlation Matrix							
	Upstream	Land	SLR	Tide	Easting	Northing	Water
Upstream	1.00000	-0.11676	-0.00074	-0.04894	0.10613	0.00613	0.09747
Land	-0.11676	1.00000	0.00256	-0.16233	0.06134	0.12301	0.09040
SLR	-0.00074	0.00256	1.00000	0.00162	-0.02496	0.01817	0.00463
Tide	-0.04894	-0.16233	0.00162	1.00000	-0.05422	0.07801	0.04129
Easting	0.10613	0.06134	-0.02496	-0.05422	1.00000	0.01425	0.21441
Northing	0.00613	0.12301	0.01817	0.07801	0.01425	1.00000	0.83219
Water	0.09747	0.09040	0.00463	0.04129	0.21441	0.83219	1.00000

Table 25. Atlantic Model Principal Component Layers

	1	2	3	4	5	6	7
Eigenvalues							
	1.8e-1	7.3e-2	1.0e-2	7.4e-3	5.4e-3	4. 6e-3	4.7e-4
Input Layer	Eigenvectors						
Upstream	7.96e-5	2.18e-2	1.52e-1	4.20e-1	5.62e-1	6.96e-1	1.72e-2
Land	7.86e-4	4.25e-2	9.04e-1	2.35e-1	3.50e-1	5.34e-2	1.82e-2
SLR	10.00e-1	9.13e-3	6.29e-4	2.20e-3	2.48e-3	3.04e-3	9.79e-4
Tide	4.13e-4	1.76e-2	3.91e-1	7.82e-1	4.84e-1	4.89e-3	6.46e-3
Easting	1.36e-3	1.48e-2	7.23e-3	5.33e-2	7.74e-2	6.91e-2	9.93e-1
Northing	8.35e-3	5.00e-1	5.24e-2	3.32e-1	5.08e-1	6.09e-1	9.19e-2
Water	5.71e-3	8.64e-1	6.32e-2	2.08e-1	2.51e-1	3.72e-1	6.90e-2

References

Allen, J. R. L. and J. E. Rae. 1988. Vertical salt-marsh accretion since the Roman period in the Severn Estuary, Southwest Britain. Marine Geology 83:225-235.

Anastasiou, C. J. and J. R. Brooks. 2003. Effects of soil pH, redox potential, and elevation on survival of *Spartina patens* planted at a west central Florida salt marsh restoration site. Wetlands 23:845-859.

Anselin, L. 1988. Spatial Econometrics: Methods and Models. Kluwer Academic Publishers, Dordrecht, The Netherlands.

Asrar, G., Kanemasu, E. T. and J. L. Hatfield. 1984. Estimating absorbed photosynthetic radiation and leaf area index from spectral reflectance in wheat. Agronomy Journal 76:300-306.

Baret, F. and G. Guyot. 1991. Potentials and limits of vegetation indices for LAI and APAR assessment. Remote Sensing of Environment 35:161-173.

Bierwirth, P. N. 1990a. Mineral mapping and vegetation removal via data-calibrated pixel unmixing, using multispectral images. International Journal of Remote Sensing 11:1999-2017.

Bierwirth, P. 1990b. Mineral and vegetation mapping over mound spring deposits near Lake Eyre: An application of data-calibrated pixel unmixing using Landsat TM data. Fifth Australian Remote Sensing Conference. Perth, Australia.

Boesch, D. F., M. N. Josselyn, A. J. Mehta, J. T. Morris, W. K. Nuttle, C. A. Simenstad and D. J. P. Swift. 1994. Scientific Assessment of Coastal Wetland Loss, Restoration and Management in Louisiana. Journal of Coastal Research Special Issue No. 20:1-103.

Boggs, K. and M. Shepherd. 1999. Response of marine deltaic surfaces to major earthquake uplifts in southcentral Alaska. Wetlands 19:13-27.

Borel, C. C. and S. A. W. Gerstl. 1994. Nonlinear Spectral Mixing Models for Vegetative and Soil Surfaces. Remote Sensing of Environment 47:403-351.

Bricker-Urso, S., S. W. Nixon, J. K. Cochran, D. J. Hirschberg and C. Hunt. 1989. Accretion Rates and Sediment Accumulation in Rhode Island Salt Marshes. Estuaries 12:300-317.

Bryant, J. C. and R. H. Chabreck. 1998. Effects of Impoundment on Vertical Accretion of Coastal Marsh. Estuaries 21:416-422.

Cahoon, D. R. and D. J. Reed. 1995. Relationships among Marsh Surface topography, Hydroperiod and Soil Accretion in a Deteriorating Lousiana Salt Marsh. Journal of Coastal Research 11:357-369.

Carter J., A. L. Foote and L. A. Johnson-Randall. 1999. Modeling the effects of *Nutria* (*Myocastor coypus*) on wetland loss. Wetlands 19: 209-219.

Childers, D. L., S. Cofer-Shabica and L. Nakashima. 1993. Spatial and temporal variability in marsh-water column interactions in a southeastern USA salt marsh estuary. Marine Ecology Progress Series 95:25-38.

Cherchali, S. and G. Flouzat. 1994. Linear mixture modelling applied to AVHRR data for monitoring vegetation. p. 1242-1244. Proceedings IGARSS ´94: Surface and Atmospheric Remote Sensing: Technologies, Data Analysis and Interpretation, IEEE, Pasadena, CA, USA.

Chmura, G. L. and P. Aharon. 1995. Stable Carbon Isotope Signatures of Sedimentary Carbon in Coastal Wetlands as Indicators of Salinity Regime, 11:124-135.

Civco, D. L., J. D. Hurd, P. L. August and C. L. LaBash. 1994. Coastal wetland mapping and change detection in the Northeast United States. CoastWatch Change Analysis Program (C-CAP), Washington, DC, USA. NOAA Project NA90AA-D-SG4433: 1-79.

Cliff, A.D. and J. K. Ord.1973. Spatial autocorrelation. Pion, London, England.

Cowardin, L. 1979. Classification of Wetlands and Deepwater Habitats of the United States. U.S. Fish and Wildlife Service, Washington, DC, USA. FWS/OBS-79/31.

Craft, C. B. and S. W. Broome. 1993. Vertical Accretion in Microtidal Regularly and Irregularly Flooded Estuarine Marshes. Estuarine Coastal and Shelf Science 37: 371-386.

Dahl, T.E. 1990. Wetlands losses in the United States: 1780's to 1980's. U.S. Department of the Interior, Fish and Wildlife Service, Washington, DC, USA.

Daborn, G. R., C. L. Amos, M. Brylinsky, H. Christian, G. Drapeau, R. W. Faas, J. Grant, B. Long, D. M. Paterson, G. M. E. Perillo and M. C. Piccolo. 1993. An ecological cascade effect: Migratory birds affect stability of intertidal sediments. Limnology and Oceanography 38:225-231.

Dame, R. and D. Childers. 1992. A Geohydrologic Continuum Theory for the Spatial and Temporal Evolution of Marsh-Estuarine Ecosystems. Netherlands Journal of Sea Research 30:63-72.

Daughtry, C., 2001, Discriminating Crop Residues from Soil by Shortwave Infrared Reflectance. Agronomy Journal 93:125-131.

Davis, J. C. 2003. Statistics And Data Analysis In Geology, Third Edition, John Wiley & Sons, New York, NY, USA.

DeLaune, R. D., C. J. Smith and W. H. Patrick, Jr. 1983. Relationship of marsh elevation, redox potential and sulfide to *Spartina Alterniflora* productivity. Soil Science Society of America. Journal 47:930-935.

DeLaune, R. D., R. H. Baumann and J. G. Gosselink. 1983. Relationships among vertical accretion, coastal submergence and erosion in a Louisiana Gulf Coast marsh. Journal of Sedimentary Petrology 53:147-157.

Dijkema, K. S. 1997. Impact prognosis for salt marshes from subsidence by gas extraction in the Wadden Sea. Journal of Coastal Research 13:1294-1304.

Donoghue, D. N. M., D. C. R.Thomas and Y. Zong. 1994. Mapping and monitoring the intertidal zone of the East coast of England using remote sensing techniques and a coastal monitoring GIS. Remote sensing for Marine and Coastal Environments; Marine Technology Society Journal 28:19-29.

Downs, L. L., R. J. Nicholls, S. P.Leatherman and J. Hautzenroder. 1994. Historic Evolution of a Marsh Island: Bloodsworth Island, Maryland. Journal of Coastal Research 10:1031– 1044.

EPA. 1982. Chesapeake Bay, Introduction to an Ecosystem. Environmental Protection Agency, Washington, DC, USA.

Erwin, R. M. 1996. Dependence of Waterbirds and Shorebirds on Shallow-Water Habitats in the Mid-Atlantic Coastal Region: An Ecological Profile and Management Recommendations. Estuaries 19:213-219.

Esselink, P., K. S. Dijkema, S. Reents and G. Hageman. 1998. Vertical Accretion and Profile Changes in Abandoned Man-Made Tidal Marshes in the Dollard Estuary, the Netherlands. Journal of Coastal Research 14:570-582.

Evers, D. E., C. E. Sasser, J. G. Gosselink, D. A. Fuller and J. M. Visser. 1998, The Impact of Vertebrate Herbivores on Wetland Vegetation in Atchafalaya Bay, Louisiana. Estuaries, 21 (1), 1-13.

Fallah-Adl, H., J. JaJa, S. Liang, J. Townshend and Y. Kaufman. 1996. Fast Algorithms for Removing Atmospheric Effects from Satellite Images. IEEE Computational Science and Engineering. 3:66-77.

Foody, G. M. and D. P. Cox. 1994. Sub-pixel land cover composition estimation using a linear mixture model and fuzzy membership functions. International Journal of Remote Sensing 15:619-631.

French, Jonathan R. and Tom Spencer. 1993. Dynamics of sedimentation in a tide-dominated backbarrier salt marsh, Norfolk, UK. Marine Geology 110:315-331.

Frey, R.W. and P. B. Basan. 1985. Coastal salt marshes. p. 225-301. In R. A.Davis (ed.) Coastal Sedimentary Environments. Springer-Verlag, New York. NY, USA.

Fung, T. and E. F. LeDrew. 1987. Land cover change detection with Thematic Mapper spectral/textural data at the rural-urban fringe. Proceedings of 21st Symposium on Remote Sensing of Environment, Ann Arbor, MI, USA.

Gabrey, S. W., A. D. Afton and B. C. Wilson. 1999. Effects of winter burning and structural marsh management on vegetation and winter bird abundance in the Gulf Coast Chenier Plain, USA. Wetlands 19:584-594.

Gammill, S. P. and P. E. Hosier. 1992. Coastal Saltmarsh Development at Southern Topsail Sound, North Carolina. Estuaries 15:122-129.

Gates D.M., H. J. Keegan, J. C. Schleter and V. R. Weidner. 1965. Spectral properties of plants. Applied Optics 4:11–20.

Gausman, H.W., W.A. Allen, V.I. Myers, and R. Cardenas. 1969. Reflectance and internal structure of cotton leaves, *Gossypium hirsutum* (L.). Agronomy Journal 61:374–376.

Gausman, H., A. Gerbermann, C. Wiegand, R. Leamer, R. Rodriguez and J. Noriega. 1975. Reflectance differences between crop residues and bare soils. Soil Science Society of America Proceedings. 39:752-755.

Gong, P., J. Miller, J. Freemantle and B. Chen. 1991. Spectral Decomposition of Landsat Thematic Mapper data for urban land-cover mapping. p. 458-461. In Proceedings of the 14th Canadian Symposium on Remote Sensing. Canadian Remote Sensing Society, Calgary, Alberta, Canada.

Gosselink, J. G. and C. J. Kirby. 1974. Decomposition of salt marsh grass, *Spartina alterniflora* Loisel. Limnology and Oceanography 19:825-832.

Gosselink, J. G. and R. H. Baumann. 1980. Wetland inventories: wetland loss along the United States coast. Zeitschrift für Geomorphologie, 30:173-187

Grace, J. B. and Mark A. Ford. 1996. The Potential Impact of Herbivores on the Susceptibility of the Marsh Plant *Sagittaria Lancifolia* to Saltwater Intrusion in Coastal Wetlands. Estuaries 19:13-20.

Gross, M. F., M. A. Hardisky, Wolf, P. L. and V. Klemas. 1993. Relationships among *Typha* biomass, pore water methane and reflectance in a Delaware (U.S.A.) brackish marsh.. Journal of Coastal Research 9:339-355.

Halupa, P. J. and B. L. Howes. 1995. Effects of tidally mediated moisture content on decomposition of *Spartina alterniflora* and *Spartina patens*. Marine Biology 123:379-391.

Harsanyi, J. C. and C. Chein-I. 1994. Hyperspectral image classification and dimensionality reduction: An orthogonal subspace projection approach. Institute of Electrical and Electronic Engineers Transactions on Geoscience and Remote Sensing 32:779-832.

Hartig, E. K., V. Gornitz, A. Kolker, F. Mushacke and D. Fallon. Anthropogenic and climate-change impacts on salt marsches of Jamaica Bay. New York City. Wetlands 22:71-89.

Haslett, S.K., A. B. Cundy, C. F. C. Davies, E. S. Powell. and I. W. Croudace. 2003. Salt marsh sedimentation over the past c. 120 years along the West Cotentin Coast of Normandy (France): Relationship to sea –level rise and sediment supply. Journal of Coastal Research 19:600-620.

Hatton, R. S., R. D. DeLaune and W. H. Patrick, Jr. 1983. Sedimentation, accretion and subsidence in marshes of Barataria Basin, Louisiana. Limnology and Oceanography 28:494-502.

Hazelden, J. and L. A. Boorman. 1999. The role of soil and vegetation processes in the control of organic and mineral fluxes in some Western European salr marshes. Journal of Coastal Research 15:15-31.

Heinle, D.R. and D.A. Flemer. 1976. Flows of materials between poorly flooded tidal marshes and an estuary. Marine Biology 35:359-373.

Hinson, J. M., German, C. D., Pulich, W. Jr., 1994, Accuracy assessment and validation of classified satellite imagery of Texas coastal wetlands. Remote sensing for Marine and Coastal Environments, 83.

Holben, B. and Y. Shimabukuro. 1993. Linear mixing model applied to coarse spatial resolution data from multispectral satellite sensors. International Journal of Remote Sensing 14:2231-2240.

Hosmer, D. W. and S. Lemeshow. 2000. Applied Logistic Regression, Second Edition. John Wiley & Sons, Inc. New York, NY, USA.

Huete, A. R. 1986. Separation of Soil-Plant Spectral Mixtures by Factor Analysis. Remote Sensing of Environment, 19:237-251.

Huete, A. R. 1989. Soil Influences in Remotely Sensed Vegetation-Canopy Spectra. p. 120 In Ghassem Asrar (ed.) Theory and Applications of Optical Remote Sensing. John Wiley & Sons, Inc. New York, NY, USA.

Hutchinson, S. E., F. H. Sklar, and C. Roberts. 1995. Short Term Sediment Dynamics in a Southeastern U.S.A. *Spartina* Marsh. Journal of Coastal Research 11:370-380.

Ingle, J. D., Jr. and S. R. Crouch. 1988. Spectrochemical Analysis, Prentice Hall, Englewood Cliffs, NJ, USA.

Kaye, Clifford A. and E. S. Barghoorn. 1964. Late Quaternary Sea-Level Change and Crustal Rise at Boston, Massachusetts, with Notes on the Autocompaction of Peat. Geological Society of America Bulletin 75:63-80.

Ke, Xiankun, M. B. Colling and S. E. Poulos. 1994. Velocity structure and sea bed roughness associated with intertidal (sand and mud) flats and saltmarshes of the Wash, U.K.. Journal of Coastal Research 10:702-715.

Kearney, M. S. and J. C. Stevenson. 1989. Marsh loss and shore erosion with sea-level rise in Chesapeake Bay. Proceedings of the Second North American Conference on Preparing for Climate Change, Climate Institute. Climate Institute, Washington, DC, USA.

Kearney, M. S. 1996. Sea-level Change during the Last Thousand Years in Chesapeake Bay. Journal of Coastal Research 12:977-983.

Kearney, M.S., A. S. Rogers, J. R. G. Townshend, W. T. Lawrence, K. Dorn, K. Eldred, D. Stutzer, F. Lindsay. and E. Rizzo. 1995. Developing a model for determining

coastal marsh health, Third Thematic Conference on Remote Sensing for Marine and Coastal Environments, Seattle, Washington. Environmental Research Institute of Michigan, Ann Arbor, MI, USA.

Kearney, M.S., A. S. Rogers, J. R. G. Townshend, E. Rizzo, D. Stutzer, J. C. Stevenson and K. Sundborg. 2002. Landsat imagery shows decline of coastal marshes in Chesapeake and Delaware Bays, Eos Transactions 83:173, 177-178.

Kearney, M. S., J. C. Stevenson and L. G. Ward. 1994. Spatial and Temporal Changes in Marsh Vertical Accretion Rates at Monie Bay:Implications for Sea-Level Rise. Journal of Coastal Research 10:1010-1020.

Kearney, M. S., R. E. Grace and J. C. Stevenson. 1988, Marsh loss in Nanticoke Estuary, Chesapeake Bay. Geographical Review 78:205-220.

Kearney, M.S., A. S. Rogers, J. R. G. Townshend, E. Rizzo, D. Stutzer, J. C. Stevenson and K. Sundborg. 2002. Landsat imagery shows decline of coastal marshes in Chesapeake and Delaware Bays, Eos Transactions 83:173.

Kearney, M.S., and L.G. Ward. 1986. Accretion rates in brackish marshes of a Chesapeake Bay estuarine tributary. Geo-Marine Letters 6:41-49.

Kelley, J.T., W. R. Gehrels and D. F. Belknap. 1995. Late Holocene relative sea-level rise and the geologic development of tidal marshes at Wells, Maine, U.S.A. Journal of Coastal Research 11:136-153.

Keough, J. R., T. A. Thompson, G. R. Guntenspergen and D. Wilcox. 1999. Hydrogeomorphic factors and ecosystem responses in coastal wetlands of the Great Lakes. Wetlands 19:821-834.

Kerner, M. 1993. Coupling of microbial fermentation and respiration processes in an intertidal mudflat of the Elbe estuary. Limnology and Oceanography 38:314-330

Kirk, J. T. O. 1994. Light and photosynthesis in aquatic ecosystems, 2nd ed., Cambridge University Press, New York, NY, USA

Koch, M. S. , I. A. Mendelssohn and K. L. McKee. 1990. Mechanisms for the hydrogen-sulfide induced growth limitation of *Spartina alterniflora* and *Panicum hemitomon*. Limnology and Oceanography 35:399-408

Kokot, R. R. 1997. Littoral Drift, Evolution and Management in Punta Medanos, Argentina. Journal of Coastal Research 13:192-197

Kuenzler, E.J. and H. L.Marshall. 1973. Effects of mosquito control ditching on estuarine ecosystems. University of North Carolina Water Resources Research Institute, Report no. 81, Raleigh, NC, USA

Kuhn, N. L., I. Mendelssohn and D. Reed. 1999. Altered Hydrology Effects on Louisiana Salt Marsh Function,. Wetlands 19:617-626

Latham, P. J., L. G. Pearlstine and W. M. Kitchens. 1991. Spatial distributions of the softstem bulrush, *Scirpus validus*, across a salinity gradient. Estuaries 14:192-198

Leonard, L.A., A.C. Hine and M.E. Luther. 1995. Surficial Sediment Transport and Deposition Processes in a *Juncus roemerianus* Marsh, West-Central Florida. Journal of Coastal Research 11:322-336

Leonard, L. A. and D. Reed. 2002. Hydrodynamics and sediment transport through tidal marsh canopies. Journal of Coastal Research SI 36:459-469.

Letzsch, W. S. and R. W. Frey. 1980. Deposition and erosion in a holocene salt marsh, Sapelo Island, Georgia. Journal of Sedimentary Petrology 50:529-542

Levitt, J. and R. Ben Zaken. 1975. Effects of small water stresses on cell turgor and intercellular space. Physiologia Plantarum. 34:273-279

Liang, S., H. Fallah-adl, S. Kalluri, J. JaJa, Y. J. Kaufman and J. R. G. Townshend. 1997. An operational atmospheric correction algorithm for Landsat Thematic Mapper imagery over the land. Journal or Geophysical Research 102:17173-17186.

Lillesand T.M and R. W. Kiefer. 1994. Remote Sensing and Image Interpretation, Third Edition. John Wiley and Sons , New York, NY, USA

Maas, S. J. and J. R. Dunlap. 1089. Reflectance, transmittance and absorptance of light by normal, etiolated and albino corn leaves. Agronomy Journal 81:105-110.

Mackin, S., N. Drake, J. Settle and H. Rotfuss. 1990. Towards automatic mapping of imaging spectrometry data using an expert system and linear mixture model. Fifth Australian Remote Sensing Conference. Perth, Australia.

Mathieu, S., P. Leymarie and M. Berthod. 1994. Determination of proportions of land use blend in pixels of a multispectral satellite image. IEEE 1154-1156

Mathieu-Marni, S., P. Leymarie and M. Berthod. 1996a Removing ambiguities in a multi-spectral image classification. International Journal of Remote Sensing 17:1493-1504.

Mathieu-Marni, S., S. Mosian and R. Vincent. 1996b. A knowledge-based system for the computation of land cover mixing and the classification of multi-spectral satellite imagery. International Journal of Remote Sensing 17:1483-1492.

McFeeters, S. K. 1996. The use of the Normalized Difference Water Index (NDWI) in the delineation of open water features. International Journal of Remote Sensing 17:1425-1432

Meentemeyer, V. 1984. The geography of organic decomposition rates. Annals of the Association of American Geographers 74:551-560

Mendelssohn, I.A. and M. T. Postek. 1982. Elemental analysis of deposits on the roots of *Spartina alterniflora* Loisel. American Journal of Botany 69:904-912

Minello, T. J., R. J. Zimmerman and R. Medina. 1994. The importance of edge for natant macrofauna in a created salt marsh. Wetlands 14:184-198

Mitsch, W. J. and J. G. Gosselink. 2000, Wetlands, Third Edition. John Wiley & Sons, New York, NY, USA

Morris, J. T., P. V. Sundareshwar, C. T. Nietch, B. Kjerfve and D. R. Cahoon. 2002,. Reponses of coastal wetlands to rising sea level. Ecology 83:2869 – 2877

Morrison, M. C., M. E. Hines and H. G. Bingemer. 1990. The variability of biogenic sulfur flux from a temperate salt marsh on short time and space scales. Atmospheric Environment 24:1771-1779

Murray, A. L. and T. Spencer. 1997. On the wisdom of calculating annual material budgets in tidal wetlands. Marine Ecology Progress Series, 150:207-216

Myneni, R.B. and G. Asrar. 1994. Atmospheric effects and spectral vegetation indices. Remote Sensing Environment 47:390-402

Netto, S. A. and P. C. Lana. 1997. Influence of *Spartina alterniflora* on Superficial Sediment Characteristics of Tidal Flats in Paranagua Bay (South-eastern Brazil). Estuarine, Coastal and Shelf Science 44:641-648

Novo, E.M. and Y. E. Shimabukuro. 1994. Spectral mixture analysis of inland tropical waters. International Journal of Remote Sensing 15:1351-1356

Nyman, J. A, R. D. DeLaune, S. R. Pezeshki and W. H. Patrick Jr. 1995. Organic Matter Fluxes and Marsh Stability in a Rapidly Submerging Estuarine Marsh. Estuaries 18:207-218.

Odum, W. E., E. P. Odum and H. T. Odum. 1995. Nature's pulsing paradigm. Estuaries, 18:547-555.

Orson, R. A. 1996. Some applications of paleoecology to the management of tidal marshes. Estuaries 19:238-246.

Orson, R. A. and B. L. Howes. 1992. Salt Marsh Development Studies at Waquoit Bay, Massachusetts:Influence of Geomorphology on Long-Term Plant Community Structure. Estuarine, Coastal and Shelf Science 35:453-471.

Orson, R. A., R. L. Simpson and R. E. Good. 1990. Rates of sediment accumulation in a tidal freshwater marsh. Journal of Sedimentary Petrology 60:859-869.

Osgood, D. T. and M. C. Santos. 1995. Sediment physico-chemistry associated with natural marsh development on a storm-deposited sand flat. Marine Ecology Progress Series 120:271-283

Peterson, B. J. and R. W. Howarth. 1987. Sulfur, carbon and nitrogen isotopes used to trace organic matter flow in the salt-marsh estuaries of Sapelo Island, Georgia. Limnology and Oceanography 32:1195-1213.

Peterson, D.L. and S. W. Running. 1989. Applications in forest science and management. P. 429-473 In. G. Asrar (ed.) Theory and Applications of Optical Remote Sensing. John Wiley & Sons, New York, NY, USA.

Pethick, J. S. 1981. Long-term accretion rates on tidal salt marshes. Journal of Sedimentary Petrology 51:571-577.

Pritchard, D.W. 1967. Observations of Circulation in coastal plain estuaries. P. 37-44. In G.H. Lauff (ed.), Estuaries, American Association for the Advancement of Science Publication no. 83,. Washington, DC, USA.

Puyou-Lacassies, P. G., A. Podaire, and M. Gay. 1994. Extracting crop radiometric responses from simulated low and high spatial resolution satellite data using a linear mixing model, International Journal of Remote Sensing 15:3767-3784.

Quarmby, N.A., J. R. G. Townshend, J. J. Settle, K. H. White, M. Milnes, T. L. Hindle and N. Silleos. 1992. Linear mixture modelling applied to AVHRR data for crop area estimation. International Journal of Remote Sensing, 13:415-426.

Ramsey III, E. W., D. K.Chappell and D. G. Baldwin. 1997a, AVHRR Imagery Used to Identify Hurricane Damage in a Forested Wetland of Louisiana. Photogrammetric Engineering & Remote Sensing 63:293-297.

Ramsey, E. W. III and S. C. Laine. 1997. Comparison of Landsat Thematic Mapper and high resolution photography to identify change in complex coastal wetlands. Journal of Coastal Research 13:281-292.

Ramsey, E. W. III, , G. A. Nelson, S. C. Laine, R. G. Kirkman, and W. Topham. 1997b. Generation of coastal marsh topography with radar and ground-based measurements. Journal of Coastal Research 13:1335-1341.

Ramsey, E. W., G. A. Nelson and S. K. Sapkota. 2001. Coastal Change Analysis Program implemented in Louisiana. Journal of Coastal Research, 17:53-71.

Richards, J. A. 1986. Remote Sensing Digital Image Analysis, An Introduction. Springer-Verlag New York, Inc., Secaucus, NJ, USA.

Rice, D., J. Rooth, and J.C. Stevenson. 2000. Colonization and Expansion of *Phragmites australis* in Upper Chesapeake Bay Tidal Marshes, Wetlands (2000) 20(2): 280-299.

Roberts, D. A., M. O. Smith and J. B. Adams. 1993, Green vegetation, nonphotosynthetic vegetation and soils in AVIRIS data. Remote Sensing of the Environment.

Rogers, A. S. and M. S. Kearney. 2004. Reducing signature variability in unmixing coastal marsh Thematic Mapper scenes using spectral indices. International Journal of Remote Sensing 25:1-19.

Roulet, N. T. 2000. Peatlands, carbon storage, greenhouse gases and the Kyoto Protocol prospects and significance for Canada. Wetlands, 20:605 – 615.

Rozas, L. R. 1995. Hydroperiod and Its Influence on Nekton Use of the Salt Marsh:A Pulsing Ecosystem. Estuaries 18:579-590.

Schenker, J. M. and J. M. Dean. 1979. The Utilization of an Inter-Tidal Salt Marsh Creek by Larval and Juvenile Fishes:Abundance, Diversity and Temporal Variation. Estuaries 2:145-163.

Sellers, P.J. 1985. Canopy reflectance, photosynthesis and transpiration. International Journal of Remote Sensing 6:1335-1372.

Sellers, P. J. 1987. Canopy reflectance, photosynthesis and transpiration. II. The role of biophysics in the linearity of their interdependence. Remote Sensing of Environment 21:143-183.

Settle, J. J. and N. A. Drake. 1993. Linear mixing and the estimation of ground cover proportions. International Journal of Remote Sensing 14:1159-1177.

Shi, Z., J. S. Pethick and K. Pye. 1995. Flow Structure in and above the Various Heights of a Saltmarsh Canopy. A Laboratory Flume Study. Journal of Coastal Research 11:1204-1209.

Shifrin, K. S. 1988. Physical Optics of Ocean Water, American Institute of Physics, New York , NY, USA.

Smith, M., J. Adams and A. Gillespie. 1990a. Reference endmembers for spectral mixture analysis. Fifth Australian Remote Sensing Conference. Perth, Australia.

Smith, M., D. Roberts, J. Hill, W. Mehl, B. Hosgood, J. Verdebout, G. Schmuck, C. Koechler and J. Adams. 1994. A New Approach to Quantifying Abundances of Materials in Multispectral Images. p. 2372-2374 *In* IEEE Transactions on Geoscience and Remote Sensing, Proceedings. IGARSS'94, JPL, Pasadena, CA, USA.

Smith, M., S. Ustin, J. Adams and A. Gillespieb. 1990b. Vegetation in deserts: I. A regional measure of abundance from multispectral images. Remote Sensing of Environment 29:1-26.

Stanley, D. W. 1993. Long-term trends in Pamlico River Estuary nutrients, chlorophyll, dissolved oxygen and watershed nutrient production. Water Resources Research. 29:2651-2662.

Steel, J. 1991. Albemarle-Pamlico Estuarine System: Technical Analysis of Status and Trends. Albemarle-Pamlico Estuarine Study Report 90-01. NC Department of Environment, Health and Natural Resources and EPA National Estuary Program Raleigh, NC, USA.

Stevens, J. L. 1997. Estimating coastal marsh loss with Landsat Thematic Mapper data:a verification study in Delaware.Master's Degree Thesis. University of Maryland, College Park, MD, USA.

Stevenson, J. C. and M. S. Kearney. 1996. Shoreline dynamics on the windward and leeward shores of a large temperate estuary. p. 233-259 *In* Nordstrom, K.F. and C.T. Roman. (ed.) Estuarine Shores: Hydrological, Geomorphological and Ecological Interactions. J. Wiley & Sons, New York, NY, USA.

Stevenson, J. C., L. G. Ward and M. S. Kearney. 1986. Vertical accretion in marshes with varying rates of sea level rise. p. 241-259. In Douglas A. Wolfe (ed.), Estuarine Variability, Academic Press, New York, NY, USA.

Stevenson, J. C., L. G. Ward and M. S. Kearney. 1988. Sediment transport and trapping in marsh systems:implications of tidal flux studies. Marine Geology 80:37-59.

Stevenson, J. C., M. S. Kearney and E. C. Pendleton. 1985. Sedimentation and erosion in a Chesapeake Bay brackish marsh system. Marine Geology. 67:213-235.

Stribling, J. M. and J. C. Cornwell. 2001. Nitrogen, phosphorus and sulfur dynamics in a low salinity marsh system dominated by *Spartina alterniflora*, Wetlands 21:629-638.

Stutzer, D.S. 1997. The effects of tidal inundation on measured spectral reflectance characteristics of coastal marsh vegetation. M.S. Thesis, Marine, Estuarine and Environmental Science Program, University of Maryland, College Park, MD, 109p.

Sullivan, J.K., Holderman, T., and Southerland, M., 1991, Habitat Status and Trends in the Delaware Estuary. A report by Dynamac Corp. prepared for the Delaware Estuary Program, U.S., Environmental Protection Agency.

Sun, S., Y. Cal and X. Tian. 2003. Salt marsh vegetation change after a short-term tidal restriction in the Changjiang Estuary. Wetlands 23:257-266.

Tiner, R. W., Jr. 1985. Wetlands of Delaware. U.S. Fish and Wildlife Service, National Wetlands Inventory, Newton Corner, MA and Delaware Department of Natural Resources and Environmental Control, Wetlands Section, Dover, DE.

Titus, J. G. 1998. Rising seas, coastal erosion and the Takings Clause:How to save wetlands and beaches without hurting property owners. Maryland Law Review 57:1279-1399.

Townshend, J.R.G. 1988 Thematic Mapper Data - Characteristics and Use. Natural Environmental Research Council, Swindon.

Turner, R. E. 1997. Wetland loss in the northern Gulf of Mexico:multiple working hypotheses. Estuaries 20:1-13.

Tyler, M. A. and R. P. Stumpf. 1989. Feasibility of using satallites for detection of kinetics of small phytoplankton blooms in estuaries:Tidal and migration effects. Remote Sensing of Environment 27:233-250.

Upton, G. and I. Cook. 2002. Oxford Dictionary of Statistics, Oxford University Press, Oxford, England

Van der Molen, J. 1997. Tidal Distortion and Spatial Differences in Surface Flooding Characteristics in a Salt Marsh:Implications of Sea-Level Reconstruction. Estuarine, Coastal and Shelf Science 45:221-233.

Walter-Shea, E. A., B. L. Bald, C. J. Hays, M. A. Mesarch, D. W. Deering and E. M. Middleton. 1992. Biophysical properties affecting vegetative canopy reflectance and absorbed photosynthetically active radiation at the FIFE site. Journal of Geophysical Research 97:18,925-18,934.

Wang, F. C., T. Lu and W. B. Sikora. 1993. Intertidal Marsh Suspended Sediment Transport Processes, Terrebonne Bay, Louisiana, U.S.A.. Journal of Coastal Research 9:209-220.

Weston, Roy F. Inc. 1992. Characterization of the Inland Bays Estuary, draft., Delaware Inland Bays Estuary Program, University of Delaware and Environmental Protection Agency.

White, W. A. and T. A. Tremblay. 1995. Submergence of wetlands as a result of human-induced subsidence and faulting along the upper Texas Gulf Coast. Journal of Coastal Research 11:788-807.

White, William A. and R. A. Morton. 1997. Wetland Losses Related to Fault Movement and Hydrocarbon Production, Southeastern Texas Coast. Journal of Coastal Research, 13:1305-1320| 32.

Wiens, J. A. 1989. Spatial Scaling in Ecology. Functional Ecology 3:385-397.

Williamson, H. D. 1994. Estimating sub-pixel components of a semi-arid woodland. International Journal of Remote Sensing 15:3303-3307.

Wilson, K.A. 1962. North Carolina wetlands, their distribution and management. N.C. Wildlife Resources Commission, Raleigh, NC, USA.

Wilson, K.A., 1962, North Carolina wetlands, their distribution and management. N.C. Wildlife Resources Commission, Raleigh.

Windham, L. 2001. Comparison of biomass production and decomposition between *Phragmites australis* (common reed) and *Spartina patens* (salt hay grass) in brackish marshes of New Jersey, USA, Wetlands 21:179-188.

Wray, R. D., S. P. Leatherman and R. J. Nicholls. 1995. Historic and future land loss for upland and marsh islands in the Chesapeake Bay, Maryland, U.S.A. Journal of Coastal Research, 11:1195-1203.